nagra.

Technical Report 03-02

Grimsel Test Site Investigation Phase V

The CRR Final Project Report Series II:

Supporting Laboratory Experiments with Radionuclides and Bentonite Colloids

July 2006

T. Missana and H. Geckeis (editors)

National Cooperative
for the Disposal of
Radioactive Waste

Hardstrasse 73
CH-5430 Wettingen
Switzerland
Tel. +41 56 437 11 11

www.nagra.ch

nagra.

Technical Report 03-02

Grimsel Test Site Investigation Phase V

The CRR Final Project Report Series II:

Supporting Laboratory Experiments with Radionuclides and Bentonite Colloids

July 2006

T. Missana[1] and H. Geckeis[2] (editors)

Contributors:
Ú. Alonso[1], M. García-Gutiérrez[1],W. Hauser[2], K. Iijima[3], M. Mingarro[1], K. Ota[3], Th. Rabung[2], Th. Schäfer[2], P. Vejmelka[2]

[1] CIEMAT, Madrid, Spain
[2] FZK-INE, Karlsruhe, Germany
[3] JAEA (former JNC), Tokai, Japan

National Cooperative for the Disposal of Radioactive Waste

Hardstrasse 73
CH-5430 Wettingen
Switzerland
Tel. +41 56 437 11 11

www.nagra.ch

This report was prepared on behalf of Nagra. The viewpoints presented and conclusions reached are those of the author(s) and do not necessarily represent those of Nagra.

ISSN 1015-2636

Foreword

Concepts for the disposal of radioactive waste in geological formations depend crucially on a thorough knowledge of relevant processes in the host rock and on an understanding of the whole repository system, comprising both engineered and geological barriers. The Grimsel Test Site (GTS) is a first-generation underground rock laboratory which is used to investigate many of these processes in hard, fractured rocks. It has been operated since 1984 by the Swiss National Cooperative for the Disposal of Radioactive Waste (NAGRA).

The laboratory is located in the crystalline rock of the Central Aar Massif, 450 m below the eastern flank of the Juchlistock at an altitude of 1730 m. It is reached via a 1200 m horizontal access tunnel, operated by the hydropower plant KWO. The layout of the tunnels that comprise the GTS allowed the establishment of a radiation controlled zone (IAEA type B/C) in 1990 in which experiments with radioactive tracers are carried out. With increasing experience in the implementation of in-situ experiments, improved process understanding and more advanced repository concepts, the experimental programmes at the GTS have gradually become more complex and more directly related to open questions defined by performance assessors or by regulatory bodies. Demonstration of disposal concepts by performing large- or full-scale, long-term experiments has also become a key aspect of investigations in the rock laboratory.

The investigation phase V of the Grimsel Rock Laboratory was initiated in 1997 in close co-operation with international partner organisations. Seven experimental programmes and projects are included in this Phase, covering a broad spectrum of investigations.

This report documents the laboratory results of the 'Colloid and Radionuclide Retardation' (CRR) project. The aims of the CRR project are to examine the migration of bentonite colloids in fractured rocks, to investigate the interaction between safety relevant radionuclides and bentonite colloids and to test the applicability of numerical codes for colloid-mediated radionuclide transport.

In addition to the laboratory programme, the project partners, namely ANDRA (F), ENRESA (E), FZK-INE (D), JNC (now JAEA, J), Nagra (CH) and the USDoE/Sandia (USA), funded a series of *in situ* dipole tracer experiments carried out at the Grimsel Test Site (GTS) and modelling investigations, the results of which are reported elsewhere in the CRR final report series (NTB 03-01 and 03-03).

Vorwort

Bei der Entsorgung radioaktiver Abfälle wird aus Sicherheitsüberlegungen die Endlagerung in geologischen Formationen vorgesehen. Dafür sind Kenntnis über das Wirtgestein sowie ein vertieftes Verständnis der technischen Sicherheitsbarrieren von entscheidender Bedeutung.

Seit 1984 betreibt die Nagra (Nationale Genossenschaft für die Lagerung radioaktiver Abfälle) ein standortunabhängiges Felslabor im Grimselgebiet (FLG), in den granitischen Gesteinen des Zentralen Aar Massivs.

Das FLG liegt 450 m unter der Ostflanke des Juchlistocks auf einer Höhe von 1730 m ü.M. und kann durch einen 1200 m langen horizontalen Zugangsstollen der Kraftwerke Oberhasli AG (KWO) erreicht werden. Im Jahr 1990 wurde in einem der Stollenabschnitte des FLG's eine kontrollierte Zone (IAEA Typ B/C) für Versuche mit radioaktiven Tracern eingerichtet.

Mit zunehmender Erfahrung in der Durchführung von Feldversuchen, verbessertem Systemverständnis der geologischen und technischen Barrieren sowie der weiterentwickelten Lagerkonzepte, verlagerten sich die Programm-Schwerpunkte zu komplexen, direkt auf die Anforderungen der Sicherheitsanalyse ausgerichteten Versuche. Langzeitdemonstrationsversuche gewannen in den letzten Jahren immer mehr an Bedeutung.

Die Untersuchungsphase V des FLG wurde 1997 in enger Zusammenarbeit mit den Partnerorganisationen geplant. Sie beteiligen sich wesentlich bei der Durchführung der insgesamt 7 Versuchsprogramme, die ein breites Spektrum wissenschaftlicher und technischer Fragestellungen abdecken.

Der vorliegende Bericht präsentiert die Resultate des Laborprogramms, welches im Rahmen des Projekts 'Kolloid- und Radionuklid-Retardierung' (CRR) durchgeführt wurde. Die Hauptzielsetzungen des CRR-Experiments waren die Untersuchung des Transportverhaltens von Bentonitkolloiden in einer Scherzone, die Wechselwirkung von sicherheitsrelevanten Radionukliden mit Bentonitkolloiden sowie die Überprüfung und Weiterentwicklung von Transportmodellen zur Vorhersage von kolloidalem Radionuklidtransport.

Zusätzlich zu den umfangreichen Laborexperimenten ermöglichten die beteiligten Projektpartner ANDRA (F), ENRESA (E), FZK-INE (D), JNC (heute JAEA, J), USDoE/Sandia (USA) und Nagra (CH) die Durchführung einer Vielzahl von *in situ* Dipol-Tracer-Experimenten, welche im Felslabor Grimsel (FLG) durchgeführt wurden und von Transportmodellierungen, welche ebenfalls in der Serie der Schlussberichte zum CRR-Projekt dokumentiert sind (NTB 03-01 und 03-03).

Préface

Le stockage définitif des déchets radioactifs est prévu, pour des questions de sûreté, dans des formations géologiques. La connaissance détaillée des roches d'accueil et une compréhension approfondie des processus se déroulant dans la roche et dans les barrières techniques de sûreté sont d'une importance décisive.

Le laboratoire souterrain du Grimsel (LSG) est un laboratoire de première génération en fonction depuis 1984, exploité par la Société coopérative nationale pour l'entreposage de déchets radioactifs (NAGRA).

Le laboratoire est situé à une altitude de 1730 m dans les roches granitiques du Massif Central de l'Aar, à 450 m de profondeur sous le flanc est du Juchlistock. On l'atteint par un tunnel d'accès horizontal exploité par la centrale électrique Oberhasli AG de la société KWO. En 1990, on a aménagé dans le LSG une zone de radiation contrôlée (type B/C de l'AIEA) pour des essais avec traceurs radioactifs.

Avec l'expérience croissante dans la conduite d'essais in-situ, une meilleure compréhension des barrières géologiques et techniques, le programme de recherche s'est orienté vers des essais toujours plus complexes liés aux exigences des analyses de sûreté. La démonstration de faisabilité de concepts de dépôt à grande échelle et sur de longues durées est devenue l'un des points forts des recherches dans le laboratoire souterrain.

La phase de recherche actuelle du LSG, qui a débuté en 1997, a été planifiée en concertation étroite avec les partenaires internationaux. Elle comprend sept projets et programmes d'essais couvrant un large spectre de questions scientifiques et techniques.

Ce rapport présente les résultats du programme d'expériences en laboratoire réalisé dans le cadre du projet 'Retard des colloïdes et des radionucléides' (CRR). Les objectifs principaux de l'expérience CRR étaient les suivants: observer la migration des colloïdes de la bentonite dans une zone de cisaillement, étudier les interactions entre les colloïdes de la bentonite et les radionucléides importants pour la sûreté du dépôt, et enfin tester les codes numériques visant à modéliser le transport des radionucléides qui s'effectue par le biais des colloïdes.

En marge du programme d'expériences en laboratoire, les partenaires du projet – à savoir l'ANDRA (F), ENRESA (E), FZK-INE (D), JNC (aujourd'hui JAEA, J), la Nagra (CH) et USDoE/Sandia (USA) – ont rendu possible une série de tests de traçage en dipôle *in situ*, réalisés au Laboratoire souterrain du Grimsel (LSG), ainsi que des essais de modélisation du transport des radionucléides, dont les résultats ont également été publiés dans la série des rapports finals du projet CRR (NTB 03-01 et 03-03).

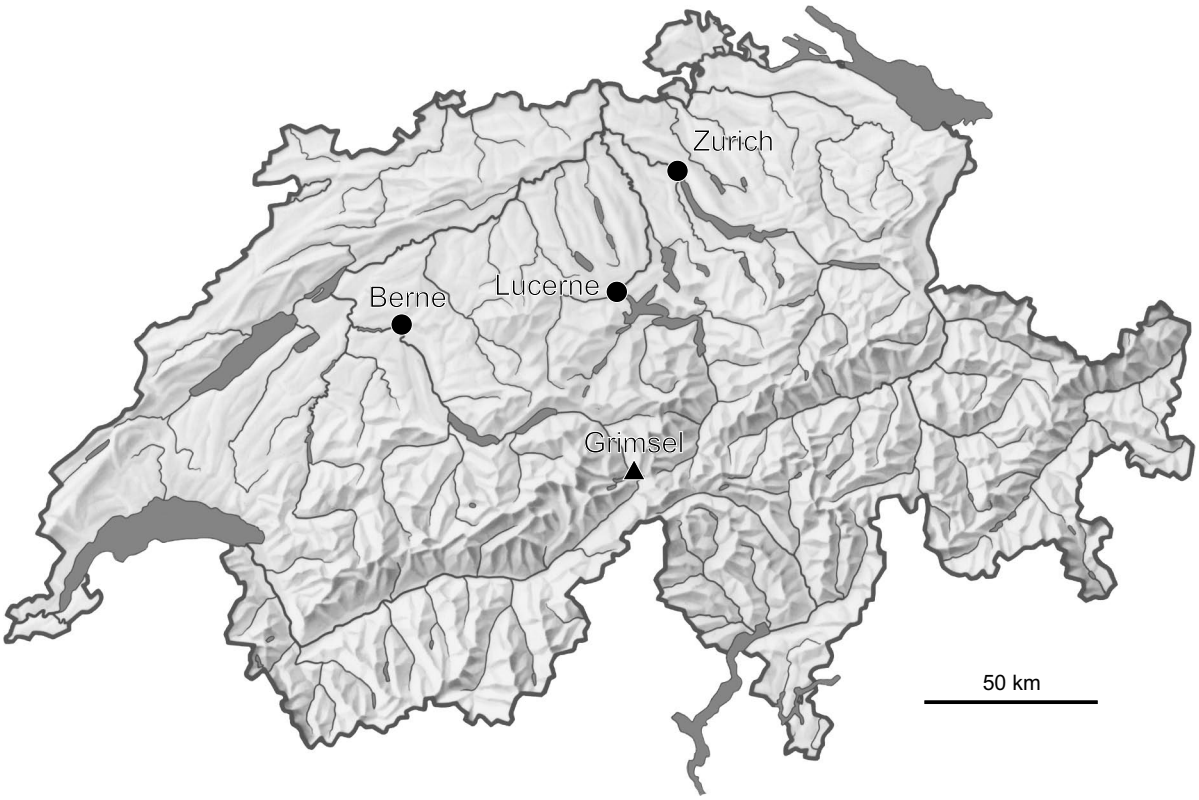

Location of Nagra's underground test facility at the Grimsel Pass in the Central Alps (Bernese Alps) of Switzerland

Grimsel area (view to the west)

1 Grimsel Test Site 2 Lake Raeterichsboden 3 Lake Grimsel 4 Juchlistock

Grimsel Test Site (GTS)

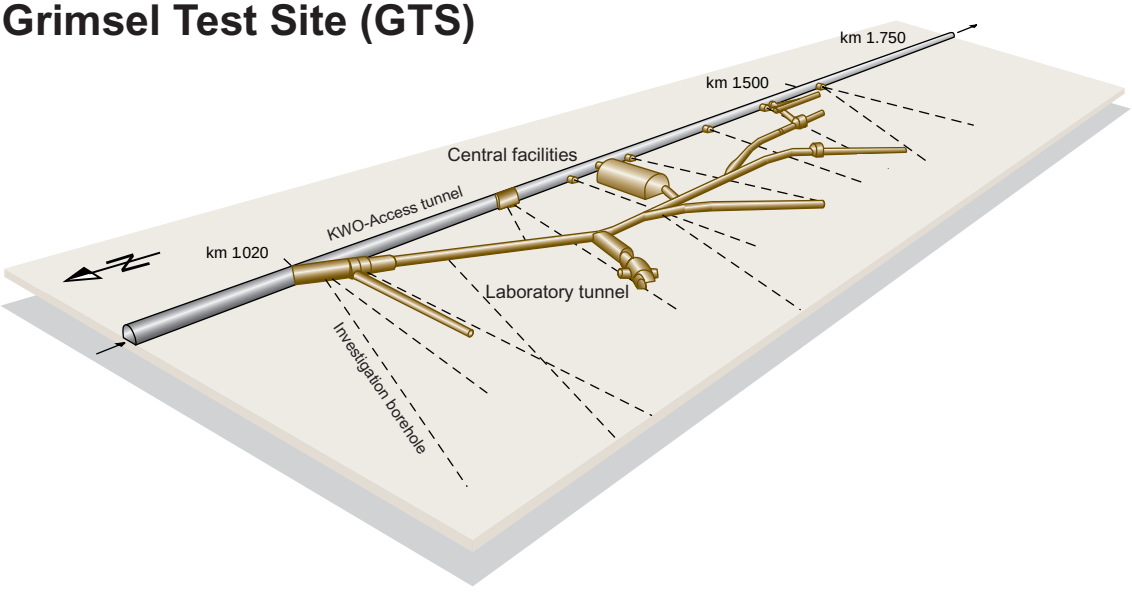

Grimsel Test Site
GTS

KWO-Access tunnel

Laboratory tunnel

Central Aaregranite (CAGR)
High biotite content CAGR

Grimsel-Granodiorite

Shear zone

Lamprophyre

SB — Investigation borehole

ZB — Central facilities

GTS Phase V 1997-2002

HPF — Hyperalkaline Plume

CRR — Colloid and Radionuclide Retardation

GAM — Gastransport in the Geosphere

FEBEX — 1:1 EBS – Demonstration (HLW)

GMT — Gas Migration Test in the EBS

GMB — Geophysical Methods in Boreholes

EFP — Effective Parameters

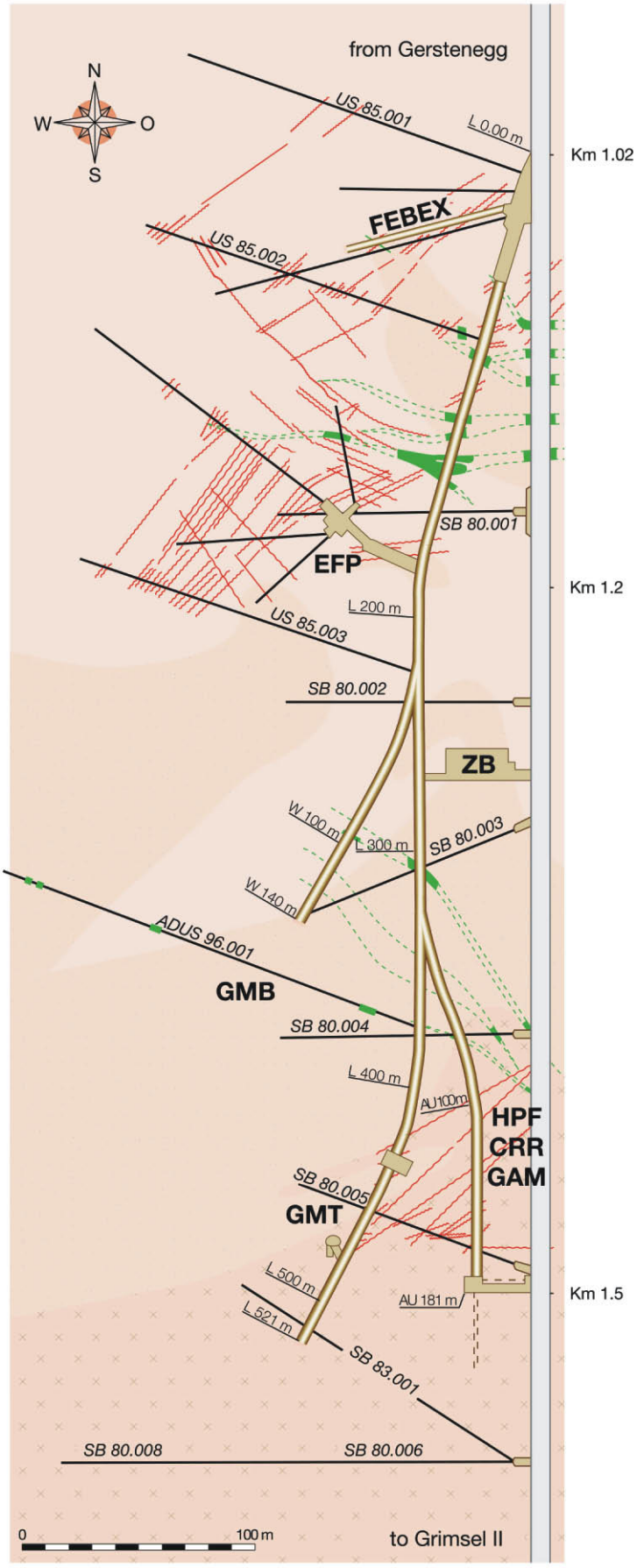

Abstract

A series of laboratory experiments was carried out in support of the *in situ* programme and of the modelling studies of the 'Colloid and Radionuclide Retardation Project' (CRR) at Nagra's Grimsel Test Site (GTS). The aim of those experiments was to study the geochemical interaction of radionuclides in the system Grimsel groundwater – granodiorite / fracture filling material – bentonite and to provide the necessary data for the final planning of the *in situ* migration experiments. The laboratory studies showed that:

- the chemistry of the Grimsel groundwater favours the stabilization of aquatic colloids, specifically of colloidal smectite particles derived from bentonite barrier material. A concentration of 20 mg L^{-1} was shown to provide enough sorption sites to bind all the radionuclides which would be injected at the CRR field experiment
- colloids can considerably influence the transportation of the actinides U, Pu and Am and the fission product Cs (distribution of radionuclides between the aqueous and solid phases in presence and absence of colloids). For ^{75}Se(IV), ^{99}Tc(VII) and Np(V) the influence of colloids appears to be of less importance
- the sorption reactions of Cs, U, Pu and Am are characterized by slow kinetics – sorption (or other uptake) reaction onto granodiorite and fracture filling does not appear to reach equilibrium on a timescale of weeks
- the extent of uptake of Cs, U and, in particular Pu and Am onto fracture filling or granodiorite decreases in the presence of smectite colloids
- there are clear indications of, at least, partial reversibility for Pu and Am

Distribution coefficients (Rd) were determined for the main elements considered in the *in situ* experiment for the three main solids, namely, bentonite colloids, granodiorite and fracture filling material. Sorption isotherms have been determined for U, Sr and Cs, in order to illustrate the concentration dependency of the sorption of these elements. The experimental observations made in this work with regard to colloid formation and sorption kinetics of Pu and Am give an indication of the complexity of uptake processes in this multi-phase system. Because the residence times of the radionuclides and colloids in the CRR experimental site are many orders of magnitude shorter than expected in a repository, additional processes, such as sorption kinetics, which may be of little relevance to an actual repository, needed to be considered for the design and interpretation of the *in situ* experiment.

Zusammenfassung

Zur Unterstützung des *in situ* Versuchsprogramms und der Modellierungsstudien für das Projekt 'Kolloid- und Radionuklid-Retardierung' (CRR) im Felslabor Grimsel (FLG) der Nagra wurde eine Reihe von Laborexperimenten durchgeführt. Das Ziel dieser Experimente waren die Untersuchung der geochemischen Wechselwirkung von Radionukliden im System Grimsel Grundwasser – Granodiorit / Kluftfüllungsmaterial – Bentonit sowie die Bereitstellung der nötigen Daten für die Abschlussplanung der *in situ* Migrationsexperimente. Die Laborexperimente zeigten, dass:

- der Chemismus des Grimselgrundwassers die Stabilität der Kolloide im Wasser begünstigt, insbesondere der kolloidalen Smektitpartikel aus dem Bentonit des Barierrenmaterials und dass bei einer Konzentration von 20 mg/l genügend Sorptionsplätze vorhanden sind, um alle Radionuklide, die während des CRR-Feldversuchs injiziert werden, zu binden
- Kolloide den Transport der Aktinide U, Pu und Am und des Spaltprodukts Cs signifikant beeinflussen (Verteilung der Radionuklide zwischen wässriger und fester Phasen in An– oder Abwesenheit von Kolloiden) und dass für ^{75}Se(IV), ^{99}Tc(VII) und Np(V) der Einfluss der Kolloide weniger bedeutend zu sein scheint
- die Sorptionsreaktionen von Cs, U, Pu und Am durch eine langsame Reaktionskinetik charakterisiert werden – Sorption (oder eine andere Form der Aufnahme) an Granodiorit und Kluftfüllungsmaterial scheint dabei kein Gleichgewicht in einem Zeitraum von Wochen zu erreichen
- die Anwesenheit von Smektitkolloiden den Umfang der Aufnahme von Cs, U und, insbesondere Pu und Am am Kluftfüllungsmaterial oder Granodiorit vermindert
- es klare Hinweise einer wenigstens teilweisen Reversibilität von Pu und Am gibt

Für die drei wichtigsten beim *in situ* Experiment in Betracht gezogenen Feststoffe – Bentonit-Kolloide, Granodiorit und Kluftfüllungsmaterial – wurden Verteilungskoeffizienten (Rd) bestimmt. Um die Konzentrationsabhängigkeit des Sorptionsverhaltens von U, Sr und Cs zu veranschaulichen, wurden Sorptionsisothermen für diese Elemente ermittelt. Die Beobachtungen in den Experimenten im Rahmen dieser Arbeit in Bezug auf Kolloidbildung und Sorptionskinetik von Pu und Am liefern Hinweise auf die Komplexität der Aufnahmeprozesse in diesem Mehrphasensystem. Da die Verweildauer der Radionuklide und Kolloide in der CRR-Testlokalität um ein Vielfaches kürzer ist als in einem Lager erwartet wird, werden für das Design und die Interpretation des *in situ* Experiments zusätzliche Prozesse, wie zum Beispiel Sorptionskinetik benötigt, welche jedoch in einem tatsächlichen Lager möglicherweise eine geringe Bedeutung aufweisen.

Résumé

Plusieurs expériences de laboratoire ont été effectuées en complément du programme d'essais *in situ* et des études de modélisation réalisés dans le cadre du projet 'Retard des colloïdes et des radionucléides' (CRR) au Laboratoire souterrain du Grimsel (LSG) de la Nagra. L'objectif de ces expériences était d'étudier l'interaction géochimique des radionucléides dans le système eaux souterraines du Grimsel – granodiorite / remplissage des failles – bentonite et de fournir les données nécessaires à la planification des essais de migration *in situ*. Les études de laboratoire ont montré que:

- la composition chimique des eaux souterraines du Grimsel est favorable à la stabilisation des colloïdes aquatiques, notamment des particules colloïdales de smectite provenant de la bentonite des barrières ouvragées. Une concentration de 20 mg L^{-1} s'est avérée suffisante pour fournir des sites d'adsorption aptes à retenir l'ensemble des radionucléides injectés dans le cadre de l'essai CRR *in situ*
- les colloïdes peuvent influencer de manière significative la migration des actinides U, Pu et Am et celle du produit de fission Cs (répartition des radionucléides entre les phases aqueuses et solides en l'absence et en présence de colloïdes). Les colloïdes semblent avoir une importance moindre dans le cas de ^{75}Se(IV), ^{99}Tc(VII) et Np(V)
- les cinétiques d'adsorption de Cs, U, Pu et Am sont lentes – après plusieurs semaines on n'a pas constaté d'équilibre d'adsorption (ou d'autre phénomène de rétention) pour la granodiorite et le remplissage des failles
- la rétention de Cs, U et en particulier de Pu et Am par le remplissage des failles ou la granodiorite décroit en présence de colloïdes de smectite
- il existe des indices montrant une réversibilité, au moins partielle, du phénomène pour Pu et Am

Pour les trois solides principaux, c'est-à-dire les colloïdes de la bentonite, la granodiorite et le remplissage des failles, on a déterminé les coefficients de répartition (Rd) des éléments principaux pris en compte dans l'essai *in situ*. On a également déterminé les isothermes d'adsorption pour U, Sr et Cs afin de montrer dans quelle mesure l'adsorption de ces éléments dépendait de la concentration utilisée. Les observations effectuées concernant la formation des colloïdes et les cinétiques d'adsorption de Pu et Am tendent à montrer que les processus de rétention dans un système multi-phases sont complexes. Du fait que, dans le cadre de l'essai CRR, les temps de résidence des radionucléides et des colloïdes étaient bien plus brefs que dans un site de stockage géologique, il a été nécessaire, pour la conception et l'interprétation de l'essai *in situ*, de prendre en compte des processus supplémentaires telles que les cinétiques d'adsorption, dont le rôle est probablement négligeable dans le contexte d'un véritable site de stockage.

Table of Contents

List of Tables

List of Figures

1 Introduction

The Colloid and Radionuclide Retardation Project (CRR) comprised a series of field tracer tests in a water-conducting feature (the Migration or MI shear zone) at Nagra's Grimsel Test Site (GTS) in southern Switzerland, supported by an intensive programme of laboratory studies and modelling at various institutions around the world. This report focuses on the laboratory studies carried out in support of the *in situ* programme and of the modelling studies, with only a short introduction to the experiment as a whole in the next section.

1.1 Background and aims of the CRR project

Colloids (suspended particles in the size range 1 nm to 1 μm) are natural and ubiquitous in groundwater, and may also be generated by physical and chemical processes resulting from the presence of a deep geological repository for radioactive waste. In most repository designs for vitrified high-level waste (HLW) and spent fuel (SF), the waste is packaged in canisters that are separated from the host rock by a layer of bentonite clay or bentonite/sand. Repository designs for other waste types also sometimes involve the use of bentonite. Although the canisters are designed to provide long-term containment of the waste and its associated radionuclides, complete containment cannot be guaranteed indefinitely, and some radionuclides may eventually be released. Subsequent transport through the bentonite is expected to be slow. This is due to its fine pore structure, which filters any radionuclides associated with colloids, its low permeability, and the operation of geochemical retention processes, collectively termed retardation.

Although bentonite is expected to act as a colloid filter, the outer surface of the bentonite may itself act as a source of colloids due, for example, to erosion by flowing water in host rock fractures. For these colloids to have any effect on radionuclide transport in the host rock, the radionuclides in question must be able (i), to migrate to the bentonite/host rock interface before they decay, and (ii) subsequently sorb to the bentonite colloids that are generated there (the colloids themselves must also fulfil a number of criteria, as discussed in Section 1.2). If the bentonite layer operates as expected, transport of any sorbing radionuclides will be slow and these conditions are unlikely to be met for most safety-relevant radionuclides. There are, however, conceivable scenarios that would allow more rapid transport of some sorbing radionuclides through the bentonite layer, including, for example, the creation of temporary flow paths through the layer by repository-induced gas (see Fig. 1.1). The impact of natural groundwater colloids on transport is also a concern in the case of fractured hard rocks.

Due largely to deficiencies in process understanding and a lack of relevant *in situ* data on colloid transport and colloid-mediated radionuclide transport in the geosphere, those safety assessment studies that consider colloids treat their impact on radionuclide transport in a highly simplified manner. This led HSK (the Swiss Federal Nuclear Safety Inspectorate) to note in 1998 that "...the generation of colloids at the bentonite surface cannot be excluded" and that possible colloid associated transport of radionuclide remains an important open question (RETROCK 2005, USDOE 2007).

CRR was started in 1998 in order to address these deficiencies. The overall aim of the project is to improve understanding of radionuclide transport in fractured geological media and, in particular, the impact of the presence of colloids on the transport of selected actinides and fission products. Improved understanding of the impact of colloids on transport should provide a firmer basis for the treatment of geosphere transport in safety assessments for such repositories. CRR is concerned primarily with the impact of bentonite colloids (released to a

host rock fracture at the bentonite/host rock interface) on radionuclide transport. The findings of CRR, however, have implications for the understanding of colloid-facilitated transport in general, including the impact of natural groundwater colloids.

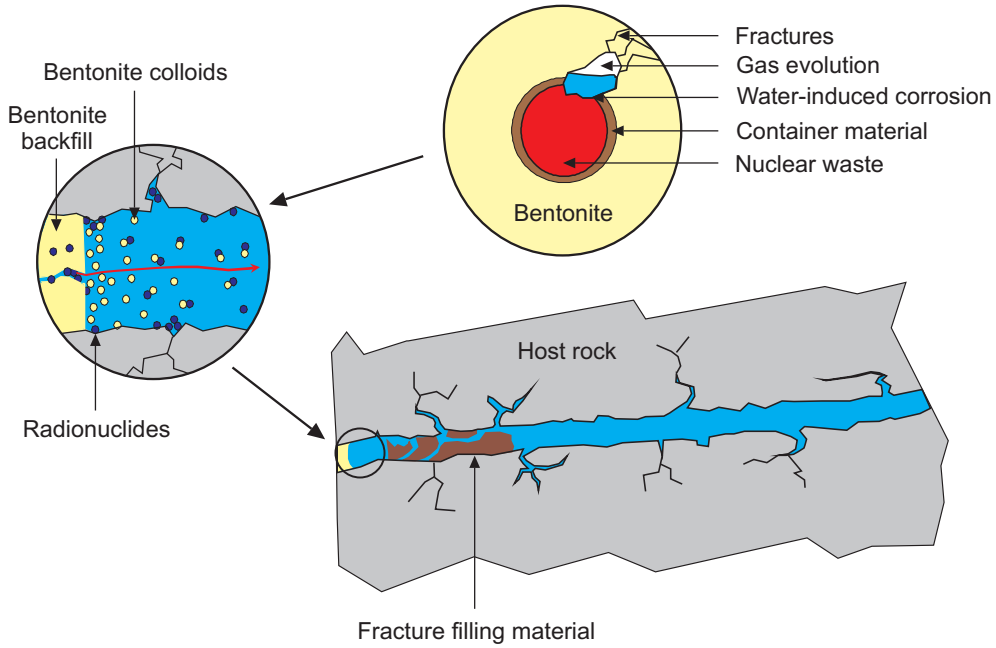

Fig. 1.1: Possible scenario for radionuclide release and bentonite colloid formation.

1.2 Key safety-relevant issues related to colloids

Although there has been little or no unambiguous evidence from field observations of natural and artificially perturbed systems for colloid facilitated transport of radionuclides over long distances under relevant conditions (Hadermann 2001), there remains concern that colloids may have an impact on the transport of radionuclides released from a repository. This remains, in part, due to observations such as those at the Nevada Test Site, in which Pu, which is generally fairly immobile in groundwater systems, was found to migrate over a distance of 1.3 km in only 30 years (Kersting et al. 1999)[1]. *In situ* experiments such as CRR are attempting to deal with this concern.

CRR addresses the transport of radionuclide-bearing colloids in a fractured hard rock. In general, there exist good arguments for assuming efficient filtration of any colloids in unfractured sedimentary clay rocks with fine pore structures (e.g. Baeyens et al. 1985) (Kim et al. 1994; Ryan & Elimelech 1996; Vilks et al. 1997; McCarthy et al. 1998). It should be noted, however, that even in the Boom Clay, which is being studied in Belgium as a potential repository host rock, field experiments have demonstrated the diffusion-dominated transport of ^{14}C-labelled natural organic matter (NOM) colloids over distances in the order of 0.5 m (Dierckx et al. 2000). However it is clear that colloid transport has a higher relevance in fractured rock, where open pore space does not delimit colloid access and migration.

[1] Conditions in this case are probably not so representative of repository systems, most obviously because of the transient flow (due to heavy pumping during sampling) and fracturing when the radioactive source material was explosively emplaced.

Several recent safety assessments have considered the possibility that radionuclides released from a repository become sorbed to colloids or incorporated within them, and subsequently transported by advection/dispersion in flowing groundwater in fractured hard rocks. Colloids may not be subject to some of the processes that retard the transport of radionuclides in solution. Indeed, they may move faster than the average groundwater flow velocity, because both their physical size and electrostatic effects can keep them away from solid surfaces where friction slows the flow of groundwater. This phenomenon is exploited in hydrodynamic chromatography, as discussed, for example, in Prieve & Hoysan (1978) and Dodds (1982). There are, however, retardation and immobilisation processes that could affect radionuclides associated with colloids. In fractured media, they could conceivably diffuse into stagnant water in the rock matrix. Their diffusion coefficient would be lower than un-complexed ions and the extent to which they penetrated into the matrix (if at all) would depend on the sizes of matrix pores with respect to the size of the colloids, as well as charge effects. The investigations of James & Chrysikopoulos (1999), for example, which considered the influence of matrix diffusion on the breakthrough of polydispersed colloids in rough fractures, showed that larger particles are the least retarded and smaller particles are more slowly transported. Colloids may, in some circumstances, become unstable through aggregation or dissolution. They may also come into contact with fixed solid surfaces, such as fracture walls and the pore surfaces of fracture infill material, to which they can become attached (although the negative charge often found on the surfaces of both colloids and solid phase surfaces acts against this process), or become trapped at constrictions in fractures or in the pore space of the rock matrix because they are too large to pass through. These processes are termed filtration: mechanical filtration, where large colloids become trapped in small pores or narrow channels, and chemical filtration, where colloids become chemically attached to fracture or pore surfaces.

Colloids may have either beneficial or detrimental effects on repository performance. A beneficial effect would be if radionuclides became irreversibly bound to colloids that are later immobilised, e.g. by filtration. A detrimental effect would be if radionuclide-bearing colloids were mobile, and excluded from matrix pores. In general, it can be stated that colloid facilitated transport may be important and detrimental to performance if the following conditions are met (e.g. Gardiner et al. 2001).

1. There is a large population of colloids occurring naturally in groundwater or arising from the presence of the repository.
2. Fracture apertures and other pore spaces conducting flowing groundwater are sufficiently large to allow colloids to pass without significant physical or chemical filtration.
3. The groundwater chemistry is favourable to colloid stability.
4. Radionuclide sorption on colloids is favoured by electrostatic attraction and groundwater chemistry, and desorption processes are irreversible, or at least slow relative to transport times through the geosphere.

This combination of conditions is illustrated schematically in Fig. 1.2. As pointed out in Gardiner et al. (2001), no chemical process, such as the sorption of radionuclides by colloids, is strictly speaking irreversible. The key issue here is whether the process is reversible over the timescales of interest to repository safety assessments. This question can also not be answered by the CRR experiments which are limited in duration and contact times of tracers with fracture surfaces. Colloid breakthrough in the *in situ* experiments took place within less than 2 hours. But combined experiments in the laboratory and in the field can at least give indications whether kinetics in radionuclide interaction with colloids may play a role.

It should also be noted that the presence of gas bubbles in the geosphere has been suggested as potentially important with respect to colloid facilitated radionuclide transport, since radionuclide-bearing colloids may accumulate at gas-water interfaces (see for example Wan & Wilson 1994 and Neretnieks & Ernstsson 1997), but this possibility is not addressed in CRR.

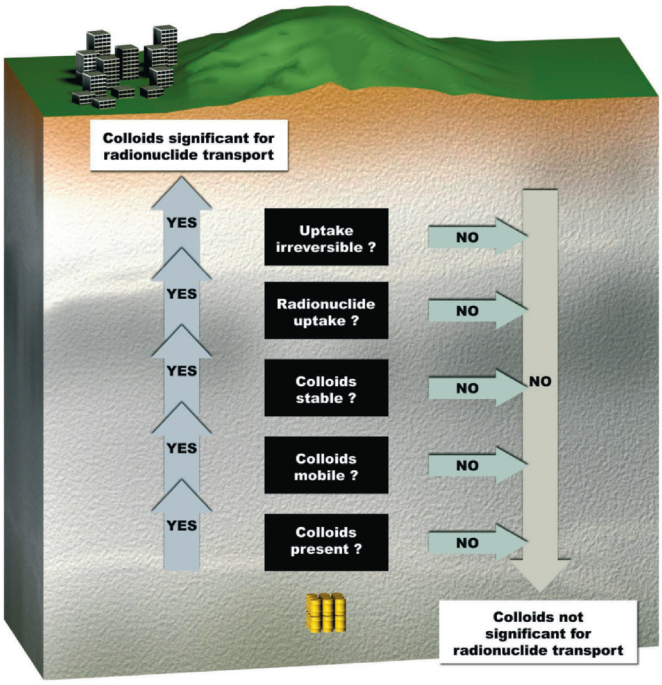

Fig. 1.2: The "colloid ladder", which indicates when colloid facilitated radionuclide transport is likely to become relevant to the long-term safety of a deep geological repository (from Miller et al. 2000).

1.3 Overview of the CRR project

1.3.1 General concept

The central component of the CRR project was a series of *in situ* tracer tests in the experimental shear zone at the GTS. The injection into the shear zone of a cocktail of tracers including, in some tests, bentonite colloids was intended to shed light on the impact of colloids released to a host rock fracture at the bentonite/host rock interface of a radioactive waste repository on radionuclide transport in fracture or shear zone (Fig. 1.3).

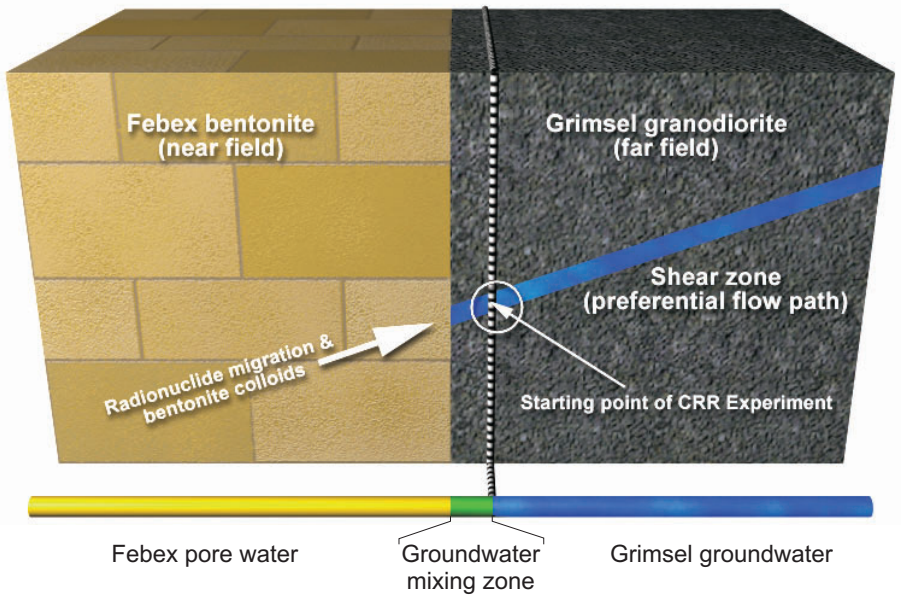

Fig. 1.3: The situation addressed by CRR - the impact of bentonite colloids released to a host rock (geosphere) fracture at the bentonite/host rock on radionuclide transport.

There are of course some key differences between the experimental situation and the bentonite/host rock interface of an actual repository, including the far higher water velocities that were used in the experiments in order to achieve manageable experimental timescales. These differences are important to keep in mind when evaluating the implications of the results for repository safety assessment.

1.3.2 CRR tasks and time schedule

In addition to the CRR *in situ* tracer tests themselves, an intensive programme of supporting field and laboratory studies and modelling work was also carried out in order to plan, implement and interpret the results of the tests.

The work was divided into two main phases:

- Phase I, in which the feasibility of conducting *in situ* tracer tests was examined (and the tests themselves planned with the aid of site characterisation), preliminary calculations, a preparatory laboratory programme and predictive transport modelling, and
- Phase II, which consisted of the tests themselves, various supporting field and laboratory studies, further transport modelling and final reporting.

The time schedules for these various tasks are summarised in Tab. 1.1.

Tab. 1.1: Major tasks and time schedule of the CRR project.

Phase	Task	1998		1999		2000		2001		2002		2003	
Phase 1 Feasibility	Site characterisation												
	Preliminary calculations												
	Preparatory laboratory programme												
	Predictive transport modelling												
Phase 2 In situ experiment	Preparatory colloid and homologue tests												
	Field experiment												
	Natural colloid background study												
	Supporting laboratory programme												
	Transport modelling												
	Final reporting												

A key consideration in designing the *in situ* tests, as well as the supporting laboratory experiments, was to minimise experimental artefacts as far as possible. Moreover, in such a highly complex experiment, where actinides and bentonite colloids are used in combination with the natural Grimsel groundwater, the chemical and hydraulic experimental conditions had to be optimised. The final layout for the tests nevertheless inevitably involved a degree of compromise that has to be taken into account in the final discussion and interpretation of the results.

1.3.3 The *in situ* tracer tests

The *in situ* tracer tests are reported in detail in Möri (2004). The tests were conducted in four different artificial asymmetric dipole flow fields in the shear zone, established by pumping water into one borehole (the injection borehole) and withdrawing water at a higher rate at a second borehole (the extraction borehole); for details see Fierz et al. (2001), Möri (2004) and this report.

In preparation for CRR, three new 86 mm boreholes (BOCR 99.001, 99.002 and 00.003) were drilled from the AU gallery of the GTS almost perpendicular to the shear zone and equipped with triple packer systems. Other boreholes (BOMI 86.004, 86.005, 87.007, 87.008, 87.010 and 87.011) were already available from the earlier GTS Migration Experiment (MI) conducted in the same shear zone (see Frick et al. 1992, Smith et al. 2001a,b for details). Figure 1.5 provides an overview of the boreholes and the different flow fields that were established between the packed-off intervals (black arrows). In each dipole, the direction of water flow was towards the gallery, thus coinciding with the unperturbed groundwater flow direction.

In the tracer tests, once the flow field had been established, individual tracers or tracer cocktails were injected at the injection borehole, and the resulting breakthrough curves measured at the withdrawal borehole. An overview of the tracer tests is given in Tab. 1.2.

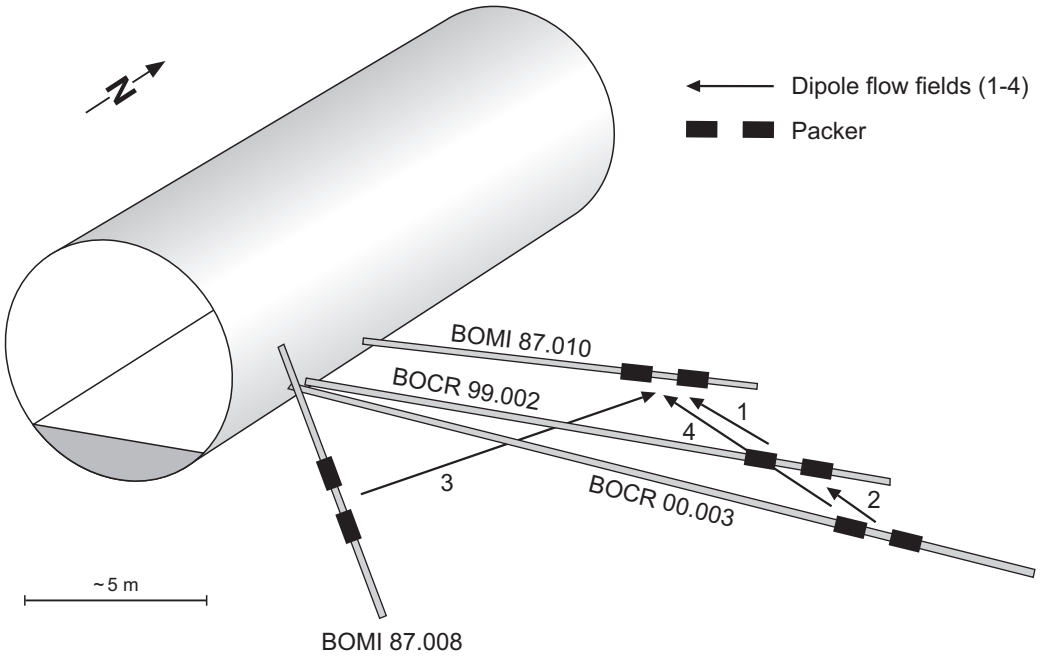

Fig. 1.4: 3D view of the CRR test site, the view direction is perpendicular to the experimental shear zone.

Tests using the conservative (i.e. non-interacting) tracer uranine were performed in order to calibrate hydraulic models of flow within the dipoles and to optimise the flow conditions so that a recovery close to 100 % was achieved. Iodine was then added to the uranine tracer cocktails in order to confirm that it was still suitable to use as a conservative tracer in later, more complex tests (see also Frick et al. 1992). Preparatory tests were also carried out with bentonite colloids and with the trivalent Tb and the tetravalent Hf and Th which provide homologues for the behaviour of a range of actinides.

Two main tracer tests were carried out in dipole D-1 with a suite of different radionuclides. These were:

- Run #31, in which ^{85}Sr, ^{131}I, ^{232}Th, ^{238}U, ^{237}Np, ^{238}Pu, ^{242}Pu and ^{243}Am were injected in the absence of bentonite colloids and
- Run #32, in which ^{85}Sr, ^{99}Tc, ^{131}I, ^{137}Cs, ^{232}Th, ^{233}U, ^{237}Np, ^{238}Pu, ^{244}Pu, and ^{241}Am were injected in the presence of 20 mg L^{-1} of bentonite colloids.

Tab. 1.2: List of dipoles with corresponding boreholes, experimental runs and tracers used.

Dipole	Length [m]	Injection/ extraction borehole	Flow rates (in/out) [ml min^{-1}]	Number of run where this dipole was tested and type of tracer composition	
D-1	2.23	CRR 99.002 /BOMI 87.010	08/120	run #1,	uranine
			06/160	run #2,	uranine
			08/213	run #3,	uranine
			10/150	run #13,	uranine
			10/150	run #14,	homologues[1]
			10/150	run #21,	uranine, ^{85}Sr & ^{82}Br
			10/150	run #28 to 30,	uranine, ^{131}I
			10/150	run #31,	RN cocktail
			10/150	run #32,	RN cocktail & colloids
			10/150	run #33 to 35	uranine, ^{131}I
D-2	1.71	CRR 00.003 /CRR 99.002	10/150	run #4,	uranine
			05/075	run #5,	uranine
			10/150	run #9,	uranine
			10/150	run #10,	homologues
			10/150	run #11,	uranine
D-3	5.25	BOMI 87.008 /BOMI 87.010	10/150	run #6 & 7,	uranine
			10/150	run #6a,	bentonite colloid injection
			10/150	run #7a,	bentonite colloid injection with homologues
			10/150	run #8,	uranine
			10/150	run #15,	homologues
			10/150	run #16,	uranine
D-4	3.94	CRR 00.003 /BOMI 87.010	10/150	run #12,	uranine

[1] The homologues are trivalent ^{159}Tb and tetravalent ^{178}Hf and ^{232}Th

1.3.4 Supporting field and laboratory studies

In addition to the *in situ* experiment, a series of supporting field and laboratory experiments and theoretical studies was carried out, addressing, most notably:

- the hydraulic characteristics of the test shear zone,
- a study of natural background colloids,
- tracer solubilities in Grimsel groundwater, and
- sorption on shear zone materials and on colloids.

Detailed discussion of the laboratory studies is the focus of this report.

1.3.5 Modelling

The aim of the modelling work carried out in support of CRR was to develop understanding of the structures and processes affecting tracer breakthrough by constructing numerical models, and comparing their output with the results of the *in situ* tests. This work is the focus of the report by Smith et al. (2006).

1.3.6 Reporting

The raw data are reported in a series of unpublished Nagra internal reports and are referenced in the corresponding sections below. Publications which have been produced as part of the CRR project are:

Biggin C., Möri A., Alexander W. R., Ota K., Frieg B., Kickmaier W. & McKinley I. G. (2002). *In situ* radionuclide retardation in groundwater conducting systems: overview of the research carried out at Nagra's Grimsel Test site, central Switzerland pp 207-228 *in* Environmental Radiochemical Analysis II (*ed* P. Warwick) RSC, London, UK.

Geckeis H., Schäfer T., Hauser W., Rabung Th., Missana T., Degueldre C., Möri A., Eikenberg J., Fierz Th. & Alexander W. R (2004). Results of the Colloid and Radionuclide Retention experiment (CRR) at the Grimsel Test Site (GTS), Switzerland - Impact of Reaction Kinetics and Speciation on Radionuclide Migration -, Radiochim. Acta 92, 765–774.

Guimerà J., Duro L. & Bruno J. (2000). Radionuclide field tests in a single fracture. Proc. Int. Conf. on tracers and modelling in hydrogeology; Liège, Belgium (Dassargues, Ed); IAHS Pub. 262, 309-314.

Hauser W., Geckeis H., Kim J. I. & Fierz Th. (2002). A mobile laser-induced breakdown detection system and its application for the *in situ*-monitoring of colloid migration. Coll. Surf. A 203, 37-45.

Kosakowski G. (2004). Anomalous transport of colloids and solutes in a shear zone, J. Contam. Hydrol. 72, 23– 46.

Kosakowski G. & Smith P. A. (2004). Modelling the transport of solutes and colloids in a water-conducting shear zone in the Grimsel Test Site. Nagra Technical Report NTB 04-01. Nagra, Wettingen, Switzerland.

Missana T. & Adell A. (2000). On the Applicability of DLVO Theory to the Prediction of Clay Colloids Stability. J. Coll. Interface Sci. 230, 150-156.

Missana T., Alonso U. & Turrero M. J. (2003). Generation and Stability of Bentonite Colloids at the Bentonite/Granite Interface of a Deep Geological Radioactive Waste Repository. J. Contam. Hydrol. 61 (1-4), 17-31.

Missana T., Garcia-Gutierrez M. & Alonso U. (2004) Kinetics and Irreversibility of Caesium and Uranium Sorption onto Bentonite Colloids. Appl. Clay Sci. 26, 137-150.

Möri A., Alexander W. R., Geckeis H., Hauser W., Schäfer Th., Eikenberg J., Fierz Th., Degueldre C. & Missana T. (2002). The Colloid and Radionuclide Retardation experiment (CRR) at the Grimsel Test Site (GTS): influence of bentonite colloids on radionuclide migration in a fractured rock. Coll. Surf. A: 217, 33-47.

Pudewills A. (2003). Modelling of flow and transport phenomena in a granitic fracture, in O. Natau, E. Fecker, E. Pimentel, Geotechnical Measurements and Modelling, Proc. of the international symposium on geotechnical measurements and modeling, 23-24 September, 2003, Karlsruhe, Germany, A. A. Balkema Publishers, Lisse, 155-160.

Pudewills A., Hauser W. & Geckeis H. (2002). Numerical modelling of flow and transport phenomena in fractured crystalline rock. Proc. 2nd Biot Conf. on Poromechanics, (Auriault et al. eds.), Balkema, 527-532.

Schäfer Th., Bauer A., Bundschuh T., Rabung Th., Geckeis H. & Kim J.I. (2000). Colloidal stability of inorganic colloids in natural and synthetic groundwater, Appl. Mineral. in Research, Economy, Technology and Culture, Proc. of the 6th Internat. Congress ICAM 2000, Göttingen, July 13-21, A. A. Balkema, Rotterdam, Vol. 2, 675-678.

Schäfer Th., Geckeis H., Bouby M. & Fanghänel Th. (2004). U, Th, Eu and colloid mobility in a granite fracture under near-natural flow conditions, Radiochim. Acta 92, 731–737.

A set of 3 final project reports summarises the findings of the CRR project:

Möri A. (ed.) (2004). The CRR final project report series I: Description of the Field Phase - Methodologies and Raw Data. Nagra Technical Report NTB 03-01.

Smith P. A., Guimerà J., Kosakowski G., Pudewills A. & Ibaraki M. (eds.) (2006). The CRR final project report series III: Results of the Supporting Modelling Programme. Nagra Technical Report NTB 03-03.

and the present one.

1.4 Overview of the present report

This report presents the results and conclusions of the different laboratory experiments which were carried out to support the CRR project between 1998 and 2003.

Chapter 1 provides an overview to the background and concept of the project.

Chapter 2 characterises the experimental shear zone, the groundwater chemistry and summarises the selection criteria for the different radionuclides used in the frame of the CRR project.

Chapter 3 presents the results of the colloid formation and stability studies and characterises the bentonite colloids used in this experiment.

Chapter 4 contains the results of the sorption and partly also of the desorption studies with the actinides ^{243}Am, ^{244}Pu, ^{237}Np and ^{233}U and the fission products ^{75}Se, ^{137}Cs and ^{99}Tc onto Grimsel granodiorite, fracture filling material, bentonite and bentonite colloids.

Chapter 5 summarises the conclusions from this work in the context of the overall CRR project.

2 Shear zone characterisation, groundwater chemistry and selection of radionuclides

This chapter presents an overview of the geochemical and geological base dataset which was used for the design and for the evaluation of the laboratory experiments. A detailed description of the FEBEX[2] bentonite and of the colloids studied is given in Chapter 3 of this report.

2.1 Shear zone characterisation

The experimental shear zone which was selected for the CRR experiment is located at tunnel point AU 96 and was investigated over many years within the MI (Migration) and EP (Excavation) projects (see Smith et al. 2001a,b and Alexander et al. 2003, respectively).

The experimental shear zone can be characterised as a re-activated mylonite in a weakly foliated granodiorite (the Grimsel granodiorite). Current movement is taken up in a brittle manner, producing a heavily brecciated zone of 1 - 30 cm width. Within the experimental area of the shear zone, water flow is assumed to be concentrated in channels, which are predominantly in the mylonite (porosity 0.1 - 0.4 %), but which may splay out into the neighbouring granodiorite (porosity 0.5 - 2 %[3]). The channels also contain fracture filling material (fault gouge, also called fracture filling material; porosity 10 - 40 %) and direct evidence exists for the diffusion of radionuclides into this material during *in situ* tracer experiments (Möri et al. 2006a). Direct evidence also exists for matrix diffusion into the mylonite and granodiorite associated with the experimental shear zone (Alexander et al. 1990). Currently, the best visualisation (e.g. Fig. 2.1) of the experimental shear zone is in Bossart & Mazurek (1991) and in Möri & Adler (2001). The characteristics of the Grimsel granite/granodiorite and fracture filling materials are largely described in the literature and are summarised in Table 2.1 and 2.2 below.

---

[2] FEBEX: Full scale Engineered Barriers Experiment (for a deep geological repository for high level radioactive waste); ongoing EU financed experiment at the Grimsel Test Site (Huertas et al. 2000).

[3] Data from the Connected Porosity project indicate that these laboratory porosity data probably overestimate *in situ* values by about 50 % (Möri et al. 2003; Ota et al. 2003).

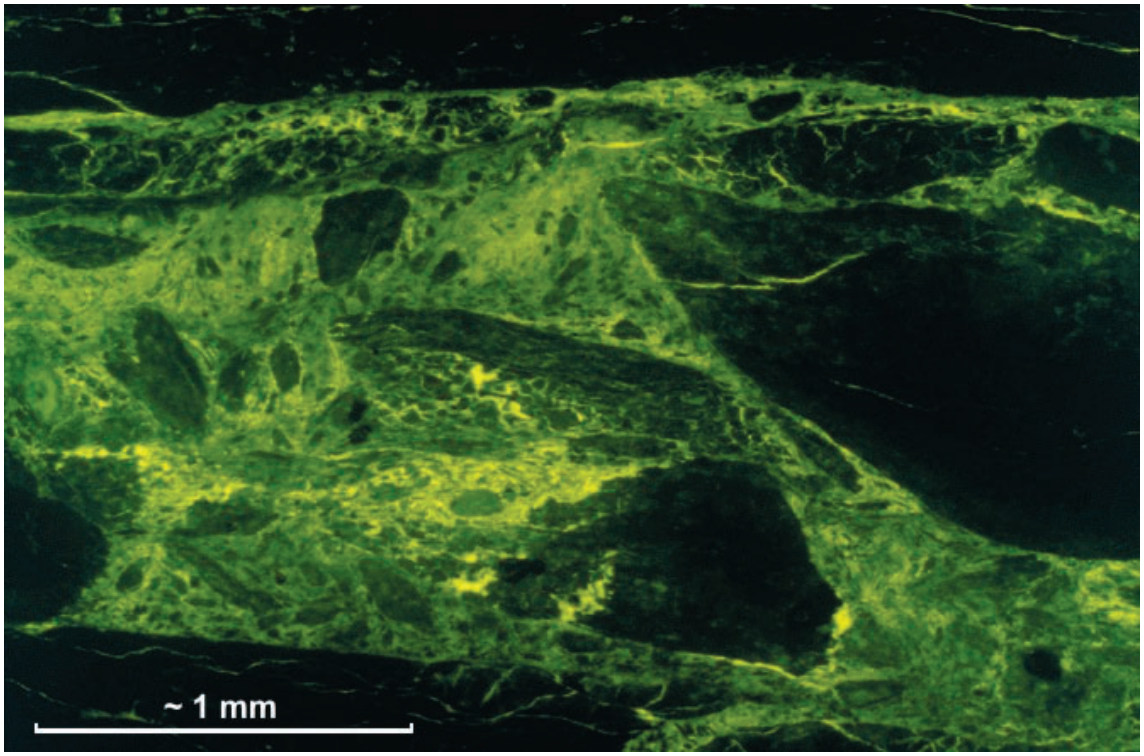

Fig. 2.1: An example of the flow path porosity in the experimental shear zone in the GTS (photomicrograph taken under UV-light and is approximately 3 mm wide).

The predominantly black areas at the top and bottom of the image represent the granodioritic wallrock with the yellow areas representing open porosity in the fracture. Particles of ground up wall rock (black, porosity < 1 %) can be seen isolated in the fine grained fracture infill (yellow to grey, porosity of 30 – 40 %). From Alexander & Kickmaier (2000).

Tab. 2.1: Mean composition of granitic and fault material from the GTS (wt%) and trace element concentration (ppm). After Meyer et al. (1989).

Rock type		**Fault gouge** (AU 96)	**Mylonite** AU 126	**Mylonite** AU 126	**Grimsel granodiorite**
Number of analyses		1 [1,2]	5 [1]	5 [1]	5
SiO_2	(wt%)	67.0	72.7	69.1	67.5
Al_2O_3	"	15.6	13.5	14.4	15.6
Na_2O	"	6.3	3.3	5.3	4.5
K_2O	"	3.8	4.1	4.8	3.9
CaO	"	1.6	0.8	0.6	2.1
FeO	"	1.5	1.1	1.5	3.3
MgO	"	1.3	1.4	1.6	1.1
Fe_2O_3	"	1.1	1.0	0.9	n.d.
H_2O	"	0.7	1.0	1.2	0.7
TiO_2	"	0.5	0.4	0.4	0.5
CO_2	"	0.4	0.3	0.2	n.d.
P_2O_5	"	0.2	0.1	0.1	0.2
MnO	"	0.05	0.04	0.05	0.07
Ba	(ppm)	579	698	646	962
Zr	"	292	235	217	245
Rb	"	164	167	189	104
Sr	"	141	126	90	293
Ce	"	98	<15	60	58
La	"	71	31	52	37
Y	"	50	36	30	36
Nd	"	40	<25	23	7
Zn	"	38	33	37	56
Th	"	13	20	<5	15
Nb	"	9	13	9	16
U	"	<10	<10	<10	<10

n.d. = no data

[1] Analyses recalculated such that Σ of major elements = 100 %.

[2] Only approximate values due to low number of analyses and heterogeneity of the material.

Tab. 2.2: Average mineralogical compositions of lithologies in, or close to, the experimental shear zone (AU 96); data (in vol%). After Meyer et al. 1989, each value represents 2-5 analyses.

Mineral	**Grimsel granodiorite**	**Mylonite**	**Fault gouge**
Quartz	23	17	15
Plagioclase / Albite	23	32	28
K-feldspar	20	11	7
Biotite	14	30	41
Chlorite	3	<1	<1
Muscovite	8	5	4
Epidote	5	3	3
Titanite	2	2	2
Rutile	trace	trace	trace
Zircon	trace	trace	trace
Apatite	trace	0.25	trace
Ilmenite	1	trace	trace
Orthite	1	< 1	< 1
Clay minerals	< 1	< 1	< 1

The mylonite has a lower FeO content (1.1 - 1.5 wt%) than that of the granite (3.3 wt%; see Tab.2.1), indicating leaching of Fe(II) from the iron-bearing minerals (predominantly biotite).

The dominant size fraction of the fracture filling material in the experimental shear zone was determined to be between 350 and 500 µm (Alexander et al. 2003). Specific area measurements are reported by Bradbury (1989) for four types of Grimsel rock material:

Grimsel granodiorite: 0.14 $m^2 g^{-1}$

Fault gouge*: 8.0 $m^2 g^{-1}$

Bulk fault gouge**: 0.5 $m^2 g^{-1}$

Sieved bulk fault gouge ***: 3.1 $m^2 g^{-1}$

* without any mylonitic material from the fracture walls
** incl. mylonitic pieces from the fracture walls
*** incl. mylonitic pieces from the fracture walls but sieved through a 250 µm sieve.

Ground fracture filling material (< 300 µm) from the experimental shear zone was analysed by X-ray and SEM-EDX. The results of the analysis showed that its main components are mainly quartz and biotite, with traces of biotite, K-feldspar and plagioclase. As accessory minerals zircon, apatite and epidote were observed.

The solid material used for the batch experiments (Grimsel granodiorite, mylonite and fracture filling material) was removed by hand from an *in situ* impregnated large diameter (380 mm) drill core at the end of November 1999. The drill core originated from the excavation project and was labelled as BOEX 97.001 (Möri et al. 2006b). The sampling interval was between 8.50 and 9.00 m along the drill core (as measured from the tunnel wall, into the matrix), well away from the resin impregnated part of the EP core.

2.2 Groundwater chemistry

The groundwater used in CRR represents one particular type of the groundwater which is present in the Grimsel Test Site. It is characterised mainly by its low salinity and by its pH of 9.6 (see below). The groundwater used for CRR is generally called "Grimsel groundwater". It was agreed by the CRR project team that all of the injection cocktails would be prepared with Grimsel groundwater only. At the beginning of the project, the possibility of injecting the radionuclides in FEBEX pore water was also contemplated, in order to simulate the geochemical processes associated with the mixing of the bentonite pore water with the Grimsel groundwater. However, this plan was abandoned as a number of precipitation/co-precipitation and additional colloid formation reactions are to be expected, adding more complexity to an already difficult experiment. However, the alkaline pH (9.6) and low ionic strength of the Grimsel groundwater will be expected to stabilise colloid populations (see Chapter 3.3), so should represent a scenario where the colloid influence on radionuclide migration will be emphasised.

Careful analysis of Grimsel groundwater samples indicates redox potentials buffered by the SO_4^{2-}/HS^- system – implying microbial catalysis (see Alexander 1991 and Mazurek et al 2001, for details). Measurements on Grimsel groundwater samples stored at FZK gave values of around -200 mV although calculations indicated an Eh of -377 mV for the SO_4^{2-}/HS^- couple, (in agreement with the above cited work).[4] In any case, for such dilute water, care must be taken interpreting any redox measurements; it is possible that solid phases present may dominate redox buffering (Barcelona & Holm 1991). Colorimetric analysis indicates the presence of $\sim 3.7 \cdot 10^{-6}$ mol/L HS^- (measured at FZK) pointing to the lower calculated redox potential being correct. A more precise statement on the groundwater redox state is difficult to derive, due to the low concentrations (Fe(II)/Fe(III)) and the slow reaction rates of potential redox partners (HS^-/ SO_4^{2-}) at electrodes.

Groundwater analyses are shown in Tab. 2.3 (compilation of pre-existing data and new data from the CRR project). The water used in all CRR laboratory experiments was sampled from the experimental shear zone[5]. It was collected at the GTS from borehole BOMI 87.008 in a 50L aluminium barrel provided by FZK. Container walls were coated with PTFE in order to minimise sorption of trace elements. The values indicated in Tab. 2.3 are the minimum and maximum value obtained over several (~ 10) measurements. Eh and pH were measured during the sampling and afterwards in the laboratory with no significant differences. All data measured by FZK and at CIEMAT (see table 2.3) are generally consistent with those from previous sampling campaigns (see Frick et al. 1992, Smith et al. 2001a).

[4] Care must be taken with all values as Alexander (1991) noted that the rock-groundwater Eh system was almost certainly not at equilibrium.

Tab. 2.3: Chemical composition of groundwater from the experimental shear zone.

		[M]*	[M]**	[M]***
Cations	Na^+	$6.9 \cdot 10^{-4}$	$7.0\text{-}7.2 \cdot 10^{-4}$	$7.0 \cdot 10^{-4}$
	K^+	$5.0 \cdot 10^{-6}$	$1.8\text{-}4.6 \cdot 10^{-6}$	$1.0\text{-}3.6 \cdot 10^{-6}$
	Mg^{2+}	$6.2 \cdot 10^{-7}$	$<1.0 \cdot 10^{-5}$	$2.0\text{-}4.1 \cdot 10^{-6}$
	Ca^{2+}	$1.4 \cdot 10^{-4}$	$1.4\text{-}1.6\ 10^{-4}$	$1.4 \cdot 10^{-4}$
	Sr^{2+}	$2.0 \cdot 10^{-6}$	$2.4\text{-}2.6 \cdot 10^{-6}$	$1.9\text{-}2.3 \cdot 10^{-6}$
	Rb^+	$2.5 \cdot 10^{-8}$	not determined	$1.6 \cdot 10^{-8}$
	Cs^+	$5.0 \cdot 10^{-9}$	$4.3 \cdot 10^{-9}$	$3.8\text{-}7.5 \cdot 10^{-9}$
	Li^+	not determined	$1.1 \cdot 10^{-5}$	$1.2 \cdot 10^{-5}$
Anions:	SO_4^{2-}	$6.1 \cdot 10^{-5}$	$2.8\text{-}6.3 \cdot 10^{-5}$	$1.8 \cdot 10^{-4}$
	F^-	$6.1 \cdot 10^{-5}$	$3.4 \cdot 10^{-4}$	$3.2 \cdot 10^{-4}$
	Cl^-	$1.6 \cdot 10^{-4}$	$1.6\text{-}2.2 \cdot 10^{-4}$	$1.4 \cdot 10^{-4}$
	Br^-	$3.8 \cdot 10^{-7}$	not determined	$3.6 \cdot 10^{-7}$
	I^-	$1.0 \cdot 10^{-9}$	$\leq 1.58 \cdot 10^{-7}$	$7.9 \cdot 10^{-10}$
	PO_4^{3-}	not determined	$<1.0 \cdot 10^{-6}$	not determined
Other Species:	Si	$2.5 \cdot 10^{-4}$	$3.4 \cdot 10^{-4}$	$2.0 \cdot 10^{-4}$
	CO_2	$<7.0 \cdot 10^{-7}$	not determined	not determined
	O_2	$<3.0 \cdot 10^{-8}$	not determined	not determined
	N_2	$7\text{-}8 \cdot 10^{-4}$	not determined	not determined
	U	not determined	$<4.2 \cdot 10^{-9}$	$1.3\text{-}6.3 \cdot 10^{-10}$
	Th	not determined	$<2.1 \cdot 10^{-9}$	$<2.2 \cdot 10^{-10}$
	Ti	not determined	$1.5 \cdot 10^{-8}$	$6.3 \cdot 10^{-8}$
	Fe	not determined	$<5.4 \cdot 10^{-7}$	$6.3 \cdot 10^{-7}$
	Al	not determined	$3.0\text{-}4.0\ 10^{-6}$	$0.5\text{-}1.7 \cdot 10^{-6}$
Calculated(3)	HCO_3^-	$2.9 \cdot 10^{-4}$	$4.7 \cdot 10^{-4}$ (measured)	$1.4 \cdot 10^{-4}$ (measured)
	CO_3^- (CO_3^{2-})	$4.2 \cdot 10^{-5}$	$<1.0 \cdot 10^{-4}$	-
	OH^-	$1.3 \cdot 10^{-5}$	not determined	not determined
	$H_3SiO_4^-$	$4.2 \cdot 10^{-5}$	not determined	not determined
	H_4SiO_4	$2.1 \cdot 10^{-4}$	not determined	not determined
pH		9.6±0.2	9.5±0.2	9.6
Ionic strength [M]		0.0012	not determined	
Temperature [°C]		12±1	not determined	
Electrical Conductivity [µS cm^{-1}]		103±5	93-103	12
Eh [mV]		<300	-200±50	106

* Data are compiled from Bajo et al. (1989), Aksoyoglu et al. (1990) and Eikenberg et al. (1991) and represent the top of the range of data reported in Tab. 3.3 of Frick et al. (1992).

** After Missana et. al. (2001)

*** Grimsel Colloid Exercise (NTB 90-01) PSI data from Degueldre et al. 1996a

2.3 Radionuclide solubility

The calculations were carried out using the measured laboratory Eh for the Grimsel groundwater of -200 mV[6]. The most stable oxidation states of Tc, Np, Pu and U were all expected to be IV. However, laboratory experiments revealed that Np, U, Tc and Se remained as oxidised species even in the reduced Grimsel groundwater at values around –200 mV. The thermodynamic calculations showed that Eh, pH data of the groundwater are very close to the stability field of oxidised species. Based on the results of laboratory tests, the kinetics of the appropriate redox reactions and practicability constraints on the *in situ* use of these elements, the final injection cocktail was then planned to contain all relevant oxidation states between I an VI (Tab. 2.4). Potential complications due to *in situ* reduction cannot be excluded and have to be taken into account in the interpretation of the test results. They are nevertheless not very likely due to the relatively short residence time of the radionuclide tracers in the shear zone during the *in situ* experiments and the obviously slow redox kinetics.

Related to the discussion on the likely oxidation state of the radionuclides was also the probability of sorption (in particular of the tri- and tetravalent actinides) on the equipment and the borehole walls. Although additional attempts were made to make the equipment sorption proof, this remained still a problem (PEEK (Poly Ether Ether Ketone) coated equipment was identified as the most promising technique, but even here some tracer loss was observed due to sorption of Am and Pu). However, sorption effects were found to be relevant only for run #31 of the final *in situ* experiment (without bentonite colloids), because of the preferred sorption of the nuclides on the added bentonite colloids in run #32. In addition to the problems with sorption on equipment and borehole walls, it was also noted that tri- and tetravalent actinides tend to be present in Grimsel groundwater as colloidal gel or bound on natural colloids which are always present in a solution (see below).

Tab. 2.4 summarises the calculated solubilities and the selected input concentrations (M_0) for the radionuclide tracer cocktails which were injected in the *in situ* experiment. The concentrations of ^{99}Tc, ^{232}Th, and $^{238/242/244}$Pu in the tracer cocktail are limited by their assumed solubility in the Grimsel groundwater. In the case of ^{85}Sr, ^{137}Cs, $^{241/243}$Am and, the concentration utilised is not solubility controlled, rather it is defined by the maximum permitted activity of these radionuclides at the site[7]. As the oxidation state for uranium and neptunium establishing in the groundwater was unclear, solubilities are given for the solids of both actinide oxidation states.

---

[6] Despite the data and calculations noted above, it was decided to use -200 mV as this would allow laboratory-based verification of the calculated solubilites (it having proved impossible to bring the GTS groundwater below -200 mV in the laboratory in the absence of the host rock).

[7] Higher activities (and therefore concentrations) are permissable, but only by re-licensing the site as an IAEA Level B laboratory once again (as was the case during the EP experiment: see Alexander et al. 1996 for details).

Tab. 2.4: Solubility values, solid phases and oxidation states of the relevant radionuclides for the injected tracer cocktail (Duro et al. 2000).

Nuclide	**Calculations**			***In situ* experiment**		
	Solid phase	**Oxidation state**	**Calculated solubility** [M or mol L^{-1}]	**Assumed oxidation state**	**Run #31: input concentration** [M or mol L^{-1}]	**Run #32: input concentration** [M or mol L^{-1}]
Cs	-	I	-	I	-	^{137}Cs: $1.4 \cdot 10^{-8}$
Sr	-	II	-	II	^{85}Sr: $1.3 \cdot 10^{-11}$	^{85}Sr: $1.1 \cdot 10^{-11}$
Tc	$TcO_2 \times H_2O$ (am)	IV	$1 \cdot 10^{-8}$	IV	---	^{99}Tc: $1.0 \cdot 10^{-8}$
Am	($AmOHCO_3$(am))	III	$1 \cdot 10^{-7}$	III	^{243}Am: $5.9 \cdot 10^{-9}$	^{241}Am: $6.6 \cdot 10^{-10}$
Th	($Th(OH)_4$(am))	IV	$1 \cdot 10^{-8}$	IV	^{232}Th: $1.1 \cdot 10^{-8}$	^{232}Th: $1.1 \cdot 10^{-8}$
U	$U(OH)_4$(am) $UO_2(OH)_2$	IV VI	$1 \cdot 10^{-8}$ $1 \cdot 10^{-4}$	VI	^{238}U: $9.5 \cdot 10^{-7}$	^{233}U: $8.7 \cdot 10^{-7}$
Np	($Np(OH)_4$(am)) $Np(V)O_2(OH)$	IV V	$1 \cdot 10^{-8}$ $1 \cdot 10^{-4}$	V	^{237}Np: $9.4 \cdot 10^{-7}$	^{237}Np: $1.1 \cdot 10^{-6}$
Pu	($Pu(OH)_4$(am))	IV	$1 \cdot 10^{-10}$	IV	^{238}Pu: $4.4 \cdot 10^{-11}$ ^{242}Pu: $9.9 \cdot 10^{-9}$	^{238}Pu: $4.8 \cdot 10^{-11}$ ^{244}Pu: $6.7 \cdot 10^{-9}$

2.4 Selection of radionuclides

The radionuclides of relevance to the performance of deep geological repositories vary depending on the waste (HLW and / or various types of SF and ILW), repository design and host rock type (Neall & Smith 2003). The list includes activation/fission products (e.g. isotopes of C, I, Ni, Se, Zr, Tc, Pd, Sn and Cs) as well as members of different actinide chains (e.g. isotopes of Am, Cm, Np, U, Pu and Th, along with their shorter-lived daughters). In addition, due to a wide range of experimental constraints for the *in situ* experiment, PA relevant radionuclides might be replaced by shorter-lived isotopes of the same element or by elements which behave in a very similar fashion but which are more amenable to the available analytical methods *etc*.

With regard to the expected oxidation state of the radionuclides in the *in situ* experiment, two possible release scenarios were discussed:

- Release of oxidised species: this scenario is based on the assumption that extensive parts of the EBS are oxidising (e.g. due to radiolysis reactions) and / or transport to the geosphere is fast enough that oxidised species released from the waste form are not reduced during transit (e.g. due to effects of gas pressurisation).
- Release of reduced species: the large EBS buffer capacity should ensure that, even if the waste surface is oxidising, radionuclides would be efficiently reduced during slow diffusive transport through the canister corrosion products and bentonite and would finally enter the geosphere in a reduced state.

The final tracer cocktail reflects compromises between safety relevance of the selected radionuclides, priorities of the project partners, considered importance of the different release scenarios above, technical feasibility and radioprotection. Below, the arguments for the tracer

selection are summarised. Different isotopes of the same element have been used where possible in the two main tracer injections to aid the identification of differing retardation mechanisms (between the injection with and without bentonite colloids). This holds for $^{233/238}$U, $^{242/244}$Pu, and $^{241/243}$Am. Actinide concentrations are analysed in the samples isotope-specific by ICP-mass spectrometry. The Pu isotope 238 has been added to both injection cocktails to allow for monitoring the actinides in collected samples additionally by α-spectrometry.

Am is the only trivalent element included in the cocktail. Am is not redox sensitive under the Grimsel groundwater conditions. The well known high sorption of this element on equipment materials must be considered in the experimental design (e.g. PEEK coatings of all materials that are in direct contact with the tracer).

The calculated stable redox state of Np under the Grimsel conditions is Np(IV). However, knowing the difficulties with the sorption properties of tetravalent radionuclides in field and laboratory experiments, it was decided to use the pentavalent form of ^{237}Np (only one isotope was available for Np), if it could be shown to be stable for the experimental conditions and time scale. In a first series of laboratory experiments ^{237}Np(V) was found to be stable in Grimsel groundwater, for at least 20 days (see also comments in Alexander et al. 2003).

Pu(IV) was calculated to be stable under the conditions of the Grimsel groundwater, mainly as the $Pu(OH)_4(aq)$ species. However, it is known that different Pu oxidation states can co-exist, even under reducing conditions and at trace concentration, due to disproportionation reactions (Guillaumont & Adloff 1992). It thus has to be accepted that the precise speciation of Pu inherently remains uncertain. In the end, questions of practicality in tracer preparation and tracer stability led to the decision to use Pu(IV), even though it was accepted that handling problems described for the other tetravalent actinides apply. The oxidation state IV was decided to be the most appropriate state which should be injected. $^{238/242}$Pu and $^{238/244}$Pu were selected as the isotopes injected in runs #31 and #32, respectively.

With respect to the Grimsel groundwater, the Eh/pH values are very close to the U(IV)/U(VI) aqueous boundary transition, making prediction of the precise speciation problematic in any case. Although it is often assumed that U is present as U(IV) in anaerobic groundwaters, it is actually likely to be present as U(VI)[8]. In addition, it was noted that, as U(IV) readily sorbs to all kind of surfaces (e.g. those of the injection equipment; see Alexander et al. 2003, for example) and that it is very easily oxidised to U(VI), even by trace oxidants[9] (much easier than Pu(IV) is oxidised to Pu(V) or Pu(VI)) it was most practicable to use U(VI) in the *in situ* experiment. Two different isotopes were suggested for the two injections: ^{238}U and ^{233}U.

There is also some uncertainty to the likely Tc speciation as the Eh/pH conditions of the Grimsel groundwater are very close to the TcO_4^-/TcO^{2+} stability boundary. In addition, Tc(VII), as pertechnetate, is easily reduced to Tc(IV) in the presence of reducing agents such as Fe(II) or S^{2-}(e.g. Cui & Eriksen 1996). From previous experience during the MI and EP projects, the extremely low solubility of Tc(IV) in the Grimsel groundwater (comparable to that of the tetravalent actinides) would make ^{99}Tc(IV) almost undetectable in the groundwater samples. Further, previous experience from MI/EP indicated that Tc(VII) would pass through a short

[8] It is noted that the reduction of U(VI) to U(IV), even in the presence of reductants, is slow unless it is microbially catalysed (e.g. Lovley et al. 1991) or surface mediated (once sorbed onto the surface of a solid, electron transference occurs more easily - Wersin et al. 1994). The reduction of U(VI) to U(IV) in aqueous solution is thus considered unlikely to be significant given the short transit time in the field experiment.

[9] For example, in CIEMAT's laboratory experiments, it was observed that U(IV) easily oxidises to U(VI) even under tightly controlled experiments in high-quality 'oxygen free' glove boxes due to the unavoidable presence of trace amounts of oxygen.

dipole in the shear zone with little or no retardation but would be completely retarded in a longer dipole, suggesting kinetically hindered reduction of soluble / poorly sorbing Tc(VII) to insoluble / strongly sorbing Tc(IV) (U. Frick, *pers comm,* 1992). Laboratory experiments confirmed this and Tc(IV) was shown to be barely soluble in Grimsel groundwater and sorbed strongly on the Grimsel granite (Möri et al. 2004). However, it was decided to use ^{99}Tc(IV) in the second injection because preliminary laboratory experiments revealed that it might be stable at higher concentrations due to its sorption onto the bentonite colloids.

^{137}Cs was intended only to be used in the second injection together with the bentonite colloids as the migration behaviour of dissolved Cs in the zone was characterised in detail during the MI experiment (see Smith et al. 2001a,b; Möri et al. 2006a). This would allow a direct comparison with the existing data on Cs migration to show the influence of the bentonite colloids.

Although not directly safety relevant (the analogy to Ra is quite weak), the behaviour of Sr in the zone was also characterised in detail during the MI experiment (see Frick et al. 1992, and Smith et al. 2001) and investigated during previous stages of the CRR project (see run #21 in Geckeis & Möri 2003). It usually displays ideal cation exchange behaviour and hence ^{85}Sr was included as a simple control for comparison with the other elements.

^{232}Th was selected in order to include a tetravalent state nuclide which is not redox sensitive. It is stable in the tetravalent state and can be taken as a reference for the behaviour of tetravalent actinides. However, the known low solubility of Th and its tendency to form colloids as known for all tetravalent actinide ions were noted as likely drawbacks. In addition, it was not possible to find an appropriate isotope which is not naturally present in the granite.

^{75}Se was examined as a potential radionuclide of interest in the early stages of the project. In agreement with the findings from EP, laboratory experiments and stability calculations revealed that the prediction of the behaviour of ^{75}Se was very difficult, even under very simple and controlled conditions. If ^{75}Se is present as IV (selenite) or -II (selenide), very little sorption would be expected for such anionic species (as shown in the EP project). The mobility of Se is believed to be predominantly controlled by formation of poorly soluble species (e.g. FeSe, $FeSe_2$; Howard 1977, Linklater et al. 1996). Although some laboratory data were measured, the experiment partners decided against the use of ^{75}Se in the CRR field experiment.

3 Colloids

Different types of colloids have been considered to be relevant for the scenario defining the framework of the CRR experiment. Colloidal species can be supplied to the near-field of a repository due to a variety of processes:

- Corrosion of container to produce metal-containing colloids.
- Corrosion of the waste form to generate colloidal silica, aluminosilicate or actinide phases (from spent fuel).
- Erosion of backfill material (smectite etc.).
- Supply from natural colloids present in groundwater.

Radionuclides can either attach to existing colloidal species by sorption or co-colloid formation (sometimes called "pseudocolloids" or "Fremdkolloide" but better termed heterogeneous radiocolloids) or may directly form colloids, for example, due to polymerisation of hydrolysed actinide species (so-called "intrinsic colloids" or "Eigenkolloide" but better termed homogenous radiocolloids).

The investigation of colloid stability in relevant groundwater is one of the major objectives of the CRR experiment. In the first stage, the stability of different colloid types was evaluated and their behaviour in the experimental flow system was investigated. Beside the analysis of concentration, size and stability of natural colloids present in Grimsel groundwater, it was necessary to establish if "near-field" generated colloids would be stable in this solution, at least during the time span of the *in situ* test, in order to assess the feasibility of this experiment and to ensure an appropriate design. An EBS consisting of compacted bentonite with small pore sizes will most likely prevent migration of such type of colloids due to the predominantly diffusive transport filtration processes. Near-field colloids produced by container and waste form corrosion are nevertheless considered here in order to discuss their possible relevance in case of gas pressuration enhancing transport through the EBS.

The different types of colloids which might be expected in the groundwater near a HLW/SF repository are shown in Tab. 3.1. A particular aim of CRR was to define the relevance of different colloid types for the *in situ* experiment with respect to the expected conditions at the bentonite-rock interface.

Tab. 3.1: Definition of different types of relevant colloids.

Name of colloid	**Definition**
Natural colloids	Colloids found in the host rock groundwater (e.g. from erosion of fracture filling material; formally includes also colloidal-sized organics and microbes).
Bentonite colloids	Colloids derived from erosion of the backfill material at the bentonite-host rock interface.
Homogeneous radiocolloids	Colloids consisting of pure radionuclide species (e.g. polymerised actinide hydroxides)
Heterogeneous radiocolloids	Colloids containing sorbed or otherwise incorporated radionuclides on / in an non-radioactive substrate

Full details of the studies on colloid generation and stability which were carried out in the frame of CRR can be found in Geckeis (1999a), Geckeis et al. (1999b) and Missana et al. (2001). The following sections summarise the key findings from these studies.

3.1 Natural colloids in granitic groundwaters

Some measured concentrations for colloids in deep granitic groundwaters are summarised in Tab. 3.2 (after Degueldre et al. 1996a). Degueldre et al. concluded from their study that under unperturbed chemical conditions and low groundwater flow rates, the relevant colloid concentration does not exceed 0.1 mg L^{-1} when the calcium concentration was greater than $1 \cdot 10^{-4}$ M (Grimsel groundwater: $1.4 \cdot 10^{-4}$ M) an /or the sodium concentration was greater than $1.0 \cdot 10^{-2}$ M (Grimsel groundwater: $6.9 \cdot 10^{-4}$ M). Under transient chemical or physical conditions, such as geothermal or tectonic activity, colloid concentrations were observed to be enhanced and reach 10 mg L^{-1} or more, providing that both calcium and sodium concentrations were not too high (Degueldre et al. 1996a).

Tab. 3.2: Comparison of natural granitic groundwater colloid concentrations for specific size ranges.

Country	**Observation site**	**Concentration** [mg L^{-1}]	**Size range of colloids measured** [nm]
Canada	Whiteshell research area (Vilks et al. 1991)	0-0.6	10-450
France	Fanay-Augeres (Moulin et al. 1991)	0.1	100-1000
Sweden	Granitic bedrock (Laaksoharju 1990)	0.4 – 1.5	50-450
Spain	El Berrocal (Turrero et al. 1995)	< 0.1	2-1000
Switzerland	Grimsel Test Site (Degueldre et al. 1996a)	0.1-0.15	10-1000

As noted previously, the Grimsel groundwater is characterised as a low salinity, Na-Ca-HCO_3-F water with a pH of 9.6 and an Eh of less than –300 mV (Frick et al. 1992, Smith et al. 2001). As the DOC (dissolved organic carbon) content might positively influence colloid stability, this parameter was also measured. Off-line measurements of the DOC (which are not very accurate below 40 μM) revealed relatively low values around 20 μM, which are unlikely to stabilise the colloid phase.

Degueldre et al. (1996b) interpreted batch experiments as indicating that the half-life of a monodispersed colloid is inversely proportional to its concentration and an "attachment factor [α]" and to the colloid. The attachment factor for the colloids at pH 9.6 was reported to lie around $1 \cdot 10^{-6}$ (for Na = $1.4 \cdot 10^{-2}$ M and Ca = $1.25 \cdot 10^{-4}$ M) which means that the half-life for a colloid concentration of 0.1 mg L^{-1} is about 80 years. High Na concentrations, such as found in the FEBEX porewater, should cause an increase of the attachment factor and therefore decrease the stability of the colloids. Changes in groundwater flow velocity, pH, pe and temperature may also influence the colloid stability and should therefore be carefully controlled during any laboratory or *in situ* tests.

The main processes affecting the mobility of colloids are "sticking" onto fracture walls and/or sedimentation after coagulation and filtration. Colloids may also dissolve in response to changes in water chemistry (can be particularly important for homogeneous colloids).

Potential temporal changes in concentration and size of the natural colloid background in Grimsel groundwater have been investigated with Laser Induced Breakdown Detection (LIBD) and are reported in Hauser et al. (2002, 2003). The concentration and average size of the natural colloids seem to be stable even after months, as determined on different sampling campaigns and over extended storage of Grimsel groundwater. The natural colloid population of the Grimsel groundwater detected with LIBD showed no significant changes in either its concentration or mean size for different sampling campaigns. The colloid diameters were found to lie in a range of 50 to 200 nm (see Möri et al. 2004). Taking into account an average colloid density of 2.0 g cm^{-3} (Hoehn et al. 1998) and assuming spherical geometry, this corresponds to a natural colloid concentration of approximately 0.3-4 µg L^{-1} of colloidal material. The natural colloid background concentration in the Grimsel groundwater determined by LIBD during the main CRR field tests was found to be around 5 µg L^{-1} which is lower than the value reported by Degueldre et al. (1996b) in Tab. 3.2. We assume that colloidal fine particles have been washed out from the shear zone fracture filling material due to the experimental activities in this area over many years and, hence, the colloid population has decreased during the time.

3.2 Near-field generated colloids

3.2.1 Radiocolloids

In several studies, actinide and rare earth element (REE) ions have been found to be predominantly present as colloidal species under deep groundwater conditions (Kim et al. 1994; Kaplan et al. 1994). Far-field groundwaters are often characterised by near-neutral pH, reducing conditions and relatively low temperatures (< ~ 50°C). Processes in the near-field of a radioactive waste repository, however, can lead to quite different conditions. In the near-field of a HLW/SF repository, temperatures up to 150°C may occur during a short time period after canister emplacement. The pH and Eh may be influenced by radiolysis (although this is often buffered by canister corrosion products) and corrosion processes of containers and of the waste form. Radionuclide concentrations will generally be considerably higher than in the far-field. Generation of radiocolloids has been observed in experiments on SF (e.g. Finn et al. 1994) and nuclear waste glass corrosion (e.g. Buck & Bates 1999). The salinity of the solution increases in case of glass corrosion and exerts a destabilising effect on radionuclide colloids. This effect is as well reported by Olofsson et al. (1982a,b), Maiti et al. (1989) and Kim (1991). The decrease in colloid concentration at increasing ionic strength is explained by the suppression of the electric surface charge, thus leading to a destabilisation and preferential retention of colloidal species by sedimentation. Furthermore, colloids can be filtered out by the buffer material (e.g. bentonite) surrounding the canisters. The role of colloids and their impact on radionuclide mobility, therefore, has to be assessed considering all these circumstances. Increased ionic strength in the repository near field and the EBS (Engineered Barrier System) consisting of nanoporous bentonite, where diffusive transport mechanism predominates, very likely prevent the migration of colloidal species to the repository far field. As conceivable pathways for a colloid-mediated radionuclide discharge remain: pressure build-up due to gas production might cause failure of the EBS/natural barriers (see GAM and GMT project) and binding to macromolecular organic matter (e.g. fulvic acid like substances) which is able to diffuse through compacted clay (Wold & Eriksen 2003).

3.2.2 Bentonite colloids

Compacted bentonite in the EBS is a potential source of colloids which can be transported into the geosphere. The mechanisms of colloid generation are primarily related to the hydration of the clay. Compacted bentonite shows a very high water uptake capability that lasts during the transient period before complete saturation is achieved (Fig. 3.1, left). Due to this hydration, a swelling pressure is developed that can extrude the clay into fractures within the rock (e.g. in the Excavation Disturbed Zone, EDZ). The smaller the clay particles, the easier extrusion is into these micro-fractures (Pusch 1999). Such intrusion can causes a local loss in density of the compacted clay and formation of a gel-like front at the clay/water interface

The transportation of colloids in the rock depends on the groundwater flow system. In low permeability, unfractured rocks, such transport might occur predominantly by diffusion through the pores of the rock matrix (if these are accessible to colloids). In host rocks characterised by an advective flow system, water usually flows predominantly in distinct regions of higher hydraulic conductivity (faults, fractures, highly conductive lithological units). These are the focus of the CRR experiment. The EDZ may also act as such a preferential flow path, but extrusion of bentonite into the fractures in this zone may actually reduce its permeability and improve its barrier performance.

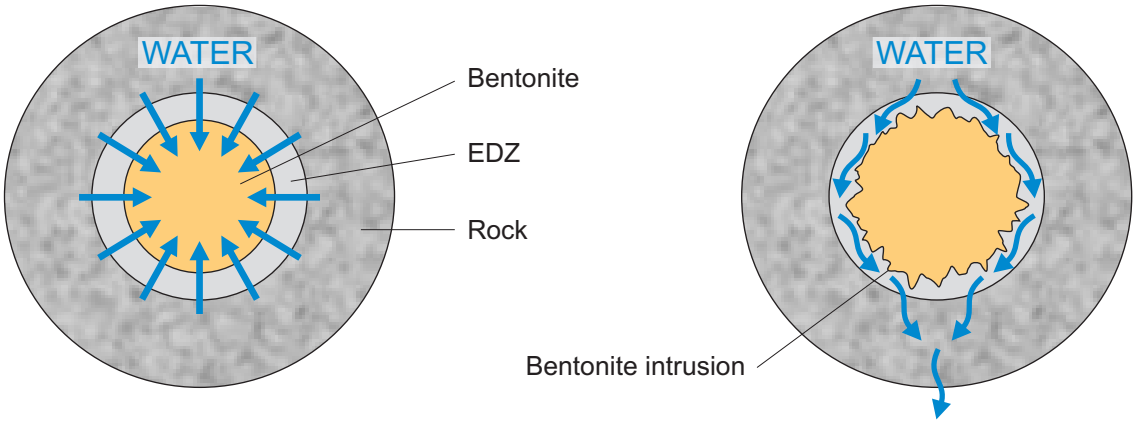

(a) During Saturation (b) After Saturation

Fig. 3.1: Water flow during saturation and after complete saturation of the bentonite buffer.

3.2.2.1 Characterisation of colloids from the FEBEX bentonite

The bentonite used in CRR is the same as used in the FEBEX project (see Huertas et al. 2000, for details) and originates from the Cortijo de Archidona deposit in Spain. This clay has a quite high smectite content (93 ± 2 %), with quartz (2 ± 1 %), plagioclase (3 ± 1 %), cristobalite (2 ± 1 %), potassium feldspar, calcite and trydimite as accessory minerals. Although illite has never been detected as a "pure" phase by XRD (X -ray diffraction) analysis, mineralogical studies indicated that the smectite phase is actually an illite-smectite mixed layer with 10 - 15 % of illite layers (Cuadros & Linares 1996). Table 3.3 shows the main chemical and mineralogical properties of the clay. Further details of this clay can be found elsewhere (e.g. Huertas et al. 2000).

Tab. 3.3a: Main chemical composition and trace elements of the FEBEX bentonite.

	(%)
SiO_2	57.89 ± 1.55
Al_2O_3	17.95 ± 0.71
Fe_2O_3	2.84 ± 0. 12
FeO	0.25 ± 0. 10
MgO	4.21 ± 0. 21
MnO	0.04 ± 0. 00
CaO	1.83 ± 0. 10
Na_2O	1.31 ± 0. 09
K_2O	1.04 ± 0. 05
TiO_2	0.23 ± 0. 01
P_2O_5	0.03 ± 0. 01
H_2O^-	8.66 ± 2. 88
H_2O^+	4.31± 0.41
CO_2 (organic)	0.35 ± 0.05
CO_2 (inorganic)	0.26 ± 0.06
SO_2 (tot)	0.21 ± 0.10
F^-	0.18 ± 0.01
	(ppm)
Ba	164±25
Sr	220±23
Ce	74±6
Co	9±3
Cr	8±2
Cu	25±9
La	40±3
Ni	20±3
V	16±2
Y	25±3
Zn	65±4
Zr	43±3
U	2±0.5
Th	19±1
Rb	41±2
Li	54±3

Tab. 3.3b: Main mineralogical composition of the FEBEX bentonite.

Mineral	**(%)**
Smectite	92±3
Quartz	2±1
Plagioclase (Na, Ca)	3±1
Cristobalite	2±1
K-Feldspar	Traces
Calcite	1±0.5

The structural formula of the FEBEX bentonite (fraction less than 2 μm (which contains more than 99 % smectite) after all exchangeable ions replaced with Ca) was determined to be (Fernández et al. 2004):

$$(Si_{7.78}Al_{0.22})(Al_{2.78}Fe^{3+}_{0.33}Fe^{2+}_{0.02}Ti_{0.02}Mg_{0.81})O_{20}(OH)_4(Ca_{0.50}Na_{0.08}K_{0.11})$$

The interlayer charge is +1.19, the charge of the tetrahedral sheet is -0.22 and that of the octahedral sheet -0.97, which indicates the dominant montmorillonitic character of this smectite.

The cation exchange capacity (CEC) of the FEBEX clay is 1.02 ± 0.04 meq g^{-1} (Huertas et al. 2000). Bentonite colloids were obtained from "natural" bentonite (crushed and sieved to size fraction < 64 μm) after washing with Milli-Q deionised water and a final equilibration with Grimsel groundwater. The colloidal fraction was obtained by centrifugation.

The structure of these colloids was investigated by electron microscopy techniques. SEM (Scanning Electron Microscope) samples were obtained by filtering 1 mL of the suspension through an Amicon XM 50 membrane (50000 MW, pore size 3 nm, 2 cm diameter), that was dried and covered by an Au film, of thickness of 200 Å, approximately. Fig. 3.2 shows a SEM image of bentonite colloids.

In the figure, smaller particle sizes are visible beside larger agglomerates. This morphology is not due simply to artefacts caused by the filtering: it seems that bentonite colloids are naturally stabilised in this intermediate size range (100-300 nm). This can be related to the fact that the clay is a cation exchanger. If Ca is present in the solid, it can be released in the liquid phase favouring a certain degree of aggregation.

The XRD peaks of the FEBEX bentonite colloids samples, previously homoionised in Na, fit very well with those of an aluminium dioctahedral smectite (Newmann 1987) and no significant mineral impurities have been found.

The characteristics of bentonite colloids in Grimsel groundwater have been examined and it has been determined that the main exchangeable cations are: Ca^{2+}(~ 29 %), Mg^{2+} (~ 31 %), Na^{+} (~29%) and K^{+}(~ 3 %).

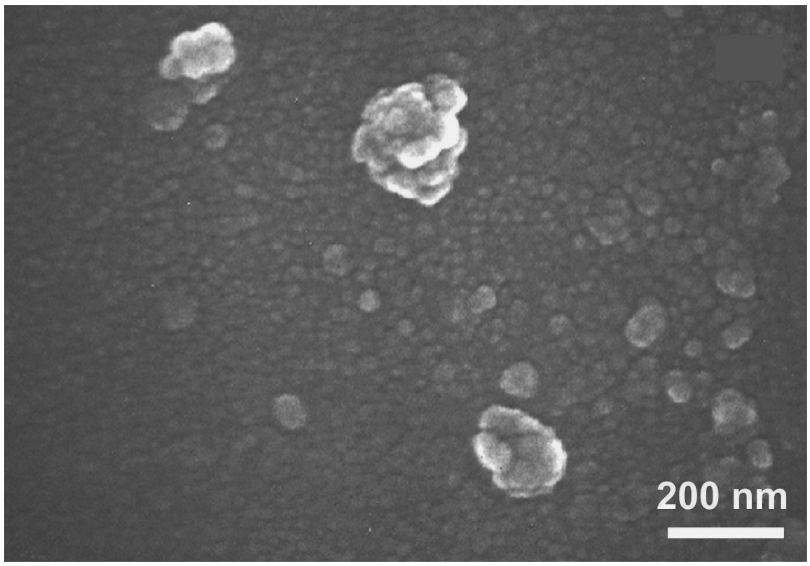

Fig. 3.2: SEM images of bentonite colloids prepared in laboratory (100 ppm).

3.2.2.2 Experiments on colloid generation from compacted bentonite

Two different experimental set-ups[10] have been designed in order to describe two different situations: first, where advection dominates colloid mobilisation (dynamic experiment) and, second, where diffusion is predominant (quasi-static experiment). However, since very low flow conditions are expected around the EBS of a repository (Nagra 1994), the water flow in the dynamic experiments were very low (from 0.17 ml day^{-1} to 0.48 ml day^{-1}, in the order of 10^{-9} ms^{-1}). Fig. 3.3 shows schematically the experimental set-up. Generation of colloids from the interface, under dynamic conditions (see Fig. 3.3, left drawing), was simulated in a half granite[11] / half compacted-bentonite composite cylinder (150 mm high and with a diameter of 38 mm) located between two sintered steel filters (pore size 10 μm) in a high-pressure cell. The two halves were held together by means of a cylindrical latex membrane. Hydration and swelling of the clay (NB density of 1.65 g cm^{-3}) was achieved without mechanical disturbance (erosion) of the bentonite and colloids were generated at the clay surface and mobilised at the bentonite-rock interface. The water was introduced parallel to the interface under a pressure of around 10 bars and a constant water flow rate was maintained. In order to balance the high swelling pressure of bentonite, the cell was filled with water and a confining pressure approximately 3 times higher than the injection pressure was applied (injection and confining pressures were slightly varied to obtain the required water flow rate).

So-called "static conditions" experiments were also performed in a cylindrical piece of granite (155 mm high and with a diameter of 85 mm) with an internal cylindrical aperture of 45 mm in diameter (drawing on the right side in Fig. 3.3). A plug of compacted bentonite (density of 1.65 g cm^{-3}), covered by a 5-mm layer of a porous and highly permeable geotextile (of polypropylene and polyethylene fibres), was placed in the core aperture and water was introduced very slowly by an HPLC pump to hydrate the geotextile layer, then the pump was

[10] In fact three were investigated – two at CIEMAT and one at JNC. Unfortunately, the JNC experiment was not completed until after CRR was completed, but a short note on the results is available in the Appendix.

[11] This experiment was performed with the El-Berrocal granite from Spain, all other experiments were done with Grimsel granodiorite.

stopped. The system was closed so that the water was initially retained by the geotextile and then progressively sorbed by the clay. When the water was adsorbed by the clay the geotextile layer was filled again by slowly introducing new water with the pump. This process was repeated several times to ensure that the bentonite surface was completely hydrated. At the end of the experiment, the small quantity of liquid remained in the geotextile was extracted with care by means of a syringe, to analyse for the presence of bentonite particles and to analyse their characteristics.

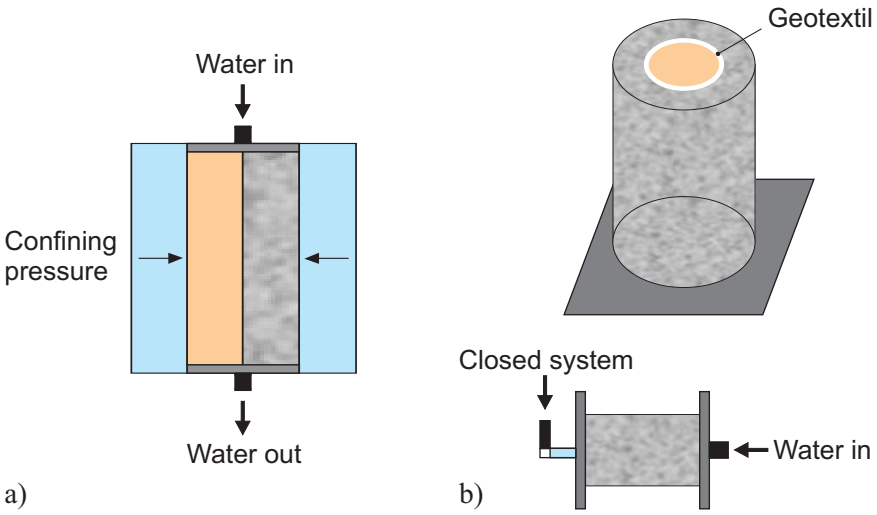

Fig. 3.3: Schematic representation of the experiments simulating the near-field/far-field interface: bentonite brown, granite grey.

The water flow at the granite/bentonite interface in the dynamic experiment produced erosion on the exposed bentonite surface and solid material was found in the eluted water. The fact that the water actually flows at the interface, and not within the clay plug or along the external walls of the column, was confirmed by adding fluoresceine dye to the injected water[12].

The particulate matter contained large fragments (up to 3 μm) and smaller particles that could be clearly observed upon filtering the eluted water with a 0.45 μm pore size filter membrane. The total solid fraction was fairly polydispersed and the colloidal fraction had a mean hydrodynamic diameter, determined by Photon Correlation Spectroscopy (PCS), ranging from 200 to 300 nm.

Fig. 3.4 shows a SEM image of a sample of the colloidal material observed in the eluted water. 10 mL of this water was filtered with an Amicon XM50 membrane. The 200 - 300 nm sized material was actually formed by a composite of smaller particles, as previously mentioned for colloids of Fig 3.2.

Chemical analysis, performed with the energy dispersive X-ray technique (EDX), indicated the presence of Si, Al, Mg, Ca and Fe as the main components. The ζ potential of this colloidal material was always negative, and lies between –20 and -30 mV. The mass of the colloidal fraction was almost two orders of magnitude smaller than the total solid fraction. The

[12] This result is surprising insofar that in most PA calculations, it has been assumed that the bentonite/rock interface will not be a preferential flowpath. It is proposed that this phenomenon is further studied before any definitive conclusions are drawn.

concentration of both colloidal and total solid fraction generated at the interface was observed to increase with increasing water flow, indicating that mechanical erosion processes could be an important factor in colloid generation at these very high imposed gradients. It is worth mentioning that colloids were observed also in the experiments performed under quasi-static conditions, implying that colloids are produced even in the absence of physical erosion processes.

In fact, at the end of a one month duration quasi-static experiment, the external surface of the bentonite plug, which was always in contact with the water of the geotextile, appeared more hydrated than the inner part and gel-like bentonite material had formed which partially extruded into the geotextile layer. This could be clearly observed. The small quantity of water in the geotextile was collected and analysed and found to contain more than 200 ppm of total solid material, of which 4 - 8 ppm represented the colloidal fraction.

These simple experiments aimed to show that the formation of colloids at the bentoite/granite interface is possible but more precise studies are still needed to understand the mechanisms of generation and its quantification.

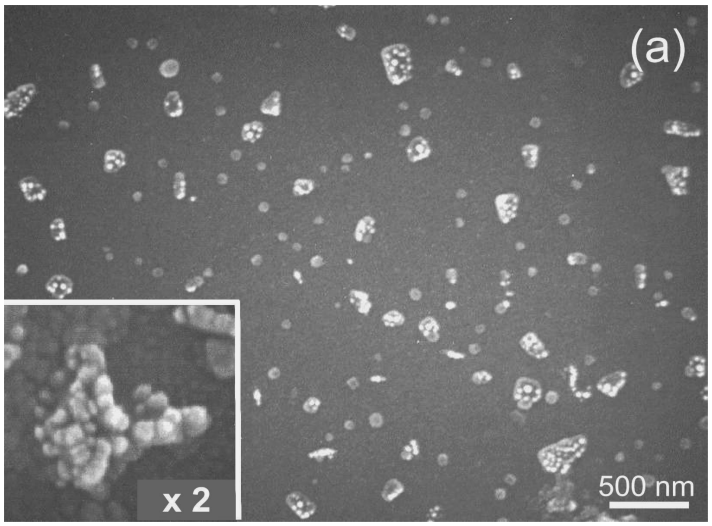

Fig. 3.4: SEM image of the bentonite colloids generated at the granite/bentonite interface (dynamic experiment).

3.3 Stability of colloids

The stability of two different types of colloids in Grimsel groundwater and FEBEX porewater were investigated: ZrO_2 colloids (as a surrogate for homogeneous radiocolloids like UO_2 or PuO_2) and FEBEX bentonite colloids. ZrO_2 colloids are taken because their surface charge properties are similar to those of tetravalent actinide particles, which may be generate in an aquifer under reducing conditions. Bentonite colloids are assumed to dominate the colloid population in the repository near-field and hence also the interaction with radionuclides to form heterogeneous radiocolloids.

Colloid stability was studied as a function of pH and ionic strength by experimentally evaluating their stability ratio (W) defined (Barringer et al. 1984) as:

$$W = \frac{k_f}{k_s} \tag{1}$$

where k_f is the rate of fast agglomeration and k_s is the rate of slow agglomeration. The rate of fast agglomeration refers to the agglomeration which is limited only by the rate of diffusion $k_f = 8\pi\ D\ r\ N_0^2$ (r=particle radius, N_0 = particle concentration, D=diffusion coefficient), *e.g.* when a potential barrier does not exist.

The rate of slow coagulation k_s is given by k_f/W where W is the stability ratio (number of collisions/number of collisions resulting in coagulation). Agglomeration rates can be experimentally determined with kinetic experiments (Barringer et al. 1984). The agglomeration rate is determined from the increase of colloid size provided by the Photon correlation spectroscopy (PCS) measurement.

The variation of the mean radius in a colloidal suspension depends on the concentration of the suspension, C, and its rate of coagulation as follows

$$\frac{\mathrm{dr}}{\mathrm{dt}}\Big|_{t\to 0} = k_s F C$$

F is an optical factor depending on the scattering angle, the radius of the particle (r) and the wavelength of the light (Einarson & Berg 1993).

The stability ratio can be therefore experimentally determined by means of the following expression:

$$W = \frac{(\frac{dr}{dt}\Big|_{t\to 0} / C)^f}{(\frac{dr}{dt}\Big|_{t\to 0} / C)}$$

by evaluating $\left.\frac{dr_h}{dt}\right|_{t\to 0}$ from the initial slope of the curves that represent the evolution of the mean hydrodynamic diameter with time (f refers to the fast coagulation regime).

The mean hydrodynamic diameter of the particles in the starting suspension was 200-250 nm. The evolution of the mean hydrodynamic diameter was observed during one hour approximately, by carrying out the single measurements every minute and using an experimental time of 60 seconds.

In a first stage, the fast coagulation regime rate was determined. An increasing amount of $NaClO_4$ M was added at the suspension conditioned at $1 \cdot 10^{-3}$ M until observing coagulation.

3.3.1 Stability of ZrO_2 colloids

ZrO_2 batch experiments were performed in Grimsel groundwater and in NaCl solutions of different ionic strength covering the range from 0.001 M corresponding to Grimsel groundwater conditions to the 0.2 M of FEBEX pore water. A ZrO_2 colloid stock dispersion of 40 g L^{-1} was prepared and the pH was adjusted to 4 with hydrochloric acid. The dispersion remained stable during the experimental time period (more than 3 weeks) at this pH value. The average particle radius, measured by dynamic light scattering (Zetaplus, Brookhaven Inc.) was about 70 nm. The point of zero charge (pH_{pzc} = 8.2) was determined by measuring electro mobility as a function of pH. Colloid stability experiments were conducted as a function of pH ($3 \leq pH \leq 11$), ionic strength (0.001, 0.01 and 0.1 M NaCl) and ZrO_2 colloid concentration (20 - 800 mgL^{-1}).

An example of the stability behaviour of these colloids as a function of pH and ionic strength is shown in Fig. 3.5.

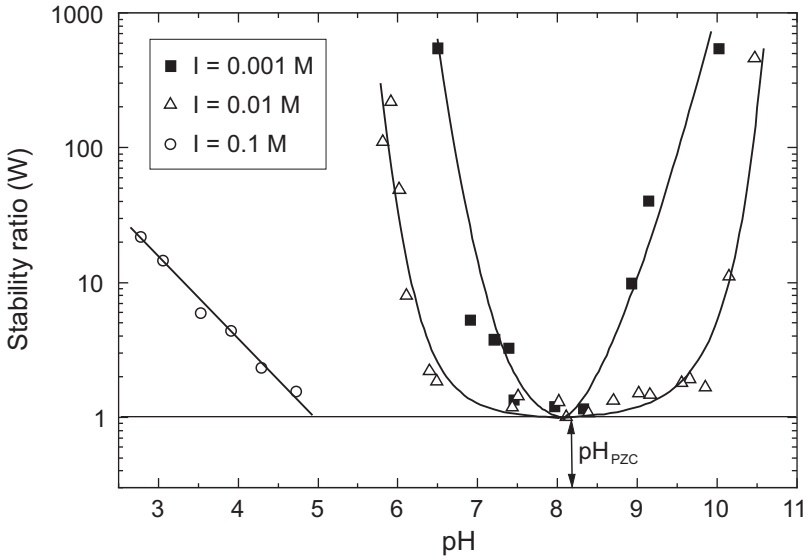

Fig. 3.5: Stability ratio (W) for ZrO_2 colloids (0.4 g L^{-1}) for I = 0.1, 0.01, 0.001 M NaCl. pH_{pzc} = pH of the point of zero charge.

The increase of W (corresponding to an increase of colloid stability) is observed when decreasing the ionic strength at constant pH and with increasing deviation from the pH_{pzc} at constant ionic strength. Fig. 3.6 shows the kinetics of coagulation of ZrO_2 colloids in Grimsel groundwater. Fast aggregation of ZrO_2 colloids, with an initial rate of ~ 3 - 4 nm s^{-1} for the increase of the mean particle diameter, occurred in the pH range of the Grimsel groundwater, presumably because it is quite close to the pH_{pzc} of the ZrO_2. Agglomeration is compared with that of clay colloids.

The pH_{pzc} of PuO_2 is reported in the literature to be at 8.5 - 9 and, for ThO_2, values of 7 - 9.5 are given (Parks 1965). Accordingly, it is not expected that significant concentrations of colloidal PuO_2 or ThO_2 species would be stable under the hydro chemical conditions of the Grimsel groundwater. It should, however, be mentioned that recent studies on the solubility of Th(IV) oxide / hydroxides using the LIBD revealed the presence of stable colloids even at elevated ionic strengths of 0.5 M (Neck et al. 2002), although it is not yet clear what is the real nature of these colloids. Presently, they are assumed to be polynuclear $Th(OH)_4$ species which behave differently to oxide colloids. Nevertheless, in the presence of the compacted bentonite or

bentonite colloids surfaces, the existence of homogeneous actinide colloids will be highly improbable and sorption of actinide species to compacted bentonite or bentonite colloids will be of much higher relevance. The influence of pH, ionic strength and reaction kinetics on the stability of radiocolloids is reported in more detail in Geckeis et al. (1998). Agglomeration of bentonite colloids is discussed in more detail in the next section.

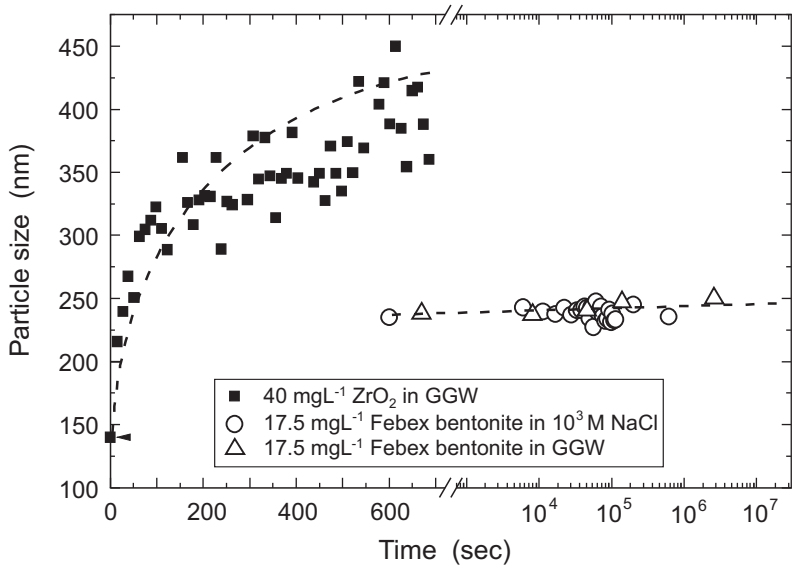

Fig. 3.6: Agglomeration of ZrO_2 and bentonite colloids in Grimsel groundwater and in a 10^{-3} mol/L NaCl solution (pH=9.5) as recorded by the change of the mean particle size with time.

3.3.2 Stability of bentonite colloids

Stable colloid dispersions of FEBEX bentonite were obtained by washing 100 mg bentonite 10-15 times with Milli-Q water and centrifuging the suspension for 2 min. at 15'000 rpm. The final stock solution has a pH of 7.1, a zetapotential (Zetaplus, PALS system; Brookhaven Inc.) of -40 ± 2 mV using the Hückel zetapotential model, and conductivity comparable to that of de-ionised water and a gravimetrically determined solid concentration of 175 mg L^{-1}. Colloid size of the stable suspension determined with photon correlation spectroscopy (PCS) using the Zetaplus showed a mean diameter of 235 ± 90 nm in the scattering intensity size distribution and a maximum around 70 nm in the colloid number size distribution using multimodal size distribution (MSD) analysis of the correlation function.

From general considerations, it would be expected that the importance of radiocolloid formation should decrease at low pH. 1) Radionuclide solubility is high at low pH and precipitation and colloid formation is only conceivable at very high radionuclide concentrations. 2) Radionuclide sorption to preexisting aquatic colloids in most cases is pH dependent and increases with increasing pH. Former experimental observations by FZK substantiate such a trend (Geckeis 1999a), which also is reported in the literature (e.g. Olofsson et al. 1982a,b, Kim 1991). Theoretical considerations predict a low stability of colloids in saline solutions (Liang & Morgan 1990) due to suppression of electrostatic repulsion. This is especially expected in the presence of divalent alkaline earth elements such as Ca^{2+} and Mg^{2+} due to their properties as flocculation reagents (Degueldre et al. 1996a,b). Further colloid analyses in natural granite groundwaters have been reported by Hauser et al. (2005). Those studies confirm the general observation that at groundwater ionic strength > 0.1 M strongly destabilizes aquatic colloids. In

absence of fast groundwater flow rates or strong chemical disequilibria (redox fronts or pH gradients), colloid concentrations decreased to < 25 µg/L.

To investigate the influence of ionic strength on the colloid stability of FEBEX bentonite, gradual concentration changes from I = 0.001 M (comparable to the ionic strength in Grimsel groundwater) to I = 0.11 M (somewhat less than in FEBEX porewater: 0.22 M) using $NaClO_4$ or $CaCl_2$ solution were examined, the pH was varied by adding 0.1 M NaOH or HCl. Colloid concentration was determined by gravimetry. Measurements were carried out in the middle of the cuvette.

Fig. 3.7 shows the evolution of the hydrodynamic mean diameter obtained by dynamic light scattering of colloids obtained from bentonite as a function of the ionic strength of the water phase. An increase in the mean size clearly indicates that coagulation is occurring. It should be noted that the colloids investigated in this study belong to a different batch than those shown in Fig. 3.6. Sizes are therefore slightly different. The pH of the suspensions varied slightly with the addition of the electrolyte, but all the final values were in the range of pH 8.7 ± 0.5.

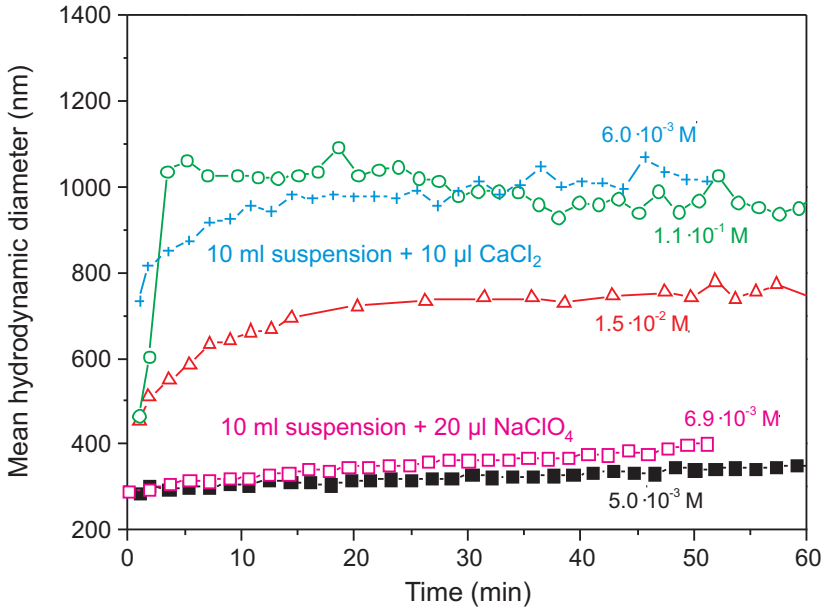

Fig. 3.7: Evolution of the hydrodynamic mean diameter of bentonite colloids (1 g/L) at different ionic strengths. (pH 8.7 ± 0.5). Scattering angle 90º.

The increase in ionic strength was obtained by adding 0.1 M $NaClO_4$. Only the curve plotted with the symbol (+) was obtained by adding 0.1 M $CaCl_2$. As can be seen, at $1 \cdot 10^{-3}$ M the curves are practically flat and only a slow increase of colloid size occurs whereas at an ionic strength of $1.5 \cdot 10^{-2}$ M, rapid coagulation can be observed. The curve obtained at $1.1 \cdot 10^{-1}$ M reflects complete screening of colloid charge and thus reveals the establishment of the fast agglomeration regime. Hence colloid repulsion does not play a significant role and colloid-colloid collisions result in agglomeration. It is interesting to observe that the addition of 10 µl of $CaCl_2$ to 10 ml ($6 \cdot 10^{-3}$ M corresponding to an ionic strength of $1.8 \cdot 10^{-2}$ M) of the suspension leads to an immediate destabilisation of the suspension whereas the addition of 20 µl of $NaClO_4$ ($6.9 \cdot 10^{-3}$ M) only produces a slow coagulation kinetic effect. In the $1.5 \cdot 10^{-2}$ M $NaClO_4$, i.e. at comparable ionic strength, the agglomeration rate is still less rapid as in the $CaCl_2$ solution. This result, which is in agreement with the Schulze-Hardly rule (van Olphen 1977), indicates that

Ca^{2+} is more effective than Na^{+} as an aggregating agent. These results showed that, in a suspension with ionic strength similar to that of the FEBEX porewater, colloids will be highly unstable whereas at a lower ionic strength ($1 \cdot 10^{-3}$ M), the increase in size is negligible at least over a 60 min period.

Another set of experiments was performed to study the effect of pH on the hydrodynamic mean diameter of bentonite colloids (see Fig. 3.8). At fixed ionic strength, the stability of the clay colloids strongly depends on the pH of the suspensions. The curves obtained for pH > 6 (pH 8 and 11) are flat and no substantial change in the mean size was observed during the experiment. The curve at pH 6 shows an increase of approximately 100 nm in the mean hydrodynamic diameter after 45 min whereas, at pH 5, the destabilisation of colloids is practically immediate. The curve at pH 2 is very similar to the curve obtained in the fast agglomeration regime.

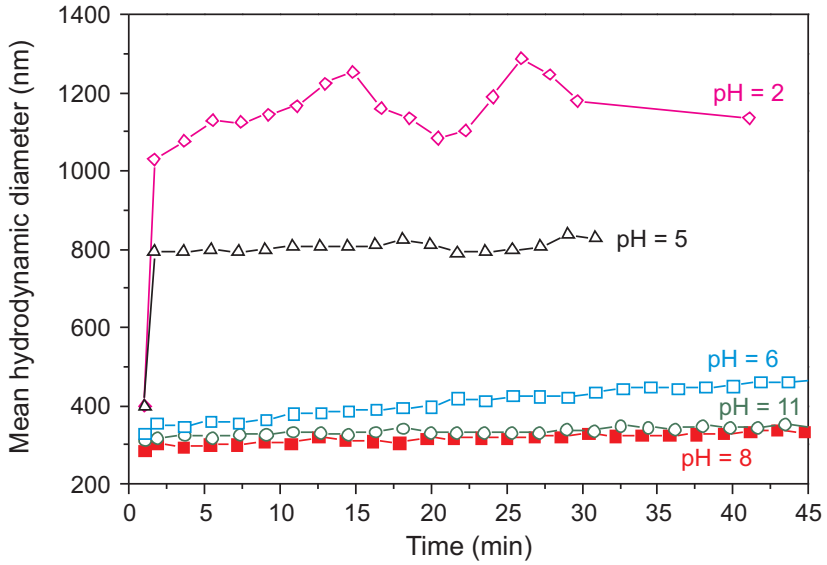

Fig. 3.8: Evolution of the hydrodynamic mean diameter of bentonite colloids (1 g/L) at different pH (I = 5E-03 M). Scattering angle 90º.

The pH-dependent stability behaviour of clay colloids depends, in fact, on the small charge existing at the edge sites. Edge to face coagulation processes occur because, at pH < 6.5, the charge developed at the edge is positive whereas the layer charge is always negative (van Olphen 1977). Under Grimsel groundwater conditions (I = $1 \cdot 10^{-3}$ M and pH = 9.6), bentonite colloids are expected to show high stability. In order to verify this, the size distribution spectra were also investigated at longer time scales. Colloids obtained from previously washed bentonite and conditioned in Grimsel groundwater were prepared. The concentration of the suspension was approximately 2 g L^{-1}. The size distribution spectra of the colloids, obtained approximately five months after preparation, is very similar to that measured just after the preparation of the sample (see Fig. 3.9).

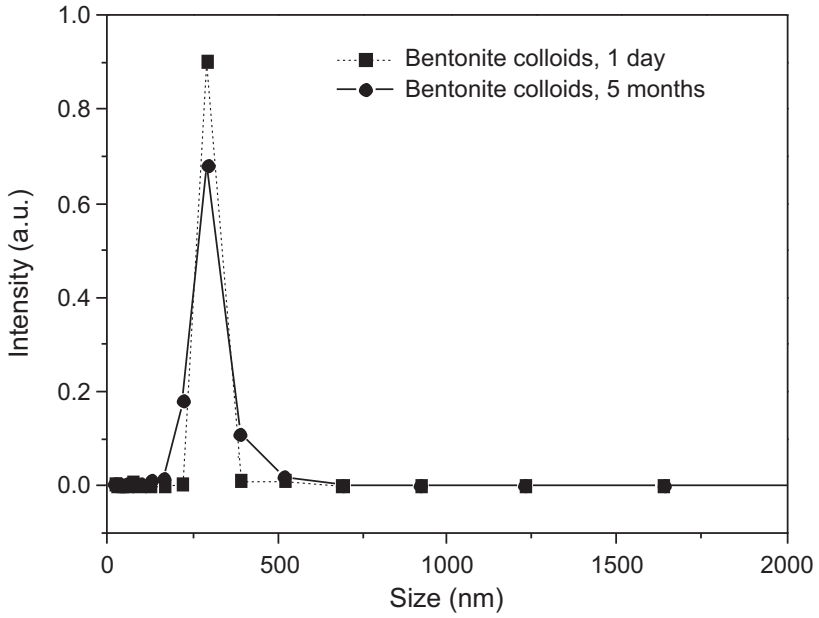

Fig. 3.9: Intensity spectra as a function of size for a bentonite colloids suspension (≈ 2 g L^{-1}) in Grimsel groundwater after one day and 5 months after preparation.

3.4 Comparison of FEBEX and Kunigel V1 bentonite

JAEA (former JNC) compared the stability of FEBEX bentonite colloids with the colloids from JNC's Kunigel V1 bentonite (JNC, 2000) in order to attain a more general understanding of the stability of bentonite colloids. For these batch experiments, 0.5 g crushed FEBEX bentonite was contacted with distilled water, a $NaClO_4$ solution representing the artificial Grimsel groundwater and three other $NaClO_4$ solutions of different ionic strength, $1 \cdot 10^{-3}$ M, $1 \cdot 10^{-2}$ M and $1 \cdot 10^{-1}$ M and at different pH values. Tab. 3.4 shows concentrations and physical properties of the FEBEX colloids experimentally determined under each chemical condition.

The artificial Grimsel groundwater was prepared by adding designated reagents to distilled water. The experimental solutions were then stirred for 24 hours, thereby generating FEBEX colloids in the suspension solution. For the $NaClO_4$ solution, the pH value of each solution was adjusted to three pH values, 6, 8 and 9, following addition of HCl or NaOH. The batch experiment with the artificial Grimsel groundwater was performed under a N_2 atmosphere (0.1 ppm O_2 in a glove box) and the others were carried out under aerobic conditions. The procedure and conditions for the experiments are summarised in Fig. 3.10.

At low ionic strength (i.e. distilled water and $1 \cdot 10^{-3}$ M $NaClO_4$ solution) the concentration of FEBEX colloids was higher than 100 mg L^{-1} following 2 weeks storage. Much lower concentrations of colloids were identified in the experimental solution at relatively high ionic strength (i.e. $1 \cdot 10^{-2}$ M and $1 \cdot 10^{-1}$ M $NaClO_4$ solutions).

Tab. 3.4: Characterisation of FEBEX colloids under different chemical conditions.

Experimental solution			**Colloid concentration**	**Colloid/particle size range***	**Zetapotential****
conc. [M]	Type	pH	[mg L^{-1}]	[µm]	[mV]
Distilled water		8.9***	121	0.1-1.1	-36
$1 \cdot 10^{-3}$	$NaClO_4$	6	129	0.3-2.1	-31
$1 \cdot 10^{-3}$	$NaClO_4$	8	144	0.2-1.4	-34
$1 \cdot 10^{-3}$	$NaClO_4$	9	140	0.2-1.1	-32
$1 \cdot 10^{-2}$	$NaClO_4$	6	about 1	below detection limit	below detection limit
$1 \cdot 10^{-2}$	$NaClO_4$	8	about 1	below detection limit	below detection limit
$1 \cdot 10^{-2}$	$NaClO_4$	9	about 1	below detection limit	below detection limit
$1 \cdot 10^{-1}$	$NaClO_4$	6	about 1	below detection limit	below detection limit
$1 \cdot 10^{-1}$	$NaClO_4$	8	about 1	below detection limit	below detection limit
$1 \cdot 10^{-1}$	$NaClO_4$	9	about 1	below detection limit	below detection limit
Artificial Grimsel groundwater		9.4	41	0.3-1.4	-31

* Determined by laser diffraction particle size analyser (http://www.shimadzu.com/products/test/powder/oh80jt0000001cwo.html).

** Determined by electrophoresis (grating rotation type).

*** Initial neutral value shifted to slightly alkaline value owing to contacting with the crushed FEBEX bentonite material.

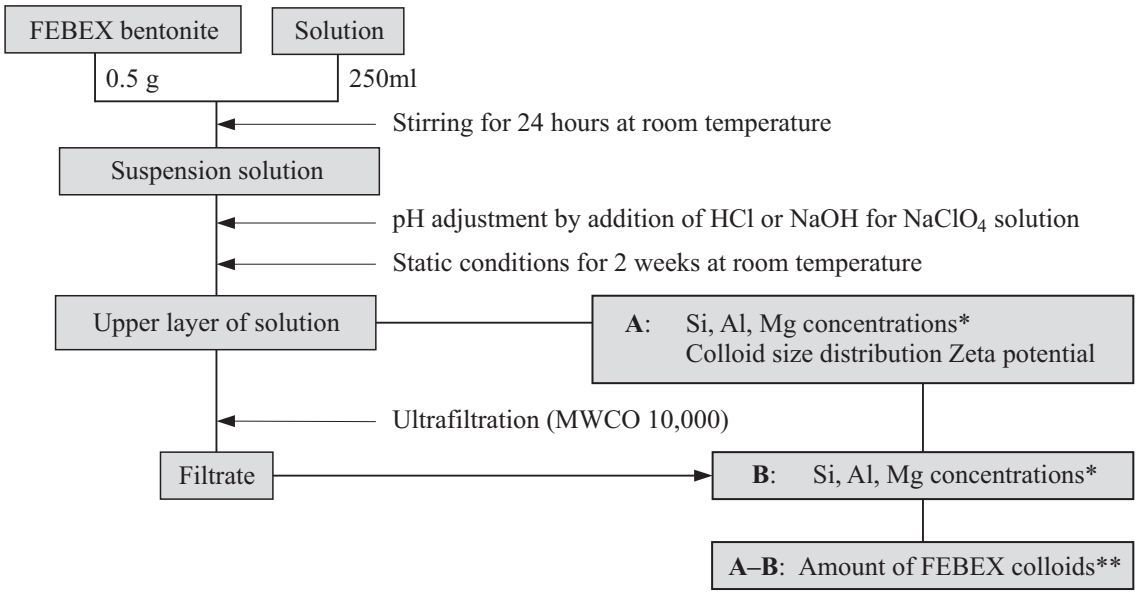

* Determined by ICP-AES

** Calculated on the basis of both analytical data and montmorillonite formula

Fig. 3.10: JNC's experimental procedure for colloid stability determination.

The amount of colloids observed in the artificial Grimsel groundwater after 2 weeks storage was 41 mg L^{-1}, which was, however, less than that of colloids generated in distilled water or in the $1 \cdot 10^{-3}$ M $NaClO_4$ solution. This might be due to the slight difference in ionic strength between the experimental solutions. The stability of the FEBEX colloids does, as expected, depend on the chemical conditions of the solution. Based on this measurement, such colloids are expected to be stable under the Grimsel groundwater conditions. Note that experimental conditions are different to those applied in Section 3.3. Colloids have been previously isolated from the bentonite in experiments described in Section 3.3 and then are used to perform dedicated experiments to study their stability. In the present experiments, the untreated bentonite has been added to the individual solutions and resulting colloid concentrations depend very much on the bentonite to solution ratio. Only a qualitative trend of colloid stability depending on ionic strength and pH may be derived from the experiments. Absolute colloid concentrations in both types of experiments can not be compared.

The concentration of the Kunigel V1 colloids, which was adjusted at the same concentration of the FEBEX colloids, also depended on the ionic strength of the experimental solution (see Tab. 3.5) and its stability behaviour is similar to that of the FEBEX colloids as described above. Both types of bentonite colloids are reasonably stable in a solution where the ionic strength is lower than $1 \cdot 10^{-2}$ M, but flocculate to a significant extent in higher ionic strength solutions.

Certain differences in colloid properties are, however, recognisable: the concentration of FEBEX colloids drops considerably at ionic strengths higher than $1 \cdot 10^{-2}$ M, whereas the concentration of Kunigel V1 colloids gradually decreases with increasing ionic strength. One possible explanation is that mineralogy of both bentonites is different with the FEBEX bentonite composed mainly of smectite whereas Kunigel V1 bentonite contains not only smectite but also a relatively large amount of chalcedony and quartz (about 40 wt%). While high Si concentrations could be detected in a high ionic strength solution containing Kunigel V1 bentonite, this was not the case for FEBEX bentonite dispersions. This suggests that silica colloids may persist in this solution, even if montmorillonite colloids were not stable.

Tab. 3.5: Characterisation of Kunigel V1 colloids under different chemical conditions.

Experimental solution			**Colloid concentration**	**Colloid size range***	**Zetapotential****
conc. [M]	Type	pH	[mg L^{-1}]	[µm]	[mV]
Distilled water		6	314	0.22-5	-41
Distilled water		9	376	0.10-0.49	-53
$1 \cdot 10^{-3}$	NaCl	9	326	0.12-0.55	-54
$3 \cdot 10^{-3}$	NaCl	9	298	0.14-0.69	-66
$7 \cdot 10^{-3}$	NaCl	9	112	0.17-0.87	-76
$6 \cdot 10^{-1}$	NaCl	8	46	n.d.	-37

* Determined by photon correlation and laser diffraction particle size analyser.

** Determined by electrophoresis (laser Doppler type).

3.5 Colloid cocktail for the *in situ* experiment

The colloid concentration selected should be sufficiently high to influence significantly the migration of those radionuclides that are assumed to undergo colloid formation (especially the actinides) and to be detected by the analytical tools available. In addition, the bentonite colloid cocktail in the Grimsel groundwater should be stable over the entire test duration (e.g. no significant aggregation).

During the laboratory experiments, it was observed that bentonite colloid concentrations up to 1000 mg L^{-1} remained stable in suspensions in the Grimsel groundwater over several weeks clearly showing that quite high concentrations of bentonite colloids can be stabilised in Grimsel groundwater. On the other hand, Degueldre et al. (1996a) state that, in natural granitic groundwater systems, colloid concentrations were observed to be much smaller (e.g. 0 – 1.4 mg L^{-1} in the granitic bedrock in Sweden and 0 – 0.6 mg L^{-1} in the Whiteshell research area in Canada). The natural colloid background in the Grimsel groundwater as determined by LIBD was found to be 0.005 mg L^{-1} by Möri (2004) in contrast to Degueldre's measurement of 0.1 – 0.15 mg L^{-1}.

Based on the experience gained from the experiments above, two studies on the sorption capacity of bentonite colloids in the Grimsel groundwater were performed by PSI and FZK (both reported in Geckeis & Möri 2003) in order to determine whether there would be enough sorption sites on 20 mg L^{-1} bentonite colloids to bind all the radionuclides which would be injected. Both studies revealed that there would be enough sites available and hence this concentration was selected for the final injection cocktail.

3.6 Summary

Laboratory experiments demonstrated that colloids can be mobilized at the bentonite granodiorite interface. At the high pH and low ionic strength conditions of the Grimsel groundwater, the stability of clay colloids prepared from FEBEX bentonite is quite high. The colloid stabilization is caused to the strong negative charge of the clay platelets reflected by clearly negative zetapotentials. It is not very surprising that colloids with a point of zero charge (pHpzc) close to the groundwater pH agglomerate even at the low ionic strength conditions. Oxihydroxides of the tetravalent actinides belong to such colloids with pHpzc around 8-10.

From these results, it has been concluded for the CRR experiment that FEBEX clay colloids and FEBEX bentonite colloids should remain stable even at over long time scales (months) in concentration much higher (up to 1 g/L) than the natural colloid background, due to very slow aggregation rates in Grimsel groundwater.

4 Sorption studies

4.1 Batch sorption experiments

The sorption of the actinides ^{233}U, ^{237}Np, ^{244}Pu and ^{243}Am and the fission products ^{75}Se, ^{99}Tc and ^{137}Cs onto Grimsel granite, fracture filling material and FEBEX bentonite colloids was experimentally investigated in the laboratories of CIEMAT and FZK. The assumed sorption processes are schematically represented in Fig. 4.1. It is, however, well known that representation of sorption by a constant distribution coefficient (Kd) is oversimplified in many cases (e.g. McKinley & Alexander 1993). For example, sorption is often observed to vary with the elemental concentration of the sorbing species and hence would be better described by a sorption isotherm rather than a constant (e.g. McKinley & Hadermann 1984). Moreover, sorption may be slow, particularly on the timescale of the planned CRR experiment, and hence kinetics has to be explicitly taken into account (as was already observed in the MI/EP experiment – Alexander et al. 2003). Simple sorption models apply only to a 2 phase system (solid & liquid) and would not be directly applicable to a 3 phase system including colloids. It may be possible to modify models to represent the case indicated in Fig. 4.1, but only if all sorption processes meet the requirements of being concentration independent, fast and completely reversible. It is, therefore, emphasised that sorption data are rather given as R_d values i.e. the phenomenological distribution ratios under given experimental conditions. They need to be used with great caution as they may not reflect the complexity of the sorption mechanisms in natural systems (see also Geckeis et al. 1999c).

Due to the restrictions given by the limited sensitivity of the detection of sorbed and migrating radionuclide species (e.g. by ICP-MS), radionuclide concentrations were often selected near the limit of solubility predicted by thermodynamic calculations (for detail see Duro et al. 2000). The limitations of the thermodynamic databases used and, indeed, the poor basis for the assumption of thermodynamic equilibrium in such systems need to be borne in mind and such "solubility limits" must be compared with observed or experimentally measured limiting concentrations in solution.

Sorption onto fracture filling material and Grimsel granodiorite will lead to retardation or, in case of an irreversible binding, to the immobilisation of radionuclides. However, sorption onto colloids is expected to lead to enhanced radionuclide mobilisation if the colloids themselves are not sorbed, especially if this binding is irreversible. The planned *in situ* migration test will be performed under experimental conditions selected from the viewpoint of practicality, but it must be remembered that the transport distances are much shorter and the flow rates involved are very much greater than those expected in a repository host rock. Consequently, the residence times of the radionuclides and colloids in the CRR experimental site are many orders of magnitude shorter than expected in a repository and it is therefore necessary to consider additional processes, such as sorption kinetics, which may be of little relevance to an actual repository. In order to allow the experiment to be put into a practical PA context, therefore, laboratory tests ran on timescales of up to several months.

For technical reasons, it was not always possible for the two laboratories involved in the investigations to work under identical conditions using identical methods. Moreover, the laboratories investigated different elements:

- **FZK** focused on the sorption of the actinides ^{237}Np, ^{244}Pu and ^{243}Am on Grimsel granodiorite in the absence and presence of bentonite colloids, on fracture filling material and on bentonite colloids.
- **CIEMAT** studied the sorption behaviour of ^{137}Cs, ^{233}U, ^{75}Se and ^{99}Tc on Grimsel granodiorite, fracture filling material, bentonite colloids and bentonite.

The sorption of the oxidised species of Tc(VII), U(VI) and Np(V) was studied at this stage of the experiment in order to check whether these species would be stable or not under the reducing conditions of the experiment (thermodynamic modelling predicted instability but, in laboratory experiments, it was found that the reducing capacity of the groundwater[13] was insufficient to reduce these species and that they seem to be kinetically stable for a long time period).

The outcome from these two groups is reported separately below and summarised in a concluding section at the end of the chapter.

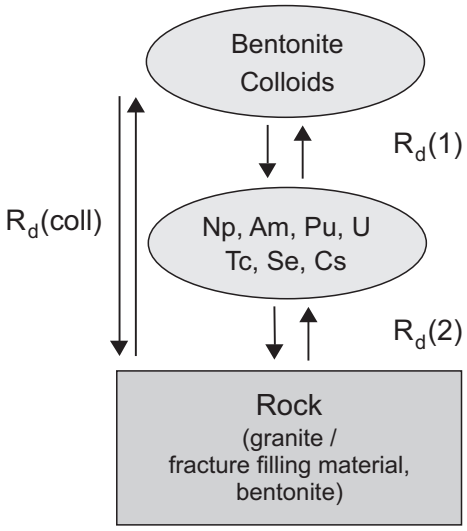

Fig. 4.1: Investigated sorption reactions for radionuclides in the frame of CRR where the R_d value describes the distribution of colloids and/or radionuclides between the individual phases (dissolved, colloidal or solid) under given conditions (definition see Section 4.2).

The distribution ratio between the solid and liquid phases (Rd) was calculated by the usual formula:

$$R_d = \frac{C_i - C_f}{C_f} \cdot \frac{V}{m} = \frac{C_{ADS}}{C_f} \frac{V}{m} \qquad (2)$$

where:

- C_i is the initial specific activity in solution (Bq L^{-1})
- C_f is the final specific activity in the liquid phase (Bq L^{-1})
- V is the liquid volume (L)
- m is the mass of the solid (kg)
- C_{ADS} is the adsorbed activity (Bq L^{-1})

[13] As noted in Alexander (1991), while the reducing capacity of the groundwater itself is very low but the rock may catalyse the redox reactions of nuclides. Therefore such species may not remain stable in the presence of rock or under the experimental *in situ* conditions.

It is clear that Rd values given here to describe radionuclide sorption to rock minerals and bentonite colloids are operational sorption data. They do not specify with which mineral phases the radionuclides interact and do not account for varying sorbent surface areas. Surface area and thus the number of sites at colloid surfaces depend on the colloid size distribution. The bentonite colloid size distribution was not so different for the different experiments, so that the effect of variable colloid sizes on radionuclide sorption was neglected.

4.2 Sorption experiments with ^{75}Se, ^{85}Sr, ^{99}Tc, ^{137}Cs and ^{233}U

All the sorption experiments were carried out as batch experiments in anoxic glove box under N_2 atmosphere (O_2 < 1 ppm) after previous equilibration of the solids with Grimsel groundwater. Three duplicates of the same samples were prepared and three different aliquots were taken for the determination of sorption parameters. The final activity in the liquid phase of ^{99}Tc and ^{233}U was determined with a liquid scintillation counter (Packard TR-2700) and the activity of ^{75}Se, ^{85}Sr and ^{137}Cs with a NaI gamma counter (Packard Auto-Cobra).

In these experiments, attention has been focused on the kinetics of the sorption process. The contact times between the radionuclides and the solids ranged from few minutes to several weeks.

4.2.1 Sorption on bentonite colloids

The sorption behaviour of ^{233}U, ^{137}Cs, ^{99}Tc, ^{75}Se and on bentonite colloids has been investigated using a colloid mass to liquid ratio of 1:435 g ml^{-1}. In order to study the stability of the different radionuclides, a "blank" solution was also prepared by adding the radionuclide to the Grimsel groundwater without the colloids. The activity of the radionuclide in the centrifuged blank solution was periodically monitored and this allowed checking the possible precipitation of the radionuclide, spontaneous colloid formation in the Grimsel groundwater conditions or sorption onto the containers walls. The pH of the bentonite colloid suspension was 9.5 and the pH of the suspension with bentonite was slightly lower (9.1-9.3).

4.2.1.1 Sorption of ^{137}Cs on bentonite colloids

The initial concentration of ^{137}Cs used in the experiments with bentonite and bentonite colloids was $1.1 \cdot 10^{-7}$ M, as can be seen in Fig. 4.2 where the evolution of ^{137}Cs concentration in the liquid phase (C_L) is shown. In the blank solution, a slight decrease of the ^{137}Cs concentration was observed during the first three weeks of the experiment that was attributed to sorption onto the container walls. After this initial period, the concentration in solution remained stable. The evolution of ^{137}Cs concentration in the Grimsel groundwater, in presence of the colloidal phase, shows that this radionuclide is strongly sorbed onto bentonite colloids and that this sorption is fast on the timescale studied (weeks), although this study is not sensitive to the times which may be of relevance for the CRR experiment (hours). The calculated distribution coefficients (Rd) for ^{137}Cs are shown in Fig. 4.3[14]. The mean Rd for bentonite colloids is 7627 ±1163 L kg^{-1}.

[14] Note that the final solution Cs concentration is not far from the natural Cs concentration in this water – $5 \cdot 10^{-9}$ M – and that the natural Cs concentration (and isotopic exchange with this pool) was not considered in the calculations.

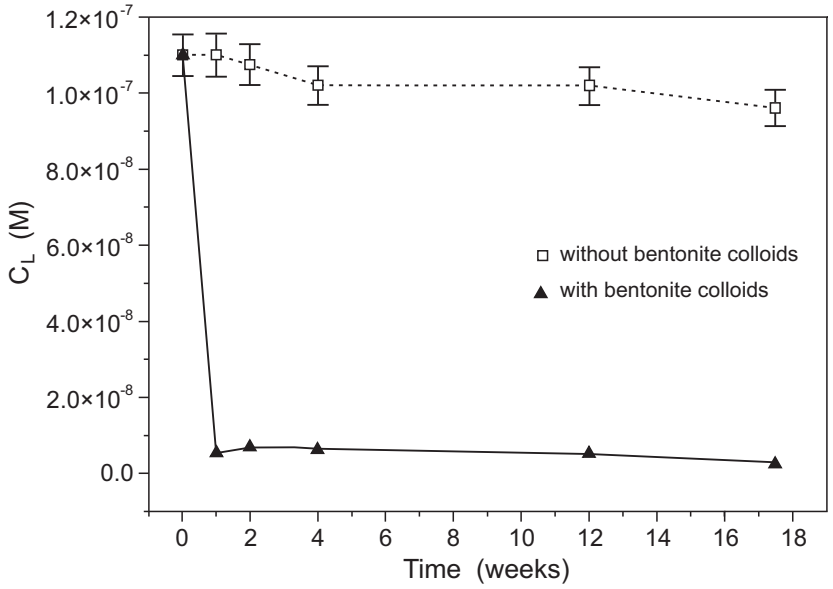

Fig. 4.2: Evolution of the ^{137}Cs concentration in Grimsel groundwater without and with bentonite colloids.

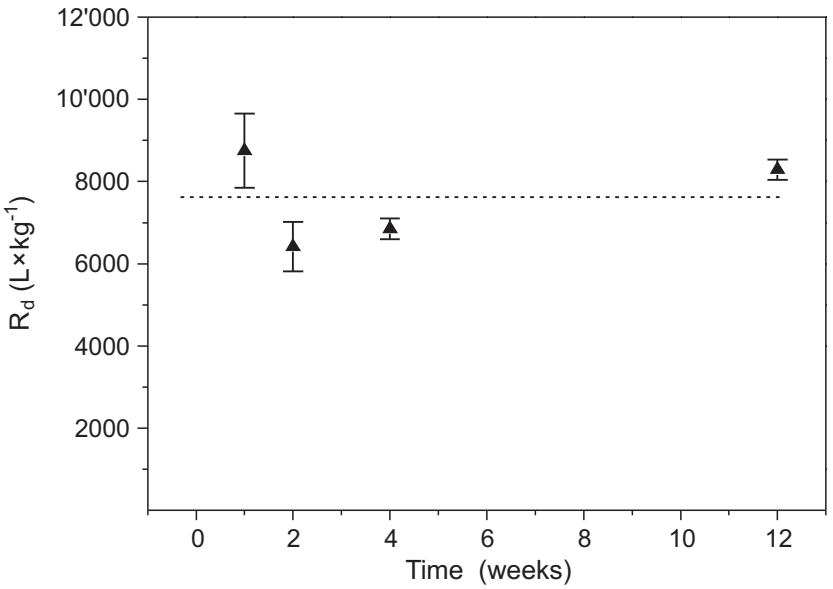

Fig. 4.3: Distribution coefficients of ^{137}Cs onto bentonite colloids in Grimsel groundwater (C_f around $1 \cdot 10^{-8}$ M).

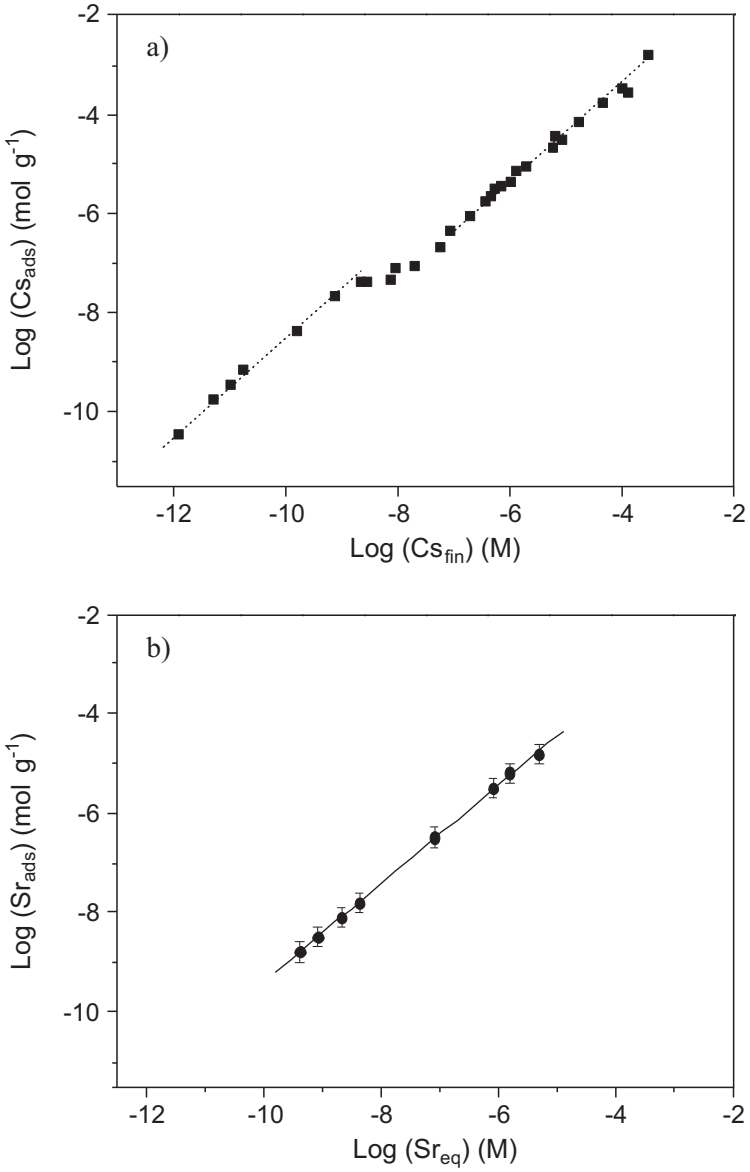

Fig. 4.4: Sorption isotherm for a) ^{137}Cs and b) ^{85}Sr onto bentonite colloids in Grimsel groundwater.

4.2.1.2 Sorption isotherms of ^{85}Sr and ^{137}Cs on bentonite colloids

Fig. 4.4a shows the sorption isotherm for ^{137}Cs interaction with bentonite colloids in Grimsel groundwater. The shape of the sorption isotherms indicated that ^{137}Cs sorption is not linear and suggests the existence of more than one sorption site (or sorption mechanism) for ^{137}Cs on bentonite colloids. The final concentration of ^{137}Cs in these experiments has been varied from approximately $1 \cdot 10^{-11}$ M to $1 \cdot 10^{-3}$ M and the contact time was 2 weeks. The plot of the logarithm of the concentration of ^{137}Cs adsorbed in colloids versus the logarithm of the final "equilibrium" ^{137}Cs concentration in solution clearly indicates a first linear zone at low ^{137}Cs concentration (the slope of the straight line is approximately 1), followed by a plateau and a further linear zone. The first type of sorption is linear below Cs concentrations in solution of around $1 \cdot 10^{-9}$M, which corresponds to the natural concentration of Cs in Grimsel water (Tab. 2.3) and hence the gradient of ~ 1 is compatible with an isotope exchange mechanism (effective Rd

~ 10,000 L kg^{-1}). Between final Cs concentrations of about $1 \cdot 10^{-9}$ and $1 \cdot 10^{-6}$ M, the gradient is one up to a saturation followed by a second range (concentration > $1 \cdot 10^{-6}$ M), where sorption is again linear (gradient ~ 1, effective Rd ~ 1,000 L kg^{-1}). It is known that K strongly competes with Cs for sorption sites and hence it is not surprising that this second linear phase occurs when final Cs concentration comes into the range of the natural concentration of K (~ 2 – $5 \cdot 10^{-6}$ M, Tab. 2.3)). Above such levels, indeed, Cs is no longer a "trace" element and lies in the range (or even above) the levels of the major solution cations. The linear sorption process is thus probably simple ion exchange. At the very highest concentrations, Cs has taken the entire exchange capacity (~ 1 meq g^{-1}). This sorption isotherm of ^{137}Cs on FEBEX bentonite colloids conditioned in Grimsel groundwater showed similar characteristics to those observed in the homoionised clay (Missana et al. 2004).

The step observed in the isotherm is not an artifact and does not depend on the Cs background concentration. Cesium sorption is not linear over the whole range of concentrations and the shape of the isotherm indicates that, at least, two different sites, with different affinity for Cs, are involved in sorption. The first site has high affinity and low capacity (~$3.2 \cdot 10^{-8}$ eq/g) and the second one with much higher capacity (~$1 \cdot 10^{-3}$ eq/g ~ CEC) but lower affinity.

The sorption isotherm of cesium in bentonite colloids conditioned to Grimsel water, presented in this study, shows similar characteristics to those previously observed by (Missana et al. 2002) in the homoionised (Na or Ca) FEBEX clay, in pure electrolytes. It was shown that sorption in the two different sites is controlled by different mechanisms. The existence of "low" and "high" affinity sites for cesium sorption in clays is usually explained considering that cesium can be exchanged with hydrated cations in basal/interlayer sites (low affinity sites) and can sorb, in a highly selective way onto frayed edge sites, FES, (high affinity sites) (Zachara et al. 2002). FES sites are not present in expanding clays like smectite but develop in weathered micas and illite.

The existence of smectite-illite mixed layer in FEBEX bentonite may possibly lead to the existence of FES-like sorption sites.

In order to compare the sorption behaviour of ^{137}Cs with the behaviour of another element which is expected to sorb mainly by ion exchange, sorption isotherms for Sr were produced. In addition, ^{85}Sr is an element that was also used in previous in situ tests in the GTS (see Frick et al. 1992).

Fig. 4.4b shows the sorption isotherm for ^{85}Sr on bentonite colloids in Grimsel groundwater. The contact time was 2 weeks. ^{85}Sr displays a different behaviour, showing linear sorption over the entire range of concentrations investigated (from $1 \cdot 10^{-10}$ to $1 \cdot 10^{-4}$ M approximately). However, this curve should not be overinterpreted as most of the concentration range lies below the natural concentration of Sr in Grimsel water (~ $2 \cdot 10^{-6}$; Tab. 2.3) when isotope exchange will dominate. Nevertheless, over the entire concentration range, the equivalent distribution coefficient measured for ^{85}Sr is Rd ~ 4,000 L kg^{-1}.

4.2.1.3 Sorption of ^{233}U on bentonite colloids

The initial concentration of U(VI) used in the experiments with bentonite colloids was $4 \cdot 10^{-7}$ M, as shown in Fig. 4.5. In the blank solution, an increase of the ^{233}U concentration was observed during the first weeks of the experiments. During this time, pH and Eh of the samples were measured extensively because they may affect the speciation, and consequently the sorption of the Redox sensitive elements. Since, in these experimental conditions, a single Eh measurement lasted few days, the bottles containing the suspensions were maintained without cap in the anoxic glove box for long periods. Evaporation is most likely the reason why the anomalous

increase of radionuclide concentration is observed in the blank solution. The fact that further increases was not observed at longer times (when pH and Eh measurements were made only in selected samples), supports this hypothesis.

Fig. 4.5 also shows the evolution of ^{233}U concentration in Grimsel groundwater in the presence of the colloidal phases. As can be seen, ^{233}U is sorbed less than ^{137}Cs on bentonite colloids. The calculated Rd values of ^{233}U are shown in Fig. 4.6. The Rd values for bentonite colloids increase significantly with time and after 18 weeks of the experiment equilibrium appears not to be completely reached.

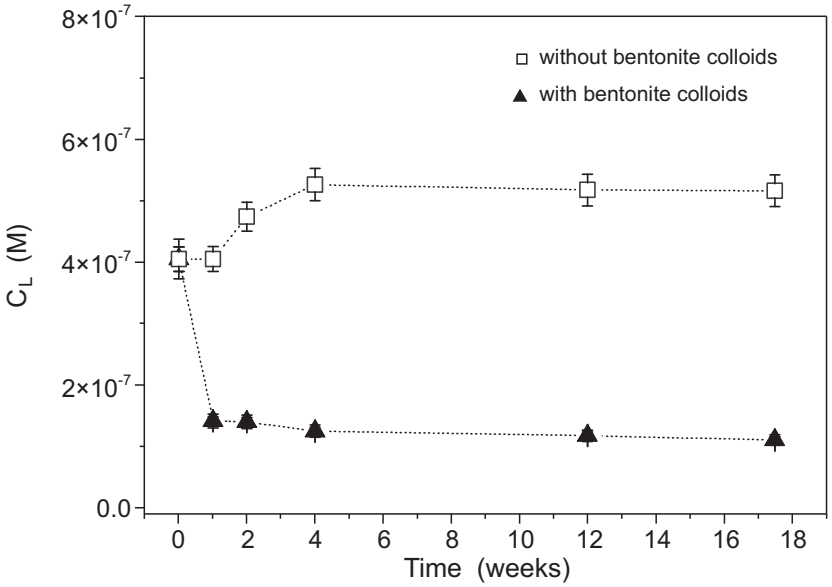

Fig. 4.5: Evolution of the concentration of ^{233}U introduced in the oxidised (VI) form in Grimsel groundwater without and with bentonite colloids.

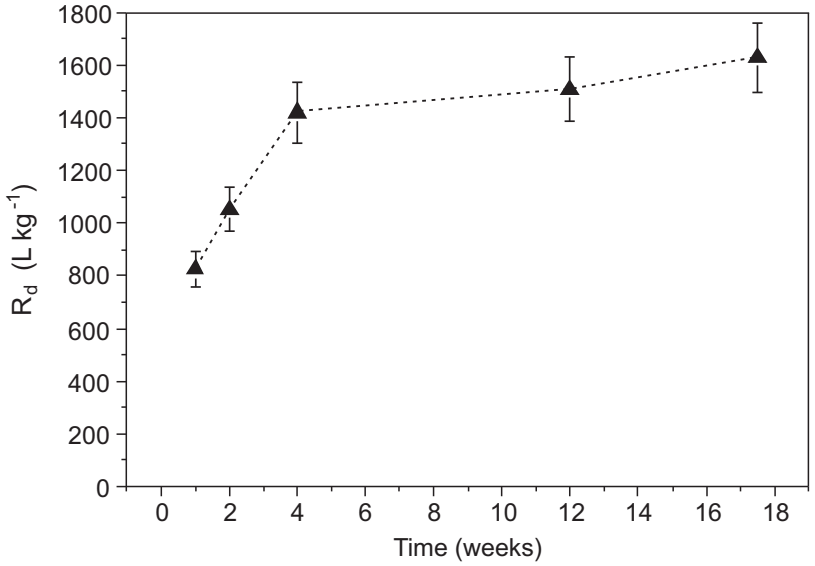

Fig. 4.6: Calculated distribution coefficients of ^{233}U introduced in the oxidised (VI) form in Grimsel groundwater onto bentonite colloids.

It has to be remarked that ^{233}U does not seem to be reduced in Grimsel groundwater in the absence of a solid phase. However, in the presence of colloids, it is very difficult to distinguish if the slow kinetic effects are due to sorption or redox changes. In the latter case, uptake onto the solid could involve precipitation (Tab. 2.4).

4.2.1.4 Sorption isotherms of ^{233}U on bentonite colloids

Fig. 4.7 shows the sorption isotherm of ^{233}U on bentonite colloids in Grimsel groundwater. The concentration of ^{233}U in these experiments has been varied from approximately $1 \cdot 10^{-7}$ M to $1 \cdot 10^{-4}$ M and the contact times were 1 day, 2 weeks and 3.5 months. Similarly to ^{137}Cs, the plot of the logarithm of the ^{233}U adsorbed on colloids *vs.* the logarithm of the equilibrium ^{233}U concentration in solution does not show linear behaviour over the entire concentration range. A line with slope 1 is included in the graph for comparison. The increase in the slope at higher concentrations might be attributed to ^{233}U precipitation. Precipitation seems to occur even at lower equilibrium concentrations in the curve for 3.5 months contact time. This could be a further indication of the partial reduction of U in the presence of the colloidal phase under the experimental anoxic / reducing conditions. A fit line with a gradient of 1 through the 5 lower concentration data measured after 1 day yields a Rd ~ 200 L kg^{-1}. After 2 weeks, the dataset with final concentrations in the range $10^{-8.5}$ to 10^{-5} M could be fit with a line of slope around 0.85, indicating than a "non-linear" Freundlich isotherm might be a better description of sorption. If, however, a line with gradient 1 is force-fit to data in the region with final concentrations in the range 10^{-7} to 10^{-5} M, an equivalent Rd of approximately 600 L kg^{-1} is obtained, which is somewhat lower than the values found in the previous series of experiments (Fig. 4.6), but is clearly in a time range where kinetics play a significant role.

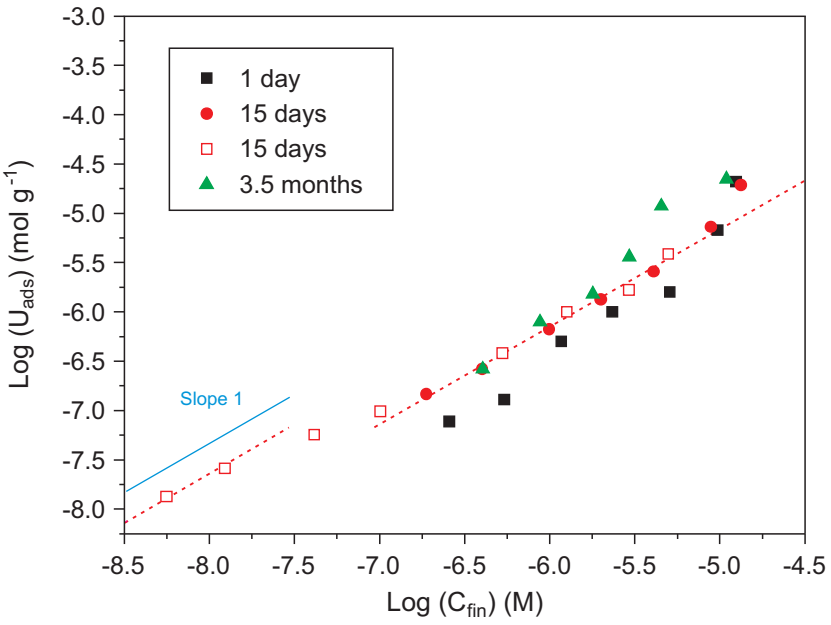

Fig. 4.7: Sorption isotherm of ^{233}U introduced in the oxidised (VI) form on bentonite colloids in Grimsel groundwater.

4.2.1.5 Sorption of ^{99}Tc(VII) on bentonite colloids

The initial concentration of Tc(VII) used in the experiments with bentonite colloids was $5.3 \cdot 10^{-7}$ M, as shown in Fig. 4.8. Also in this case, a slight (~ 10 %) increase in the ^{99}Tc concentration was observed in the blank solution during the first weeks of the experiments, attributed to evaporation of the samples. Fig. 4.8 also shows the evolution of the ^{99}Tc concentration in Grimsel groundwater in the presence of the solid phases. As can be seen in the Fig. 4.8, Tc is only weakly sorbed on bentonite colloids.

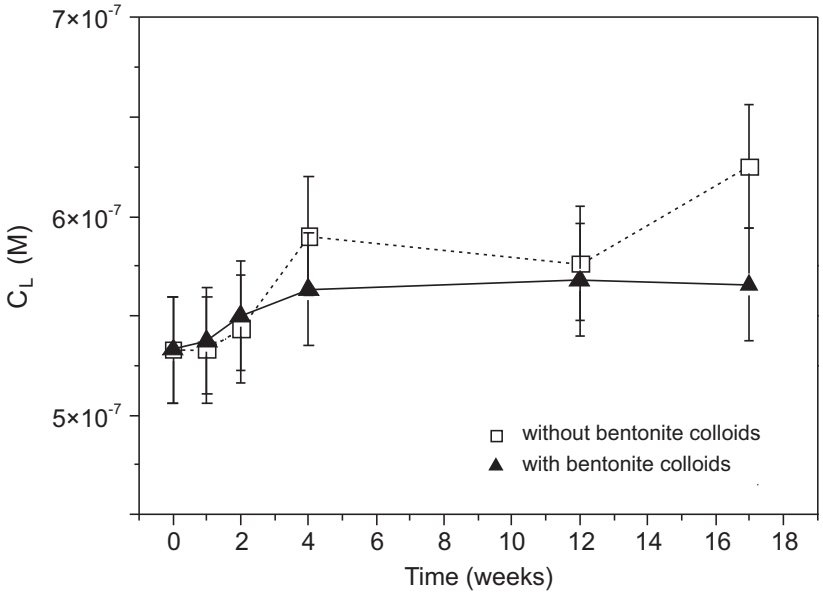

Fig. 4.8: Evolution of the concentration of ^{99}Tc introduced in the oxidised (VII) form in the Grimsel groundwater without and with bentonite colloids.

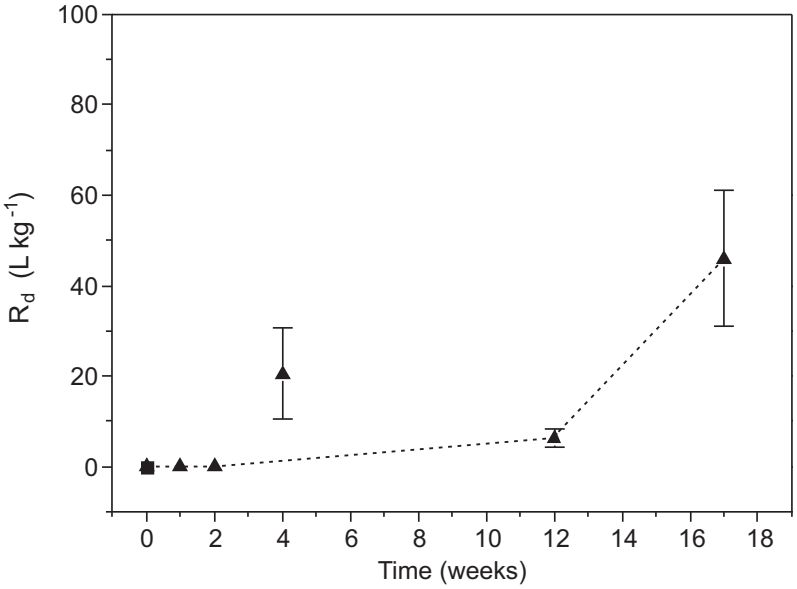

Fig. 4.9: Evolution of the distribution coefficient of ^{99}Tc introduced in the oxidised (VII) form in the Grimsel groundwater onto bentonite colloids as a function of time.

The calculated distribution ratios (Rd) for ^{99}Tc are shown in Fig. 4.9. The Rd for technetium is indistinguishable from zero at least for the first four weeks of the experiment. The positive Rd values after four weeks, plotted in Fig. 4.9, represent the mean value and range obtained averaging several samples. The progressive increase of the Rd values at longer times is, as with U, probably related to the reduction (of Tc(VII) to Tc(IV)). Indeed, again loss from solution could be partially attributed to the precipitation of the reduced species, since the concentration of Tc used in these experiments is substantially higher than the calculated solubility limit of Tc(IV).

4.2.1.6 Sorption of Tc(IV) on bentonite colloids

The ^{99}Tc(IV) solution was prepared by reducing the original ^{99}Tc(VII) solution with hydrazine. The concentration of the Tc before adding the reducing agent was $4.9 \cdot 10^{-6}$ M. After hydrazine addition, the solution was stored under a N_2 atmosphere, in an anoxic glove box. This solution was prepared in Grimsel groundwater to allow equilibration; the supernatant of the solution was periodically sampled and the activity measured. During the first few days, a continuous decrease in the activity of the supernatant was observed, reaching the steady state after approximately 10 days. After two weeks, this solution was ultracentrifuged (90,000 rpm, for 1 hour), in order to remove ^{99}Tc precipitates or colloids. The ^{99}Tc concentration in the supernatant was then measured as $7.4 \cdot 10^{-7}$ M. The supernatant was diluted again in Grimsel groundwater to produce a ^{99}Tc concentration of $4.5 \cdot 10^{-9}$ M and its activity was periodically measured following ultracentrifugation, in order to check long-term stability in these conditions; the results are plotted in Fig. 4.10. As shown in this Figure, no significant changes are observed, at least during the first month, indicating that the reduced Tc is stable in Grimsel groundwater at this concentration. The sorption behaviour in the presence of bentonite colloids is also shown in Fig. 4.10. In contrast to the behaviour of Tc(VII), the reduced species sorbs well on bentonite colloids, in fact approximately half of the radionuclide concentration has been removed from solution after one week. The calculated distribution coefficients (Rd) of reduced Tc are shown in Fig. 4.11.

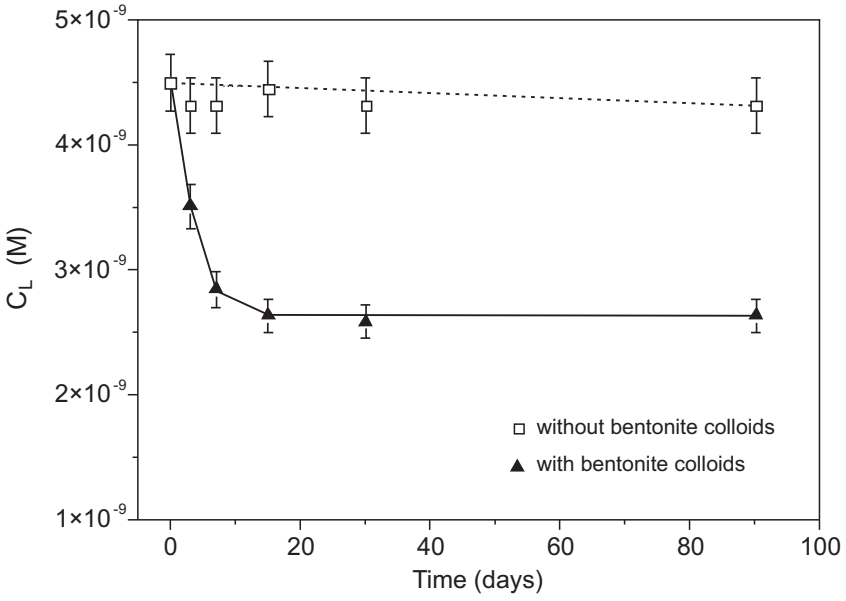

Fig. 4.10: Evolution of the concentration of ^{99}Tc introduced in the reduced (IV) form in Grimsel groundwater without and with bentonite colloids.

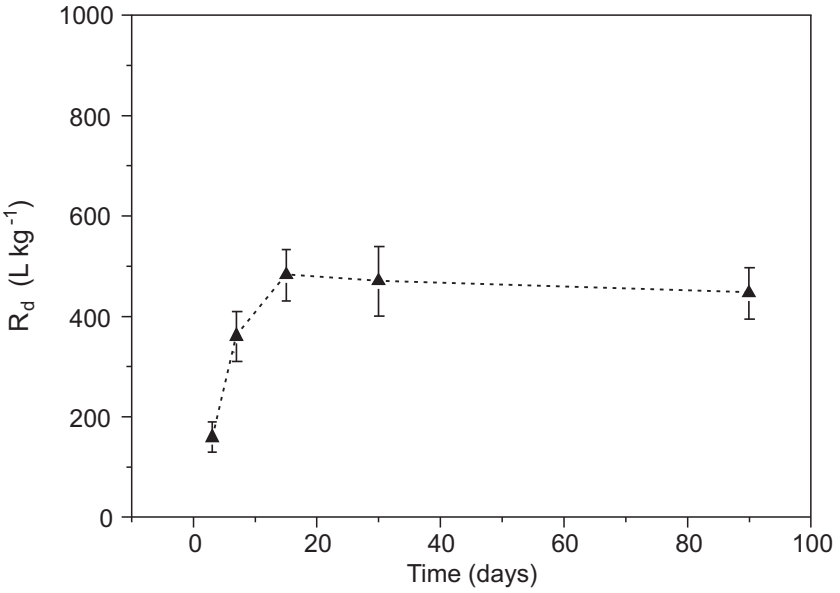

Fig. 4.11: Distribution coefficients of ^{99}Tc introduced in the reduced (IV) form in Grimsel groundwater onto bentonite colloids.

The Rd values for bentonite colloids clearly increase during the first two weeks of the experiment and, after this period, equilibrium appears to be attained. Compared to the oxidised species, as expected, the reduced ^{99}Tc is more strongly sorbed on the bentonite colloids as shown by the higher Rd values. In comparison with literature values (Rd between 10 and 100 Lkg^{-1} under reducing conditions: see, for example, Vieno & Nordman 1999) the data presented here seem high but this may be affected by the clay particle size. The degree of ^{99}Tc reduction with the used methodology, the influence of the reductant on sorption properties and the possible partial re-oxidation when introduced into Grimsel groundwater, was not checked.

4.2.1.7 Sorption of ^{75}Se on bentonite colloids

The initial concentration of ^{75}Se as selenite used in the experiments with bentonite colloids was $1.4 \cdot 10^{-7}$ M, as shown in Fig. 4.12. ^{75}Se uptake onto the clay shows slow kinetics. The calculated Rd values, shown in Fig. 4.13, tend to increase with time and it is possible that equilibrium has not been attained by the end of the experiment.

The observed kinetic dependence could be related to a progressive reduction of ^{75}Se(IV) to lower oxidation states even if this was not experimentally proven. ^{75}Se(IV) (SeO_3^{2-}), ^{75}Se(VI) (SeO_4^{2-}) and ^{75}Se(-II) all occur in anionic form and their affinity for a negatively charged clay (especially at the Grimsel groundwater pH) is expected to be very small. Values reported in the literature for the sorption of ^{75}Se in both oxidised and reduced form vary between 0 and 5 L kg^{-1} (e.g. Vandergraf and Ticknor, 1994). Oxidised Se species may be taken up by sulphate reducing bacteria which may be found as biofilms on clay surfaces (Hockin & Gadd 2003), but such analysis is outwith the scope of the present study.

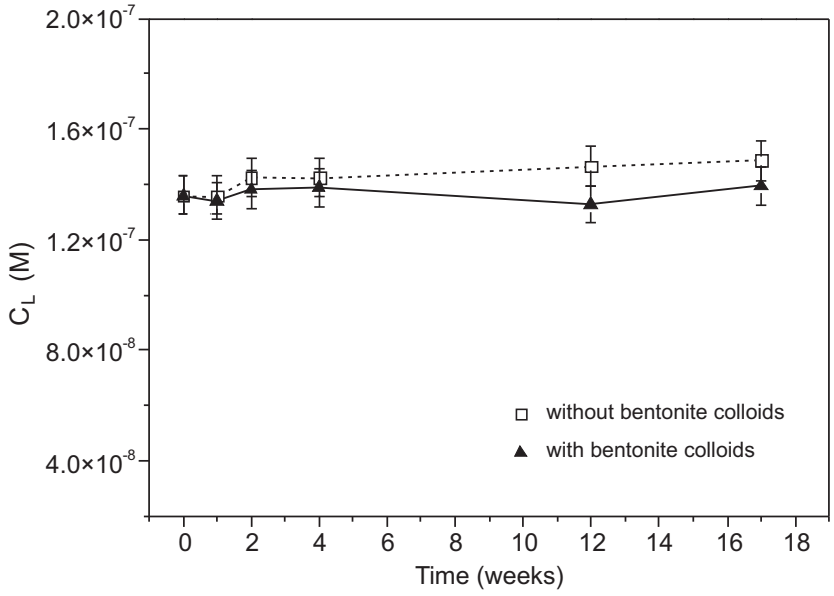

Fig. 4.12: Evolution of the concentration of ^{75}Se introduced as selenite in Grimsel groundwater without and with bentonite colloids.

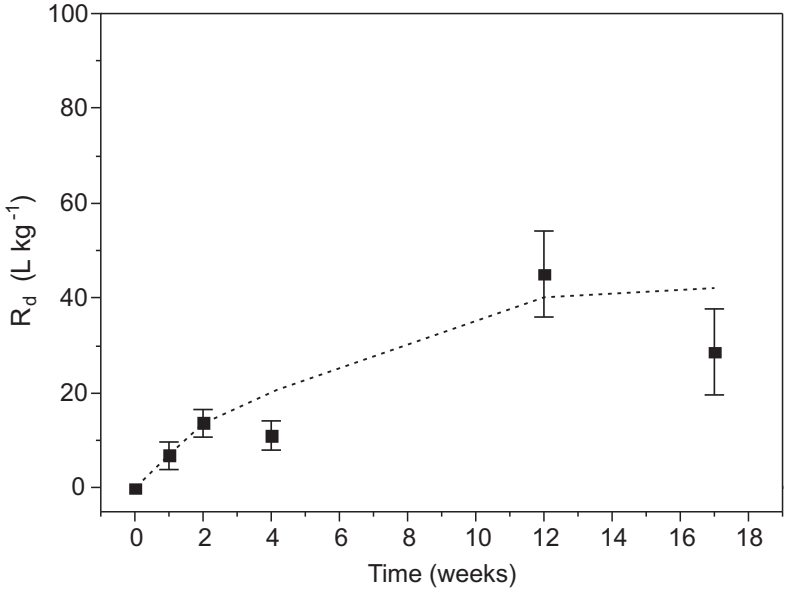

Fig. 4.13: Distribution coefficients of ^{75}Se introduced as selenite in Grimsel groundwater onto bentonite colloids.

4.2.1.8 Summary of sorption on bentonite colloids

The summary of the sorption data expressed as distribution ratios for bentonite colloids after different contact times (from 1 week up to 18 weeks) for all the investigated radionuclides is presented in Tab. 4.1. Those Rd values show that in several cases sorption is non-linear (concentration-dependence) shows slow kinetics and potential complications due to reduction and possible precipitation may appear.

Tab. 4.1: Calculated Rd values for bentonite colloids (L kg^{-1}) for radionuclides (with specified initial oxidation state for redox-sensitive species) at different contact times.

Solid	**Distribution coefficient Rd (L kg^{-1})**				
	Contact times				
	1 week	2 weeks	4 weeks	12 weeks	18 weeks
$^{75}Se(IV)$ $1.36 \cdot 10^{-7}$ M*					
Bentonite colloids	7.0 ± 3	14 ± 1	11 ± 3	45 ± 9	27 ± 9
$^{85}Sr(II)$ $1.03 \cdot 10^{-7}$ M					
Bentonite colloids	3980 ± 250	3950 ± 150	n.d	n.d	n.d
^{99} Tc(VII) $5.33 \cdot 10^{-7}$ M*					
Bentonite colloids	0	0	0	6.5 ± 2	46 ± 15
^{99} Tc(IV) $4.5 \cdot 10^{-9}$ M*					
Bentonite colloids	361 ± 50	482 ± 50	470 ± 70	446 ± 50	n.d.
^{137}Cs $1.10 \cdot 10^{-7}$ M*					
Bentonite colloids	8746 ± 900	6422 ± 600	6849 ± 250	8492 ± 250	n.d.
$^{233}U(VI)$ $4.04 \cdot 10^{-7}$ M*					
Bentonite colloids	824 ± 50	1050 ± 50	1420 ± 50	1508 ± 50	1628 ± 50

n.d. = not determined; * initial concentration

4.2.2 Sorption reversibility on bentonite colloids

Solute transport codes often adopt the "Kd" concept to predict retardation of dissolved radionuclides, accepting the major simplifications involved in this concept. Sorption is thus assumed to be instantaneous, linear and reversible. In the "linear" sorption concept the uptake of the contaminant is not affected by its concentration in the liquid phase which is clearly not true for many elements (as indicated in the previous section) and is well known from the literature (for example Cs in many rock and soil systems; see e.g. Oscarson et al. 1987; Staunton & Roubaud 1997).

The issue of reversibility of radionuclide uptake onto colloids is central to the CRR project. The impact of colloids on the long-range transport of radionuclides is very dependent on the extent of irreversibility of sorption because, if radionuclides readily desorb, small concentrations of colloids need to compete for radionuclides with the large quantity of sorbing minerals along the transport path. Calculations indicate that such reversible uptake would have very little (or no) effect on radionuclide migration in most relevant geological systems (Ryan & Elimelech 1996). In the CRR scenario, where the bentonite colloids are generated at the backfill/host rock interface, these would immediately contact "fresh" Grimsel groundwater, so the key question is whether any sorbed radionuclides would be released back into solution.

Desorption experiments were performed by carrying several re-equilibrations of the colloidal phase with Grimsel water after the initial sorption step. The study has been performed at CIEMAT with two nuclides that are of interest for the CRR project, ^{137}Cs and ^{233}U and which have shown to sorb on bentonite colloids. Both these elements show non-linear sorption and additional special attention has to be paid to possible differences in the kinetics of sorption / desorption processes.

In the "reversible" sorption concept, sorption and desorption rates should both be fast and the distribution coefficient measured in experiments where tracer is initially in the dissolved phase (Rd_{sor}) should be identical the distribution coefficient measured by desorption from sorbed phase into solution (Rd_{des}). Many of the commonly studied sorption processes occur in the time frame of seconds to weeks but, in natural environments, surface reactions can be significantly slower - on the time scale of years. The problem, however, is distinguishing slow sorption / desorption reactions from associated reactions such as solid-phase (or matrix porosity) diffusion or the formation / dissolution of surface precipitate / co-precipitate layers.

4.2.2.1 Dialysis bag desorption method

Different methods were used to study the reversibility of sorption onto bentonite colloids. The first utilised a dialysis bag method.

Here, 25 ml of bentonite colloid suspension (0.78 g L^{-1}) was sealed in a dialysis bag. The bag was then introduced into a polypropylene test tube filled with 35 ml of Grimsel groundwater, producing a total solution volume of 60 ml and an effective colloid concentration of 0.325 gL^{-1}. Experimental conditions are not exactly the same as described for the batch experiments in 4.2.1 (S:L 1:435)[15]. This water was spiked with ^{233}U or ^{137}Cs ($3.3 \cdot 10^{-7}$ M) and then the tube was closed and agitated constantly. Different samples were used for determining the "sorption" Rd at different contact times (Sample 1, 2, 3 or 4 corresponds to 1, 2, 3 or 4 weeks of contact time).

The "sorption" distribution ratio (Rd_{sor}) was calculated, as in the previous section. After the selected contact time, the water in the test tube was sampled in order to determine the radionuclide concentration and the Rd value was calculated assuming the total volume of solution in the test tube was well mixed. In order to verify this, a 5 ml sample of the colloidal suspension from the dialysis bag was centrifuged and the tracer measured in the supernatant. Exchange between the solution in the test tube and in the dialysis bag was shown to be kinetically hindered for contact times less than 1 hour, so sorption kinetics at very short contact time cannot be evaluated with this method.

After the sorption step, desorption was initiated. The bag containing the colloidal suspension was removed from the test tube, washed outside with Grimsel groundwater and located again in a test tube filled with 28 ml[16] of fresh Grimsel groundwater. The system was allowed to equilibrate with the fresh water during 1 week and then the radionuclide concentration in the solution was determined. After this determination, the bag was extracted from the test tube, washed with Grimsel groundwater and located in a test tube filled with 28 ml of fresh Grimsel groundwater. The "desorption" distribution ratios (Rd_{des}) were calculated by the following formula:

---

[15] The conditions were changed to ensure that the experiment was in the second part of the non-linear isotherm, where ionic exchange in the planar sites is dominating.

[16] Note that 28 ml and not 35 ml were removed as part of the suspension in the dialysis bag for measuring the activity. Therefore it was necessary to decrease the external liquid to maintain the initial solid to liquid ratio.

$$Rd_{des} = \frac{C_{ADS} - C_f^*}{C_f^*} \cdot \frac{V}{m} \qquad (3)$$

where:

- C_{ADS} is the initial calculated concentration of the element sorbed on the colloidal material in suspension (M)
- C^*_f is the final concentration measured in the liquid following re-equilibration (M)
- m is the mass of the sorbing phase (kg)
- V is the *total* liquid volume (L)

The desorption process was repeated up to three times. At the end of the experiment, the colloidal suspension within the dialysis bag was also sampled in order to determine the radionuclide concentration and to perform mass balance calculations for the sorbing species[17].

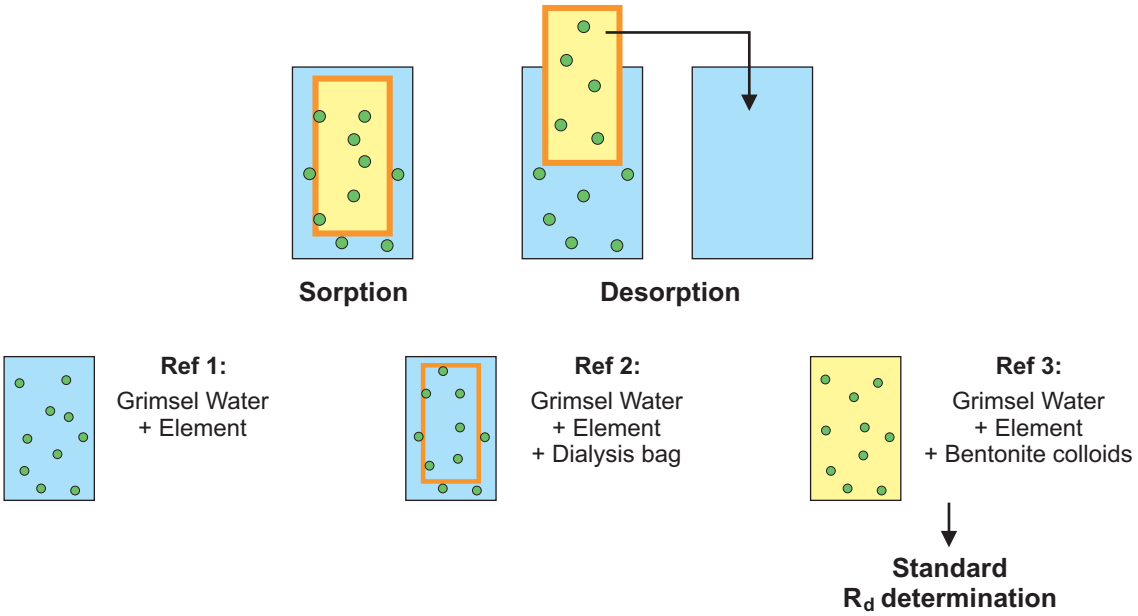

Fig. 4.14: Schematic diagram of the experimental measurement of desorption from bentonite colloids using the dialysis bag method.

In this experimental configuration, three different "references" were considered, as can be seen in Fig. 4.14:

- Reference 1 (Ref 1) consisted of 60 ml of Grimsel groundwater spiked with the element of interest, and it was used to check the stability of the element in the system without any bentonite colloids and to assess any possible sorption onto the test tube walls.
- The second "reference" (Ref 2) was used to check possible sorption on the dialysis bags and the test tube together, and consisted of 35 ml of Grimsel groundwater spiked with the radionuclide plus the dialysis bag filled with 25 ml of Grimsel groundwater.

[17] Note that, because of error propagation, mass balance was always checked during the experiments.

- In order to compare the Rd values obtained in this configuration with those obtained in a conventional batch sorption experiment, a third reference was considered (Ref 3), which consisted of a conventional Rd determination, using a colloidal suspension of 0.325 g L^{-1}.

4.2.2.2 Results and discussion

The main problem observed for this experimental method is that it is not reliable for all radionuclides. Fig. 4.15 shows the evolution of ^{137}Cs and ^{233}U in Grimsel groundwater in the presence of the dialysis bag (Ref 2) and without a bag (Ref 1). As can be seen, the measured ^{137}Cs concentration with or without the dialysis bag corresponds fairly well to the concentration added to the system. However, the concentration of ^{233}U for Ref 2 is well below the input value, presumably due to ^{233}U uptake on the dialysis bag (sorption in the bag?).

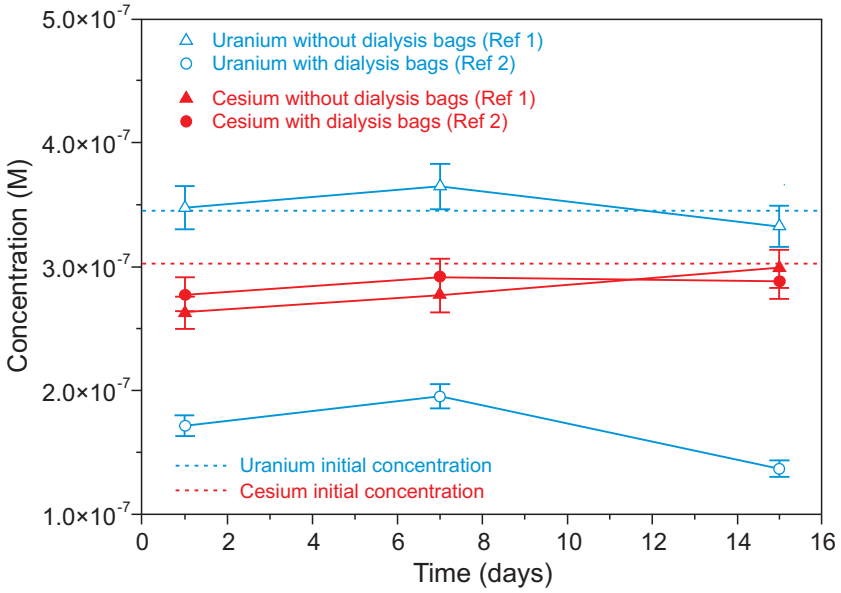

Fig. 4.15: Evolution of ^{233}U (open symbols) and ^{137}Cs (solid symbols) concentration with and without the dialysis bags. The dotted lines correspond to the calculated initial concentrations.

Therefore, Fig. 4.16 shows the results obtained with this method only for ^{137}Cs. Four different samples were initially considered, each of them having been in contact with ^{137}Cs for different time periods, (1, 2, 3 or 4 week). The Rd values obtained with the dialysis bag configuration varied between 7,000 and 7,500 L kg^{-1}; similar values, with less data scatter, were measured with the "standard" Rd determination (Ref 3).

The initial Rd_{des}, measured in samples 1 and 2, appears slightly lower than that observed for the sorption (Rd_{sor}), but values are within the given error bars and hence the significance should not be over-interpreted. Upon further washing, the Rd_{des}, values significantly increase. This could be interpreted as an indication of partial irreversibility but such a conclusion must be treated with great caution. The measured Cs sorption isotherm is strongly non-linear in the concentration range below $1 \cdot 10^{-7}$ M (Fig. 4.4a) and hence, even if sorption was fully reversible, decreasing the solution concentration of Cs in desorption steps would be expected to result in an increase of Rd.

As previously mentioned, only the samples 1 and 2 were used for the desorption experiment. The method was not practically reliable because the manipulation and washing of the bags in the anoxic glove box was complicated and because, occasionally, some leaking of colloidal suspension from the dialysis bag into the outer test tube water was observed. For this reason, the method was abandoned and a classical desorption approach was used.

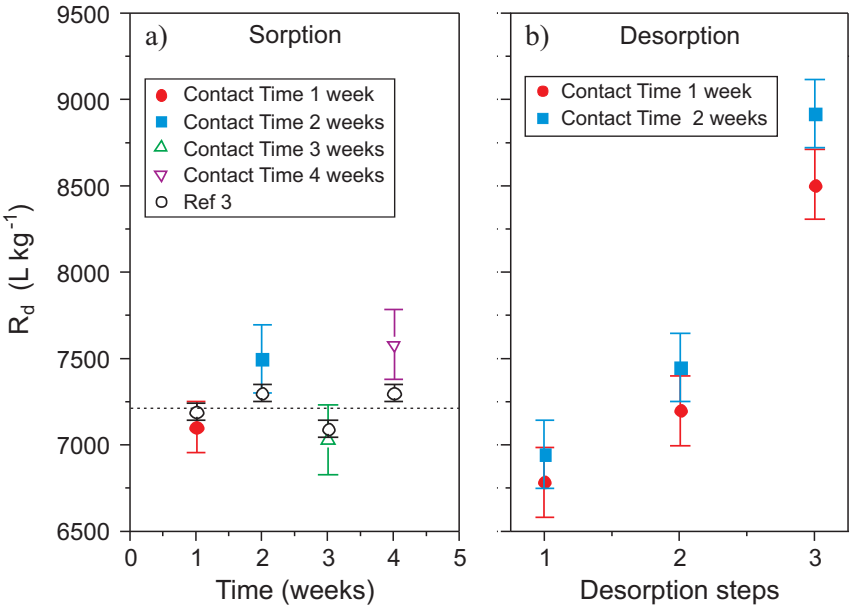

Fig. 4.16: ^{137}Cs desorption experiment with the dialysis bags.

a) "Sorption Rd" obtained in different samples maintained in contact with the tracer during different times. (Ref 3 corresponds to the standard Rd determination without dialysis bags). b) Rd obtained in successive desorption steps for the first and second sample (contact time: 1 week and 2 weeks) (Errors correspond to the results of triplicate experiments).

4.2.2.3 Classical desorption method

The second configuration used for desorption experiments was a "classical" one, consisting of a sorption experiment followed by separation of the solid and liquid phase, by centrifugation, and re-suspension of the solid phase in fresh solution. The main advantage of this configuration, with respect to the previous one, is that the behaviour of both elements of interest could be studied by the same method.

A bentonite colloid suspension of 2 g L^{-1} (S:L = 1:500 close to that used in experiments described in 4.2.1) was used for these experiments. This colloidal suspension was spiked with ^{233}U ($1 \cdot 10^{-7}$ M) or ^{137}Cs ($9 \cdot 10^{-8}$ M). In order to study sorption / desorption kinetics, after a defined contact time (1 day, 1 week, 2 weeks, 5 weeks or 8 weeks) two aliquots were removed from the test tube and centrifuged. Upon centrifugation, the closed tubes were transferred (again in the anoxic glove box) and the liquid was separated. The supernatant was used for the radionuclide analysis and the determination of the Rd_{sor}. Following this, the solid was contacted again with fresh Grimsel groundwater (maintaining the initial solid to liquid ratio) and carefully suspended again.

In the first desorption experiment, the clay was maintained in contact with the fresh solution for the same time as for the sorption experiment. The liquid was separated from the solid and the activity in the liquid phase was measured. In order to observe to what extent it is possible to "extract" further radionuclide fractions from the clay, it was contacted with fresh water and suspended again. This process was repeated on the same sample up to 4 times and the resulting Rd values obtained were compared with Rd_{sor}.

4.2.2.4 Results and discussion

a) Cesium

The results of this experiment, with ^{137}Cs are shown in Fig. 4.17. Sorption results are plotted in the right part of the graph and desorption results on the left part. This representation of sorption/desorption data is very useful to analyse sorption reversibility at a glance. The same symbol always refers to the same sample, in which sorption and then successive desorptions were performed. If sorption and first desorption graphs are symmetrical then sorption is reversible. For a reversible sorption process, it is generally assumed that not only $Rd_{sor} \approx Rd_{des}$ but also that sorption and desorption rates are similar.

In this concentration range, ^{137}Cs sorption appears to be fast on a timescale of days, in agreement with previous kinetics studies so that the variation in the sorption data can be attributed to inherent scatter (i.e. a measure of uncertainty). The mean value for the Rd, calculated for these experimental conditions and indicated in the Fig. 4.17 as a continuous line, is approximately 8,400 L kg^{-1}, which is similar to data measured previously (Figs. 4.3, 4.16).

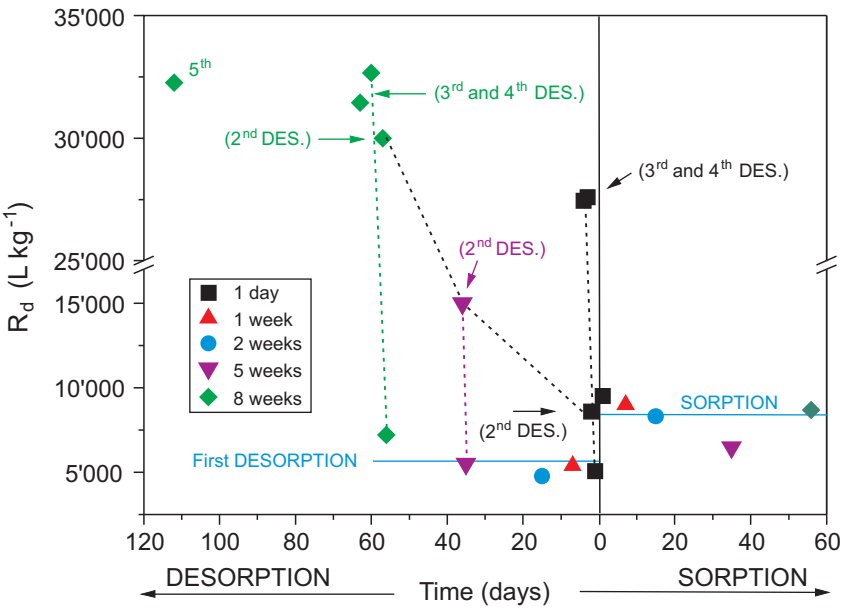

Fig. 4.17: Sorption and desorption kinetics of ^{137}Cs on bentonite colloids conditioned to Grimsel groundwater.

The same symbols refer to the same sample, on which sorption and then successive desorptions were performed. The estimated error is lower than 10 % in Rd values.

The first Rd_{des} values are always lower than the Rd_{sor} and, in spite of the different initial contact time, very similar. The mean value for the first Rd_{des} considering all the samples, is approximately 5600 L kg^{-1}. This result is similar to that observed in the previous experiment with the dialysis bags (Fig. 4.16). This finding is very surprising as both the effects of partial irreversibility of sorption and decreasing Cs concentration in the system (due to the shape of the isotherm in this concentration range) would be expected to result in Rd_{des} being higher than Rd_{sor}. Possible explanations would be either a small systematic error in the analytical procedure or an effect of slight changes in the chemistry of the system associated with the first desorption step.

For the sample that has been contacted with ^{137}Cs for one day, the Rd value obtained in the second desorption experiment is lower (~ 8,600 L kg^{-1}) than that of the samples contacted 5 or 8 weeks (~ 15,000 and ~ 30,000 L kg^{-1} respectively). The same occurs for the third and fourth desorption step. After the third desorption, the Rd_{des} values appear reasonably constant. These numerical values should be treated with caution due to error propagation during repeated desorption steps. Nevertheless, there seems a clear trend of an increase of calculated Rd for the second desorption step followed by effectively constant values thereafter. If the latter observation is correct, it suggests that Cs sorption is effectively completely reversible. The increase in Rd during the 2^{nd} desorption step reflects the strong non-linearity of the "plateau" in the isotherm (Fig. 4.4). At yet lower concentrations, sorption falls into the linear range – again as would be expected for an isotope exchange mechanism operating at tracer concentrations below the natural concentration of Cs in this system.

The non-linearity of Cs sorption is well documented and has been extensively discussed (Bradbury & Baeyens 1992). Even if the process is interpreted as an exchange process, part of the Cs has been considered to diffuse towards more energetically stable locations in the clay structure that are not immediately accessible. When ^{137}Cs is transferred to less available sites, "fixation" of the ion may also take place (Comans et al. 1991). The ^{137}Cs fixation in 2:1 clays has been reported to occur at the hexagonal cavity of the tetrahedral surface, and it is more favoured in montmorillonite-like than in illite-like smectites, as reported by Onodera et al. (1998).

Further interpretations focus on the fact that bentonite colloids are mainly formed by smectite. Smectite is a 2:1 layer silicate mineral, whose basic structure is composed of two tetrahedral (T) and one octahedral (O) sheets. The T-O-T layers are stacked and form the clay particles. These particles carry a permanent negative charge, due to isomorphic substitutions in the sheets (Al^{3+} for Si^{4+} in the tetrahedral sheet, and bivalent ions for Al^{3+} in the octahedral sheet). Cations are adsorbed at the surface of the clay particles and in the interlayers, to balance the structural negative charge.

In addition, on the edges of the layers, a pH dependent charge exists, due to protonation / deprotonation of the silanol (≡SiOH) and aluminol groups (>AlOH) and it can be either positive or negative. In smectites, this charge is very small in relation to the total charge of the clay (approximately 5 % in the FEBEX clay). However the surface reactions with these groups can significantly contribute to the sorption of certain radionuclides, especially actinides.

At the external surface of the clay particles, cations can adsorb both on basal planes (negatively charged) and negatively or positively charged edges or Frayed Edge Sites (FES). The other sites accessible to certain cations are, as was noted above, in the interlayer region. Sorption of ions in "basal / interlayer" and "edge" sites occurs predominantly as ion-exchange and surface complexation, respectively.

Surface complexation processes for ^{137}Cs on the edges of the clay particles can be disregarded because ^{137}Cs sorption was found to be independent of pH (Missana & García-Gutiérrez 2005). However, it is generally accepted that, in clay minerals, different sites exist for sorption and spectroscopic evidence of "different environments" for ^{137}Cs sorbed in clays can be found in the literature (e.g. Weiss et al. 1990; Kim et al. 1996).

Sorption of ^{137}Cs on FEBEX bentonite colloids is non-linear (Fig 4.4), which can be fit with a 2-site model, with one ion-exchange site of "high" affinity and another of "low" affinity. The non-linearity of ^{137}Cs sorption has previously been described in 2:1 clays e.g. (Oscarson et al. 1987; Staunton & Roubaud 1997) and 2-sites models have already been successfully used to model ^{137}Cs sorption data (Zachara et al. 2002). It has been suggested that a 3-site model is appropriate to model Cs sorption on a number of different clay minerals and over a wide range of chemical conditions (Bradbury & Baeyens 2000). Multi site models can be represented by a Freundlich isotherm – which is often found to provide an excellent empirical fit to Cs sorption data over the range between natural background and saturation of the exchange capacity.

In the CRR *in situ* experiment, it was found that, in presence of bentonite colloids, a small quantity of ^{137}Cs was able to move unretarded in the fracture along within the colloid contamination front (Möri 2004). Interestingly, this behaviour was not observed for Sr, although it is also adsorbed by bentonite colloids. The reason why this occurred may be related to the high adsorption of ^{137}Cs at low concentrations and the relatively slow kinetics of both sorption and desorption on an experimental timescale of hours (not addressed in this experimental study).

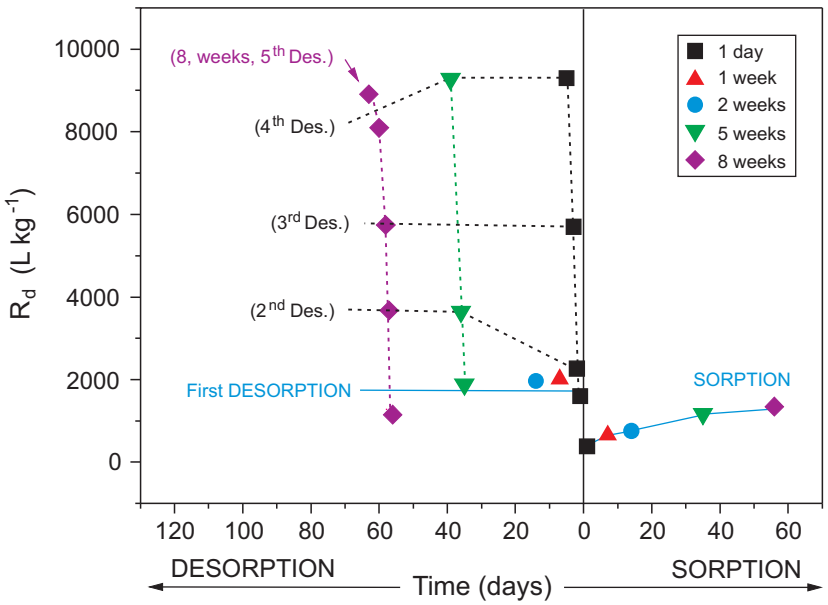

Fig. 4.18: Sorption and desorption kinetics of ^{233}U on bentonite colloids conditioned in Grimsel groundwater.

The same symbols refer to the same sample, in which sorption and then successive desorptions were performed. The experimental error is lower than a 10 % in Rd values.

b) Uranium

Fig. 4.18 shows the sorption / desorption behaviour of ^{233}U on bentonite colloids. Again, the same symbols refer to the same sample, in which sorption and then successive desorptions were

performed. An increase of the Rd_{sor} values as a function of time is observed (from ~ 390 to ~ 1'300 L kg^{-1}), although the sorption kinetics are not very fast. As already discussed in the previous section, the progressive increase in the Rd might be partially attributed to the reduction of the element[18]. As observed in previous experiments, the sorption isotherms of ^{233}U on bentonite colloids in Grimsel groundwater indicated non-linear sorption behaviour over the entire range of concentration examined. In the range of interest here (< ~ 10^{-7} M), a best fit line through the 15 days sorption data would give a gradient (Freundlich exponent) of about 0.7 - indicating that the "apparent Rd" would double for every order of magnitude decrease in aqueous concentration.

Although numerical values must be treated with caution, the mean Rd_{des} of the first desorption experiments (≈ 1,850 L kg^{-1}) is higher than measured sorption values and appears independent of the initial contact time. When further desorptions of the same sample were carried out, the Rd values for successively increase. Nevertheless, the values obtained at each desorption step are effectively independent on the initial contact time. The overall pattern is thus somewhat different from that observed previously for ^{137}Cs.

There is an extensive literature on U(VI) sorption. Previous sorption studies of U(VI) on smectites indicated that multiple surface species result both from ion exchange on planar sites and surface coordination reactions at the edge sites (Zachara & McKinley 1993; McKinley et al. 1995). U(VI) is preferentially sorbed by ionic exchange at acidic pH levels (Boult et al. 1998) and in low salinity waters. At higher pH and ionic strengths, the mechanism of surface complexation, with the formation of inner sphere complexes, will prevail (Turner et al. 1996). Several studies were made with spectroscopic techniques in order to explain the sorption mechanisms of the uranyl ion onto smectite clays. Different binding sites have been identified which are in agreement with observations in classical sorption studies. At pH< 6 and low ionic strength, the uranyl maintains its outer hydration shell so that an outer sphere mechanism (most probably cation-exchange) must be responsible of the binding (Sylvester et al. 2000). At near neutral pH, the evidence of inner sphere complexation (Sylvester et al. 2000) is shown. Above pH 5-6 the deprotonation of the silanol and aluminol groups provides additional sorption sites and, in addition, uranyl-hydroxide species start to form. Finally at "low" ^{233}U concentrations, the edge seems to be most important sites for ^{233}U uptake (Morris et al. 1994), with the formation of inner sphere complexes. As surface coverage increases, a less close approach of the uranyl to the surface and the formation of outer sphere complexes were observed (Chisholm-Brause et al. 1994).

The fact that the first Rd_{des} are always higher than Rd_{sor} could indicate that the U sorption process in bentonite colloids is not totally reversible within the experimental observation time frame, which might be a further corroboration of the hypothesis of the existence of surface complexation reactions, since a rapidly reversible process would be expected for a purely ionic exchange. Hysteresis of sorption / desorption has been already shown for actinides surface complexation onto colloidal phases (Lu et al. 1998). However, this may be rather simplistic for this particular case.

The strong increase of the measured Rd_{des} values beyond any obtained Rd_{sor} values suggests the occurrence of multiple reactions. U(VI) reduction might be one possibility. Because of this strong isotherm non-linearity and possible Redox disequilibria it is not possible to distinguish which are the causes for the observed irreversibility.

---

[18] Fast kinetics have been reported for sorption reactions of reduced U in the GTS groundwater/ rock system (see Alexander et al. 2003, for details).

4.2.3 Sorption on Grimsel granodiorite and fracture filling material

Sorption on Grimsel granodiorite

The initial tracer concentrations for the first sorption experiments on Grimsel granodiorite for ^{137}Cs(I), ^{233}U(VI), ^{75}Se(IV) and ^{99}Tc(VII) are the same than those used for the study of sorption kinetics described in the previous section (4.2.1). A second series of experiments was carried out to investigate sorption at shorter contact times. The calculated Rd values obtained in different experiments and the tracer concentration in each experiment are indicated in Tab. 4.2. The experiments with ^{99}Tc(IV) were carried out subsequently, to improve understanding of the behaviour of this element. A granodiorite size fraction lower than 64 μm and a solid to liquid ratio 1:4 (g ml^{-1}) were used for the sorption experiments.

The Cs results are shown in Fig. 4.19 and 4.20. The evolution of the ^{137}Cs concentration in the liquid phase, in the presence or absence of the solid phase is shown in Fig. 4.19, whereas the calculated Rd values are plotted in Fig. 4.20 (including the values obtained in the second, shorter contact time, experiment). The first three values in this plot were obtained in the second experimental batch and they are clearly higher than those measured the first time. Unfortunately, this is probably an artefact due to a factor 2 lower ^{137}Cs concentration for an element for which the isotherm is expected to be strongly non-linear as already observed in the bentonite colloid sorption studies.

The Rd values at equilibrium are not very high (~ 60 L kg^{-1}) and are much lower than those obtained for bentonite colloids. Apart of the initial decrease, which could, as noted above, be an artefact, the sorption of ^{137}Cs on Grimsel granodiorite does not seem to be affected by kinetics over the timescale of weeks.

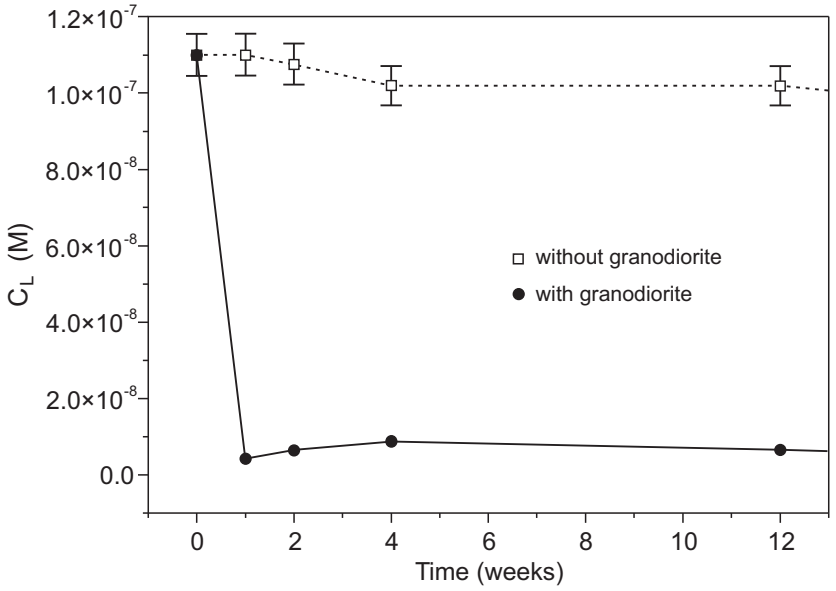

Fig. 4.19: Evolution of the ^{137}Cs concentration in Grimsel groundwater without solid added and in presence of Grimsel granodiorite.

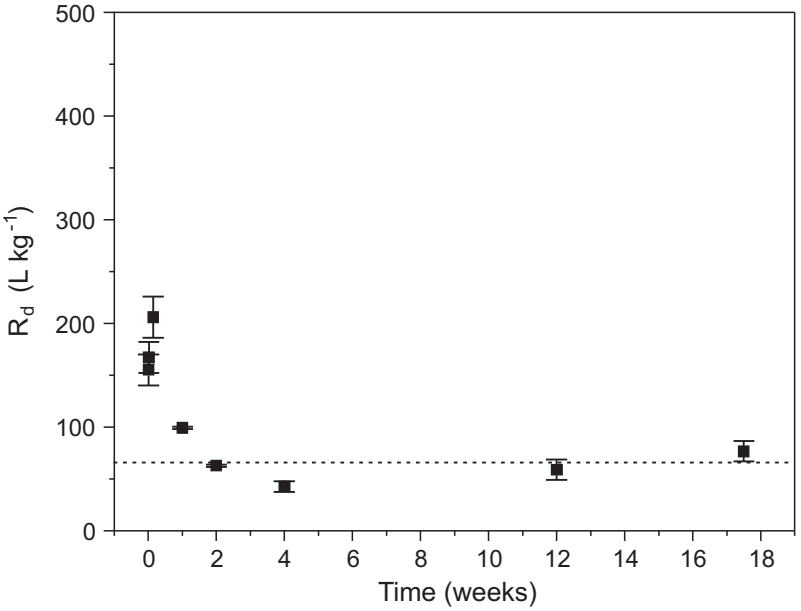

Fig. 4.20: Calculated distribution coefficients of ^{137}Cs on Grimsel granodiorite in Grimsel groundwater (Two different series of experiments are included here: note that total Cs concentrations are lower for the short term sorption studies).

The U results are shown in Fig. 4.21 and 4.22. The evolution of the ^{233}U concentration in the liquid phase, in the presence and absence of the solid phase is shown in Fig. 4.21, whereas the calculated Rds are plotted in Fig. 4.22. In this case, a significant effect of kinetics is observed, which could be related to a reduction process. In fact, the Rds calculated at times longer than two weeks are much higher than those expected for U(VI) on crystalline rocks and more typical of those expected for U(IV) (see for example García-Gutiérrez 2000). Interestingly, these results are very similar to those reported by Baston et al. (2003) for the sorption of ^{233}U(IV) on mylonite from the experimental shear zone. Here, Rd values of up to 280-430 L kg^{-1} (duplicate experiments) were reported, but with one major difference: the maximum Rd values were measured within 10 hours of the start of the experiment. This would suggest that any reduction of U(VI) to U(IV) in these CRR experiments is kinetically hindered.

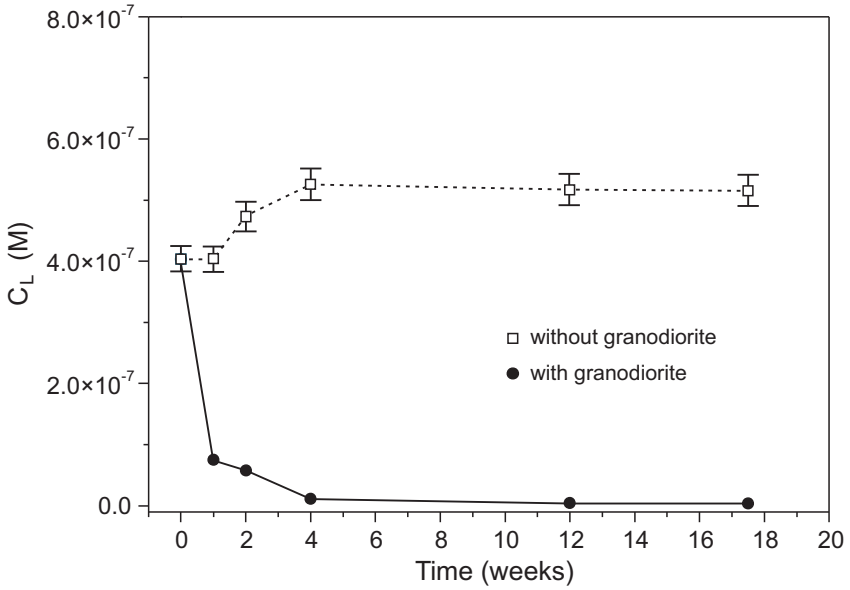

Fig. 4.21: Evolution of the ^{233}U concentration in Grimsel groundwater without solid added and in the presence of Grimsel granodiorite.

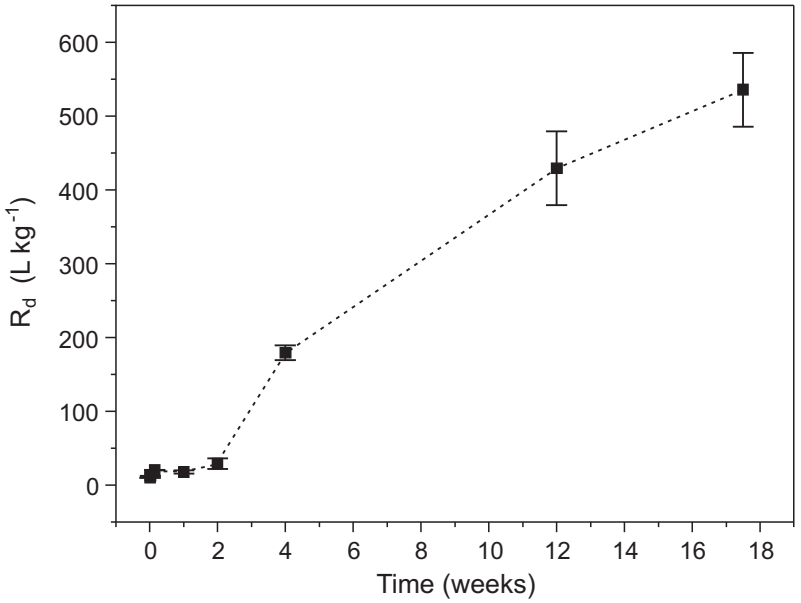

Fig. 4.22: Calculated distribution coefficients of ^{233}U on Grimsel granodiorite in Grimsel groundwater.

The ^{75}Se results are shown in Fig. 4.23 and 4.24. As for the ^{233}U experiments, the first three values in Fig. 4.24 were obtained in a different experiment.

The Rd values for ^{75}Se are very low during the first two weeks of the experiments and then, as occurred for U, start to increase. In this case, however, equilibrium seems to be attained within approximately 12 weeks. Again, the increase in the sorption values could be related to the reduction of the element and subsequent sorption or precipitation. The values expected for $^{75}Se(IV)$ sorption on crystalline rocks are generally lower than 10 L kg^{-1}, compared to the

35 – 40 L kg^{-1} measured here. Further support for this hypothesis comes from the data of Baston et al. (2003) where Rd values for the uptake of reduced ^{75}Se on mylonite (from the CRR experimental site) are as high as 57 L kg^{-1} (although they are variable due to experimental problems).

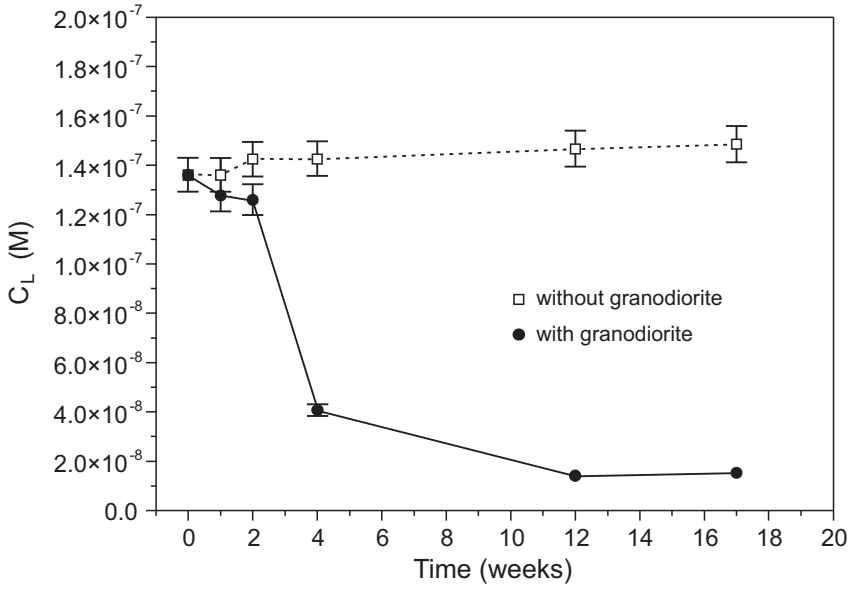

Fig. 4.23: Evolution of the ^{75}Se concentration in Grimsel groundwater without solid added and in the presence of Grimsel granodiorite.

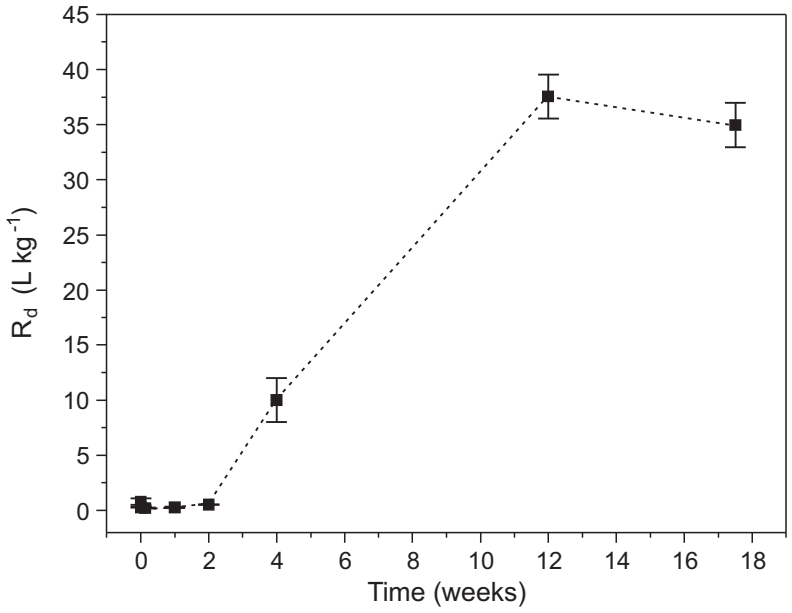

Fig. 4.24: Calculated distribution coefficients of ^{75}Se on Grimsel granodiorite in Grimsel groundwater.

The ^{99}Tc(VII) data are presented in Figs. 4.25 and 4.26. The uptake of Tc is high and Rd values increase rapidly during the first two weeks, then equilibrium appears to be attained. Indeed, the sorption kinetics on Grimsel granodiorite are much more rapid in the case of ^{99}Tc than was the case of ^{233}U or ^{75}Se. The Rd expected for Tc(VII) in crystalline rocks is near to zero, so it seems likely that some degree of reduction has occurred during the experiment. This would be in line with the observed *in situ* behaviour of Tc(VII) in the experimental shear zone (see comments in Smith et al. 2001b) where reduction of Tc(VII) to Tc(IV) is believed to take place over a period of several weeks.

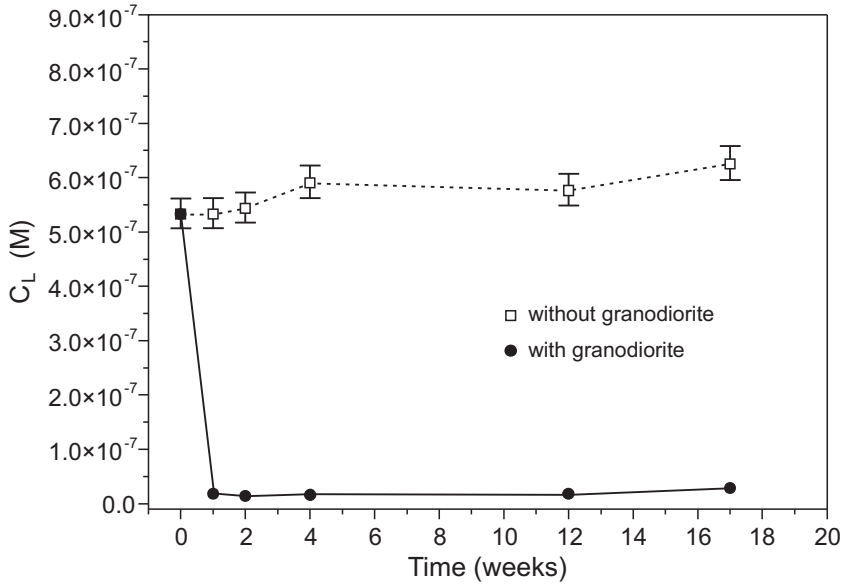

Fig. 4.25: Evolution of the concentration of ^{99}Tc introduced in the (VII) form in Grimsel groundwater without solid added and in the presence of Grimsel granodiorite.

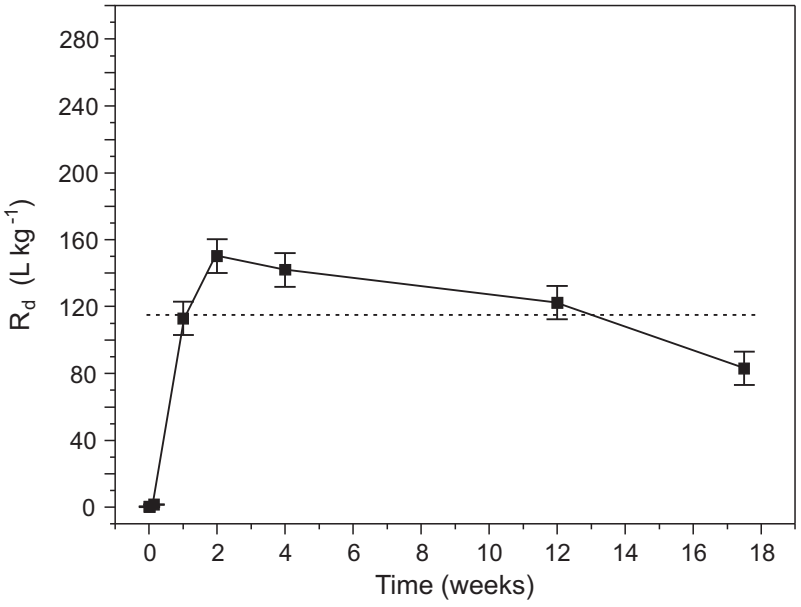

Fig. 4.26: Calculated distribution ratios for ^{99}Tc introduced in the (VII) form on Grimsel granodiorite in Grimsel groundwater.

Data for ^{99}Tc(IV) are presented in Fig. 4.27 and 4.28. The uptake of ^{99}Tc(IV) from the solution is significant and very rapid: Rd values increase significantly and attain an apparent equilibrium (about 115 L kg^{-1}) within a day. This equilibrium value is similar to that measured previously for Tc(VII) and that reported by Baston et al. (2003) for Tc(IV) sorption on mylonite from the experimental shear zone (a maximum Rd value of 180 L kg^{-1} was measured, although care must be taken with this data set as it seems likely that colloidal ^{99}Tc was present in the solution).

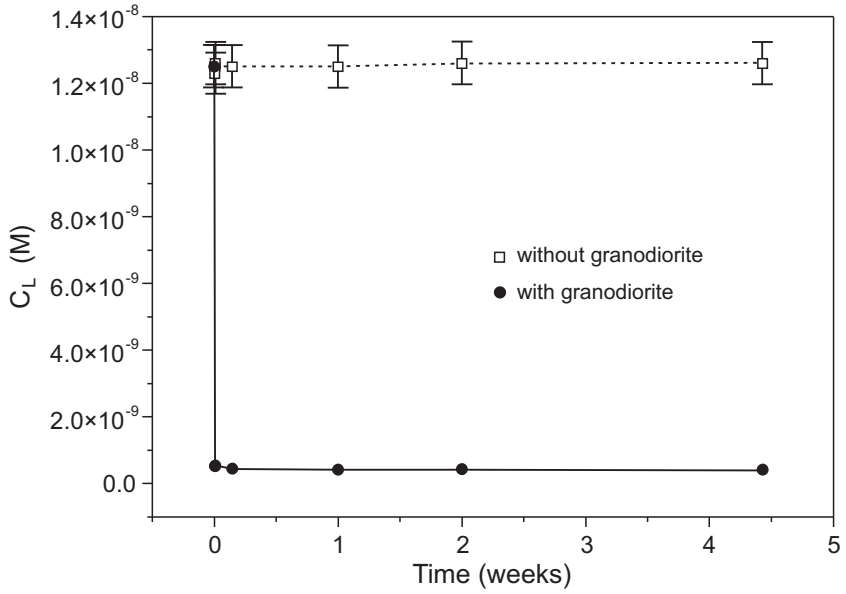

Fig. 4.27: Evolution of the concentration of ^{99}Tc introduced in the (IV) form in Grimsel groundwater without solid added and in the presence of Grimsel granodiorite.

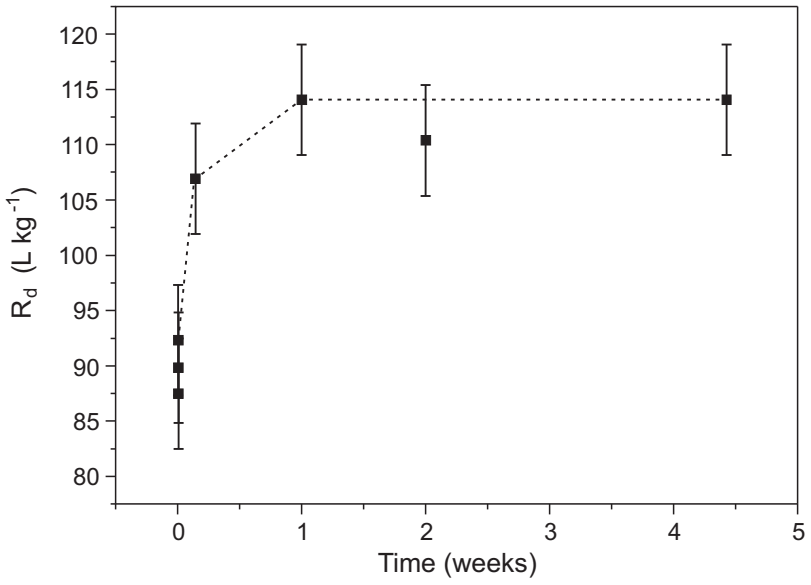

Fig. 4.28: Calculated distribution ratios for ^{99}Tc introduced in the (IV) form onto Grimsel granodiorite in Grimsel groundwater.

In general, these data compare well with literature values where the equilibrium Rd value obtained under anoxic conditions for Grimsel granodiorite (~ 140 L kg^{-1}) is significantly higher than that obtained under oxic conditions (< 1 L kg^{-1}; CIEMAT, unpubl. results). It is however clear that sorption data for reactions where redox reactions of the sorbing metal ion are included have to be considered with great care. The established distribution ratio depends very much on the overall redox potential of the system and redox disequilibria (i.e. Tc(VII) in solution and Tc(IV) sorbed) cannot be excluded. Furthermore, surface precipitation reactions may occur. The solubility of Tc(IV) with regard to TcO_2 lies in a range of 10^{-9} to 10^{-8} M (Duro et al. 2000). Final Tc concentrations fall pretty close into this range and might be also due to solubility constraints rather to pure surface sorption reactions.

Summary of Rd results on Grimsel granodiorite

The Rd values of ^{75}Se(IV), ^{99}Tc(VII), ^{99}Tc(IV), ^{137}Cs(I) and ^{233}U(VI) onto Grimsel granodiorite determined at different contact times are summarised in Tab. 4.2. In this table, the input oxidation state (where relevant) and the initial tracer concentration are also indicated.

Tab. 4.2: Rd values (L kg^{-1}) onto Grimsel granodiorite at different contact times and initial concentrations.

Solid	Distribution coefficient Rd (L kg^{-1})							
	Contact times							
	1 hour	2 hours	1 day	1 week	2 weeks	4 weeks	12 weeks	18 weeks
	^{75}Se(IV)							
Grimsel granodiorite	$1.7 \cdot 10^{-7}$ M 0.8±0.3	1.710^{-7} M 0.28±0.05	1.710^{-7} M 0.22±0.05	1.410^{-7} M 0.3±0.05	1.410^{-7} M 0.5±0.01	1.410^{-7} M 10±2	1.410^{-7} M 38±2	1.410^{-7} M 35±2
	^{99}Tc(VII)							
Grimsel granodiorite	2.810^{-7} M 0.34±0.06	2.810^{-7} M 0.18±0.09	2.810^{-7} M 1.67±0.15	5.310^{-7} M 113±10	5.310^{-7} M 150±10	5.310^{-7} M 141±10	5.310^{-7} M 122±10	5.310^{-7} M 83±10
	^{99}Tc(IV)							
Grimsel granodiorite	1.310^{-8} M 90±5	not determined	1.310^{-8} M 107±5	1.310^{-8} M 114±5	1.310^{-8} M 110±5	1.310^{-8} M 114±5	not determined	not determined
	^{137}Cs							
Grimsel granodiorite	5.810^{-8} M 155±15	5.810^{-8} M 167±15	5.810^{-8} M 206±20	$1.1 \cdot 10^{-7}$ 100±1	$1.1 \cdot 10^{-7}$ M 63±1	$1.1 \cdot 10^{-7}$ 45±5	$1.1 \cdot 10^{-7}$ M 60±10	$1.1 \cdot 10^{-7}$ M 77±10
	^{233}U(VI)							
Grimsel granodiorite	$1.1 \cdot 10^{-7}$ M 9.9±0.2	$1.1 \cdot 10^{-7}$ M 12.2±0.2	$1.1 \cdot 10^{-7}$ M 20.3±0.3	$4.0 \cdot 10^{-7}$ M 18±2	$4.0 \cdot 10^{-7}$ M 29±7	$4.0 \cdot 10^{-7}$ M 179±10	$4.0 \cdot 10^{-7}$ M 430±50	$4.0 \cdot 10^{-7}$ M 535±50

4.2.4 Sorption on fracture filling material

Four different sets of experiments were carried out to study the sorption kinetics of the selected elements on fracture material from the experimental shear zone. In the first set of experiments, three different size fractions of the solid were considered (< 71 μm, < 300 μm and < 1160 μm). The experiments were carried out using a solid to liquid ratio of 1:10 (kg L^{-1}). After equilibration between the groundwater and the solid, the pH of the suspension was very similar to that of the Grimsel groundwater (9.3). In this first set of experiments, the time span investigated for sorption was between 1 and 5 weeks.

A second set of experiments was carried out using a higher solid to liquid ratio (1:4) and focusing only on one size fraction (< 300 μm). The equilibrium pH was again very similar to that of the Grimsel groundwater (9.3). In this second set of experiments, the time span investigated was between 1 and 11 weeks.

A third set of experiments was carried out for shorter time scales (1h-1day) for a selected size fraction (< 300 μm) and both solid to liquid ratios (1:4 and 1:10). The last series of experiments has been carried out investigating very short times scales (less than 1 hour), for the size fraction < 300 μm, with a solid to liquid ratio 1:4 for ^{137}Cs and ^{233}U(VI) and ^{99}Tc(IV).

Experiments with ^{99}Tc(IV) on fracture materials were made only with the size fraction < 300 μm and the solid to liquid ratio 1:4 (kg L^{-1}). The initial concentrations of the tracers in each set of the experiment are detailed in Tab. 4.3 - 4.5. In these tables, the results of the sorption experiments on fracture materials, expressed as Rd values as a function of time, are summarised.

As can be seen in Tab. 4.3, the Rd values depend on the size fraction; larger size fractions have lower Rds, as expected, due to the lower available surface area per mass. However, the range in such values decreases at longer times (compare 1 week and 5 weeks of contact time), suggesting that diffusion processes into the bulk material are occurring and that, when the equilibrium is reached, these differences may not be very significant.

For any given size fraction, some trends can be observed: the lower solid to liquid ratios tend to have generally higher Rd values (although the differences are not large in any case) – which would be compatible with sorption non-linearity, but this is very difficult to assess because of associated changes in initial concentration.

In order to identify possible the kinetic hindrance of sorption in the *in situ* experiment, where the contact times between the injected tracer and the fracture material could be very short, it was considered necessary to make some sorption experiments at very short time scales (less than one hour). These experiments have been carried out only for ^{99}Tc(IV), ^{137}Cs and ^{233}U(VI). The results of the experiments are summarised in Tab. 4.5. Although these are difficult to compare to Tab. 2.4 because of different initial concentrations of Cs and U, in all cases it is noted that more than 50 % of the sorption at 1 hour is already reached within 5 minutes.

Tab. 4.3: Rd values (L kg^{-1}) on fracture filling material at different contact times, initial concentrations and input oxidation state (if relevant) for different fractions at a solid to liquid ratio of 1:10 kg L^{-1}.

Fracture filling material	**Distribution coefficient Rd (L kg^{-1})**			
	Contact times			
	1 hour	2 hours	1 week	5 weeks
^{75}Se(IV)				
< 71 µm	n.d.	n.d.	7.1E-08 M 7.5±0.2	n.d.
< 300 µm	$2.1 \cdot 10^{-7}$ M 1.7 ± 0.1	$2.1 \cdot 10^{-7}$ M 1.9 ± 0.1	$7.1 \cdot 10^{-8}$ M 6.6 ± 0.2	n.d.
< 1160 µm	n.d.	n.d.	$7.1 \cdot 10^{-8}$ M 2.8 ± 0.2	n.d.
^{99}Tc(VII)				
< 71 µm	n.d.	n.d.	$2.8 \cdot 10^{-7}$ M 8.7 ± 0.3	2.8E-07 M 8.1 ± 0.1
< 300 µm	$3.5 \cdot 10^{-7}$ M 0.4 ± 0.1	$3.5 \cdot 10^{-7}$ M 0.5 ± 0.1	$2.8 \cdot 10^{-7}$ M 3.0 ± 0.1	n.d.
< 1160 µm	n.d.	n.d.	$2.8 \cdot 10^{-7}$ M 0.4 ± 0.1	$2.8 \cdot 10^{-7}$ M 2.5 ± 0.1
^{137}Cs				
< 71 µm	n.d.	n.d.	$7.6 \cdot 10^{-7}$ M 910 ± 10	$7.6 \cdot 10^{-7}$ M 1640 ± 10
< 300 µm	$7.1 \cdot 10^{-8}$ M 540 ± 10	$7.1 \cdot 10^{-8}$ M 610 ± 15	$7.6 \cdot 10^{-7}$ M 720±10	$7.6 \cdot 10^{-7}$ M 1320 ± 10
< 1160 µm	n.d.	n.d.	$7.6 \cdot 10^{-7}$ M 450 ± 10	$7.6 \cdot 10^{-7}$ M 1580 ± 10
^{233}U(VI)				
< 71 µm	n.d.	n.d.	$2.2 \cdot 10^{-7}$ M 8.1 ± 0.2	$2.2 \cdot 10^{-7}$ M 15.4 ± 0.1
< 300 µm	$1.3 \cdot 10^{-7}$ M 5.2 ± 0.3	$1.3 \cdot 10^{-7}$ M 6.0 ± 0.2	$2.2 \cdot 10^{-7}$ M 5.3 ± 0.2	$2.2 \cdot 10^{-7}$ M 13.7 ± 0.1
< 1160 µm	n.d.	n.d.	$2.2 \cdot 10^{-7}$ M 1.8 ± 0.2	$2.2 \cdot 10^{-7}$ M 10.4 ± 0.1

n.d. = not determined

Tab. 4.4: Rd values ($L \cdot kg^{-1}$) on fracture filling material at different contact times, initial concentrations and input oxidation state (if relevant) for different fractions at a solid to liquid ratio of 1:4 in kg L^{-1}.

	Distribution coefficient Rd (L kg^{-1})							
Fracture filling material	Contact times							
	1 hour	2 hours	1day	1 week	2 weeks	4 weeks	6 weeks	11 weeks
				^{75}Se(IV)				
< 300 µm	$2.1 \cdot 10^{-7}$ M 1.5±0.2	$2.1 \cdot 10^{-7}$ M 1.6±0.2	n.d.	$2.9 \cdot 10^{-7}$ M 3.3±0.20	n.d.	n.d.	$2.9 \cdot 10^{-7}$ M 5.1±0.2	$2.9 \cdot 10^{-7}$ M 6.5±0.2
				^{99}Tc(VII)				
< 300 µm	$3.5 \cdot 10^{-7}$ M 0.3 ± 0.2	$3.5 \cdot 10^{-7}$ M 0.4 ± 0.1	n.d.	$2.2 \cdot 10^{-7}$ M 1.6 ± 0.3	n.d.	n.d.	$2.2 \cdot 10^{-7}$ M 6.8 ± 0.3	$2.2 \cdot 10^{-7}$ M 6.3 ± 0.3
				^{99}Tc(IV)				
< 300 µm	$1.3 \cdot 10^{-8}$ M 10±1		$1.3 \cdot 10^{-8}$ M 12±1	$1.3 \cdot 10^{-8}$ M 12±1		$1.3 \cdot 10^{-8}$ M 11±1		
				^{137}Cs				
< 300 µm	$7.1 \cdot 10^{-8}$ M 550 ± 10	$7.1 \cdot 10^{-8}$ M 600 ± 25	n.d.	$7.6 \cdot 10^{-8}$ M 690 ± 10	n.d.	n.d.	$7.6 \cdot 10^{-8}$ M 730 ± 10	$7.6 \cdot 10^{-8}$ M 1030 ± 20
				^{233}U(VI)				
< 300 µm	$1.3 \cdot 10^{-7}$ M 5.0 ± 0.4	$1.3 \cdot 10^{-7}$ M 5.6 ± 0.5	$1.3 \cdot 10^{-7}$ M 3.6 ± 0.5	$1.3 \cdot 10^{-7}$ M 4.2 ± 0.5 6.8E-07 M 5.6 ± 0.4	$1.3 \cdot 10^{-7}$ M 5.6 ± 0.5	$1.3 \cdot 10^{-7}$ M 6.3 ± 0.5	$6.8 \cdot 10^{-7}$ M 7.4 ± 0.5	$6.8 \cdot 10^{-7}$ M 6.4 ± 0.5

n.d. = not determined

Tab. 4.5: Rd values (L kg^{-1}) on fracture filling material at different contact times of less than one hour at solid to liquid ratio of 1:4.

Fracture filling material	**Distribution coefficient Rd (L kg^{-1})**			
	Contact times			
	5 min	15 min	30 min	60 min
		^{99}Tc		
< 300 µm	$1.3 \cdot 10^{-8}$ M 6 ± 1	n.d	n.d	$1.3 \cdot 10^{-8}$ M 10 ± 1
		^{137}Cs		
< 300 µm	$1.0 \cdot 10^{-7}$ M 300 ± 15	$1.0 \cdot 10^{-7}$M 350 ± 15	$1.0 \cdot 10^{-7}$M 410 ± 15	$1.0 \cdot 10^{-7}$M 450 ± 15
		^{233}U		
< 300 µm	$2.9 \cdot 10^{-7}$ M 0.8 ± 0.5	$2.9 \cdot 10^{-7}$ M 1.1 ± 0.5	n.d	$2.9 \cdot 10^{-7}$M 1.3 ± 0.5

n.d. = not determined

Fig. 4.29 to 4.33 summarise the results obtained for fracture material of the size fraction <300 μm and at a solid to liquid ratio 1:4 kg L^{-1} which is the most complete set of data. Fig. 4.29 shows the sorption kinetics of ^{137}Cs. As shown in the Fig. 4.29 and Tab. 4.4, the lowest Rd measured for ^{137}Cs (obtained after only 5 min) is 300 L kg^{-1}. This indicates extremely fast sorption of this element, which is expected to sorb preferentially by ionic exchange. Within one hour, this value is doubled and then a much slower kinetic process is observed. As discussed above with respect to bentonite colloids, this can be attributed to diffusion processes into the bulk of the particles. The extent of sorption in fracture material for ^{137}Cs is higher than in Grimsel granodiorite (Tab. 4.2), most probably due to the higher content of layer silicates and in particular biotite.

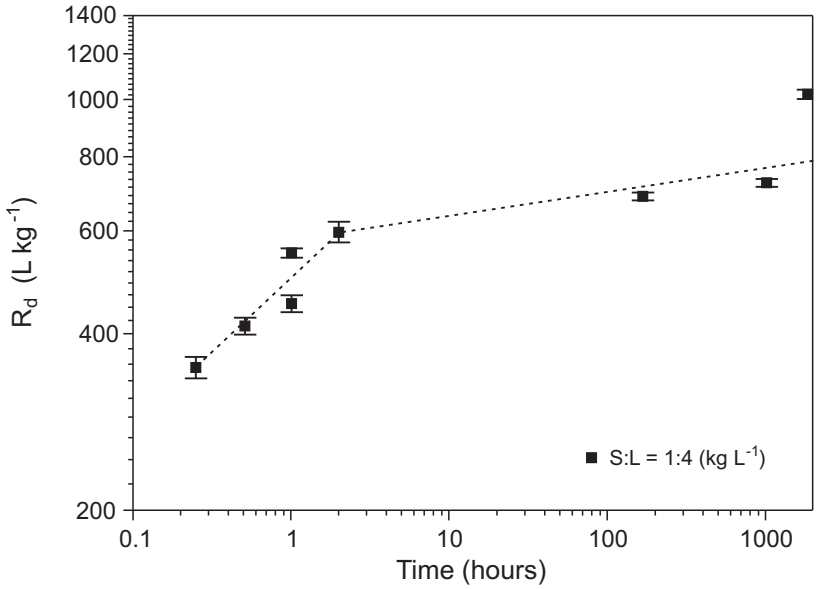

Fig. 4.29: Sorption kinetics of 137Cs on fracture material (< 300 μm) at a solid to liquid ratio of 1:4 kg L-1.

As a part of the laboratory support programme for previous field migration experiments at the GTS (MI experiment), the sorption of ^{137}Cs was also studied by Aksoyoglu et al. (1991) and Bradbury & Baeyens (1992). In particular, the authors studied the effect of the K concentration on the ^{137}Cs uptake. The Rd values that they obtained in experimental conditions similar to those here are well comparable.

Fig. 4.30 shows the sorption kinetics of ^{233}U. In this case, the lower sorption values are near to zero (0.8 ± 0.5 L kg^{-1}) and an initial rapid increase of the Rd value is observed, within the first hours, followed by a much slower increase (in agreement with Baston et al. 2003). Sorption equilibrium seems to be reached within approximately 1,000 hours (6 weeks). In this case, it is not possible to state that this kinetic effect is due to diffusion into the bulk of the particles since it could be also related to reduction of $^{233}U(VI)$ to $^{233}U(IV)$ (and possibly associated precipitation). Nevertheless, the fact that, at equilibrium, the Rd values are quite low (6 – 7 L kg^{-1}) seems to indicate that only a limited degree of reduction has taken place yet in this system. This is consistent with the data of Baston et al. (2003) for U(IV) uptake by crushed mylonite (< 250 μm size fraction) which showed Rd values climbing to 430 L kg^{-1} within 10 hours.

Of further note is the fact that the Rd values obtained on fracture filling material are much lower than those obtained on Grimsel granodiorite.

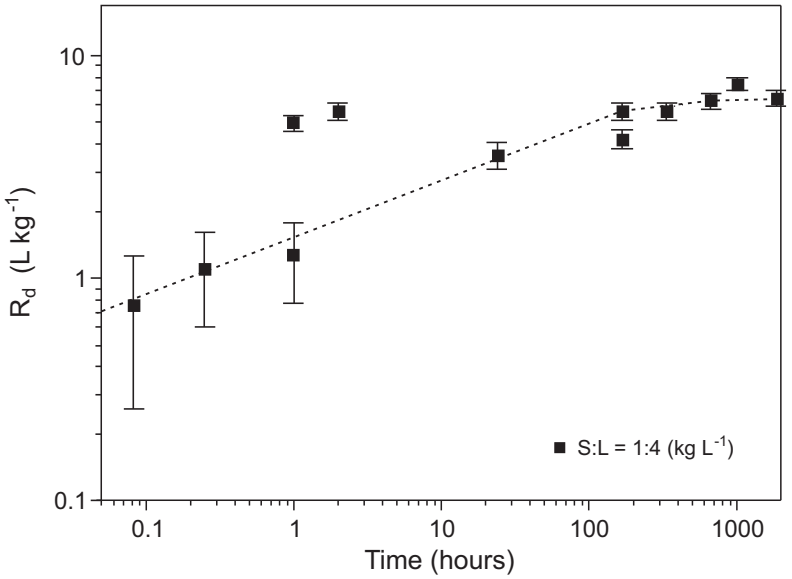

Fig. 4.30: Sorption kinetics of ^{233}U input in (VI) oxidation state on fracture material (< 300 μm) at a solid to liquid ratio of 1:4 kg L^{-1}.

For ^{75}Se(IV) and ^{99}Tc(VII) (see Figs. 4.31 and 4.32) the behaviour is somewhat different to that of ^{233}U(VI); the increase in Rd values with time is less sharp and equilibrium is not attained within 18 weeks. Baston et al. (2003), in contrast, observed little significant sorption of reduced ^{75}Se on crushed mylonite within 10 hours.

It is worth noting here that, like U, the Rd values for Se and Tc are lower for fracture filling material than for Grimsel granodiorite; which seems to indicate that the Grimsel granodiorite is acting as a more efficient reductant than the fracture filling material. This may seem counter-intuitive as, first, the smaller particle size of the fracture filling material would presumably allow more rapid access to the reducing capacity of the rock and, second, the Fe-rich mica, biotite, is relatively enriched in the fracture filling material compared to the Grimsel granodiorite. Therefore CIEMAT measured the Fe(II) / Fe(III) ratio in both, Grimsel granodiorite and fracture filling material. The results that were obtained were 1.6 and 0.6 which indicates that effectively the fracture filling material was more oxidised than the Grimsel granodiorite. This agrees with measurements by Meyer at al. (1989) indicating that the fracture filling material (which is derived from the mylonite/Grimsel granodiorite parent rock) appears to have undergone some degree of oxidation, probably due to weathering reactions. However, it cannot be ruled out that the oxidation is an experimental "artefact" due to the preparation of the sample in air.

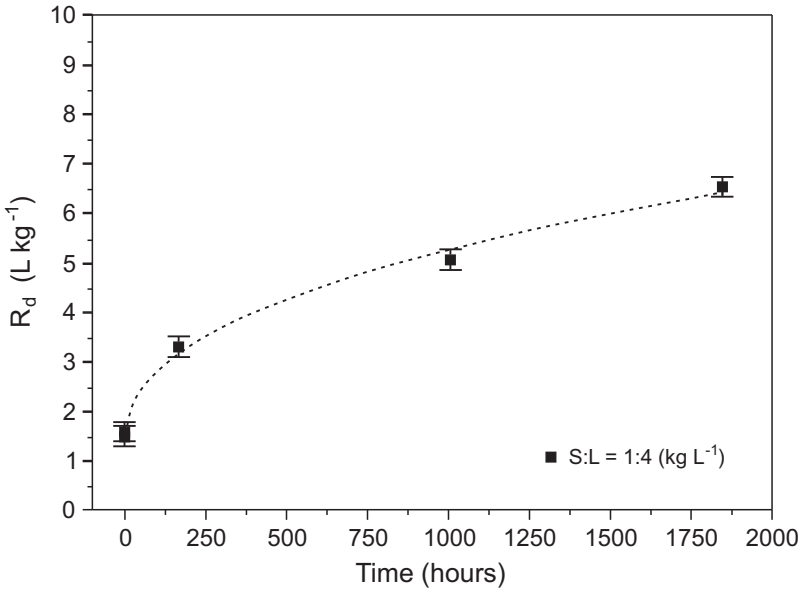

Fig. 4.31: Sorption kinetics of ^{75}Se input in (IV) oxidation state on fracture material (< 300 μm) at the solid to liquid ratio of 1:4 kg L^{-1}.

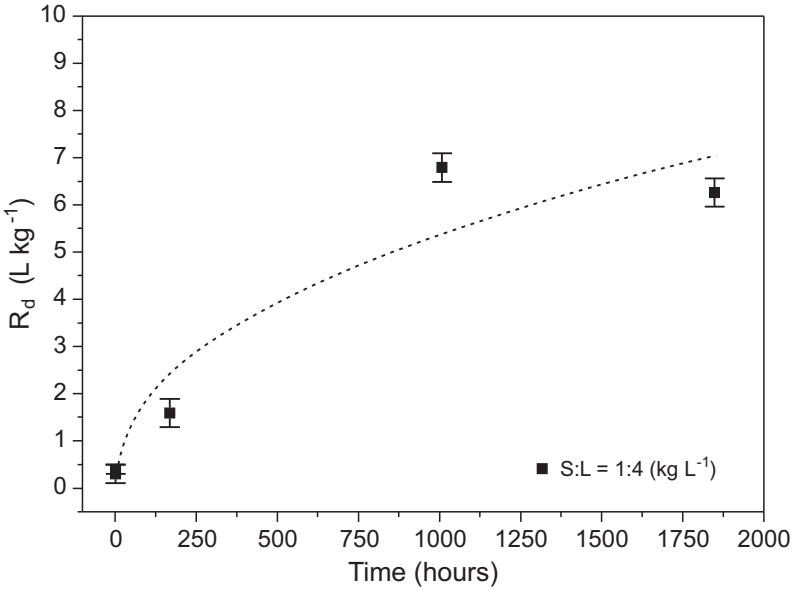

Fig. 4.32: Sorption kinetics of ^{99}Tc input in (VII) oxidation state on fracture material (< 300 μm) at a solid to liquid ratio of 1:4 kg L^{-1}.

The sorption of ^{99}Tc(IV) onto fracture materials is shown in Fig. 4.33. In this case, sorption is very rapid. After 5 minutes, more than the half of the equilibrium value (which is reached within a day) is measured. Interestingly, Baston et al. (2003) measured Rd values up to an order of magnitude higher than these for ^{99}Tc(IV) sorption on crushed mylonite, but they did note experimental problems and suggested that colloidal ^{99}Tc could have been present in the solutions.

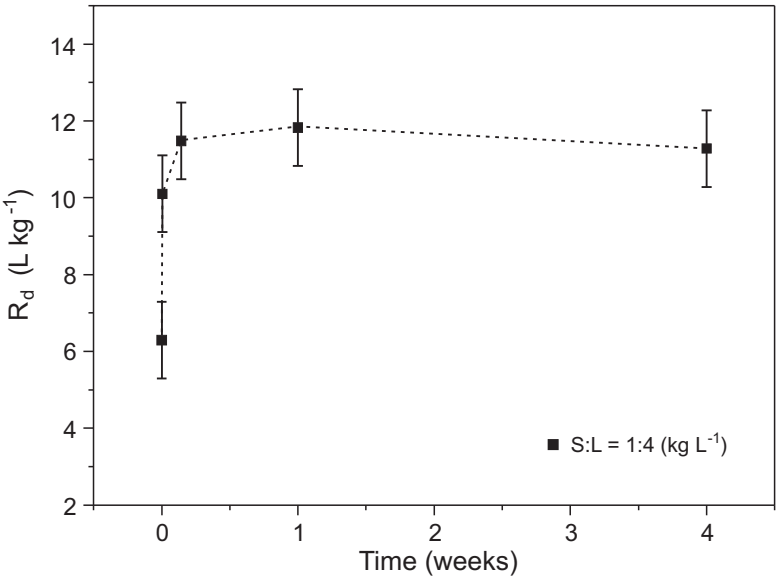

Fig. 4.33: Sorption kinetics of ^{99}Tc input in (IV) oxidation state on fracture material (<300 μm) at the solid to liquid ratio of 1:4 kg L^{-1}.

4.2.5 Sorption onto fracture filling material in the presence of bentonite colloids.

4.2.5.1 Experimental methods and results

In systems composed of more than one sorbing phase, it is of great interest to determine the distribution of the radionuclides between them and to determine if a particular phase dominates uptake of specific radionuclides. In particular, the aim of this section is to evaluate the sorption of ^{137}Cs and ^{233}U on fracture filling material in the presence of bentonite colloids. All experiments were carried out under N_2 atmosphere (O_2< 1 ppm) and two experimental configurations were considered. The first configuration included the use of dialysis bags with ^{137}Cs, as already described above (Section 4.2.2). The second method, applicable to both radionuclides, was also used to study the sorption onto small pieces of fracture filling material (millimetre sized rock pieces from the fracture walls) in presence of bentonite colloids. Small pieces of rock instead of fine-grained fractions of fracture filling material were used to simplify the separation of the phases when dialysis bags could not be used.

4.2.5.2 Dialysis bags

The first experimental configuration, with dialysis bags, was similar to that used for the studies of sorption irreversibility, but an additional phase (fracture filling material) was now added. The total volume of the Grimsel groundwater in these experiments was 30 ml. Fracture filling material (2 g, size fraction < 1180 μm) was added to a test tube containing 25 ml of Grimsel groundwater. 5 ml of 0.78 g L^{-1} colloidal suspension was added to the dialysis bag which was then placed in the test tube, giving a bentonite colloid concentration in the whole system of 0.13 g L^{-1}. The solid to liquid ratio of the fracture filling material in the system is 1:15 kg L^{-1}. The system was allowed to equilibrate for at least one day, then the water was spiked with ^{137}Cs (3.3E-7 M). Following addition of the tracer, the tubes were agitated constantly. After 1 day or 1 week, the dialysis bag was removed from the test tube and an aliquot of the suspension (Grimsel groundwater and fracture filling material) in the test tube was extracted and

centrifuged to determine the radionuclide concentration in the liquid phase. At the end of the experiment, the colloidal suspension within the bag was also sampled in order to determine the radionuclide concentration, to check the mass balance of the sorbing species.

In the system without colloids, at the equilibrium, the initial cesium mass (M_{Cs}^{in}) is distributed between the fracture material (M_{Cs}^{ffm}) and the Grimsel water (M_{Cs}^{wat}) and $M_{Cs}^{in} = M_{Cs}^{ffm} + M_{Cs}^{wat}$. In the system with colloids, the cesium will be adsorbed also in the colloidal phase and therefore: $M_{Cs}^{in} = M_{Cs}^{coll} + M^{*ffm}_{Cs} + M^{*wat}_{Cs}$, where M_{Cs}^{coll} is the mass of cesium adsorbed in the colloids and $M^{*ffm}_{Cs}, M^{*wat}_{Cs}$ represent the masses in adsorbed in the fracture material and in the water, in the three phases equilibrium, respectively.

As mentioned before, in the system with colloids, the sampling is made in the water and within the bag. The mass in the colloids can be calculated from this relation:

$$M_{Cs}^{coll} = M_{Cs}^{bag} - M^{*\mathrm{wat}}_{Cs} \frac{V^{bag}}{V} \tag{4}$$

where M_{Cs}^{bag} is the mass of cesium in the bag, V is the total volume of Grimsel water and V^{bag} is the volume of liquid in the dialysis bag.

Also the mass onto colloids can be derived, according to the following formula:

$$M^{*ffm}_{Cs} = M_{Cs}^{in} - M_{Cs}^{bag} + M^{*wat}_{Cs} \frac{V^{bag}}{V} - M^{*wat}_{Cs} \tag{5}$$

After the calculation of the radionuclide distribution, the percentage of sorption on each phase could be determined and the distribution of ^{137}Cs between the fracture filling material and the bentonite colloids estimated. The results of the experiment are summarised in Tab. 4.6.

Tab. 4.6: Adsorption of ^{137}Cs on fracture filling material (< 1150 μm) in the presence or absence of bentonite colloids.

	Initial Cs	Adsorbed Cs *(measured)*	Cs in colloid suspension* *(measured)*	Cs on colloids *(calculated)*	Cs on fracture filling material	Cs on fracture filling material
	(μg)	(μg)	(μg)	(μg)	(μg)	(%)
1 day (without colloids)	2.34	2.27	no colloids	no colloids	2.27	≈ 97
1 week (without colloids)	2.34	2.27	no colloids	no colloids	2.27	≈ 97
1 day (with colloids)	2.34	2.29	0.18	0.17	2.18	≈ 93
1 week (with colloids)	2.34	2.28	0.18	0.17	2.11	≈ 90

* without centrifugation

In the system in which the bentonite colloids were added, the percentage of ^{137}Cs adsorbed in the fracture material decreased. It seems clear that the presence of even a small quantity of bentonite colloids (4 mg, however with a large surface area for sorption) compared to the fracture material mass (2 g), can affect the uptake of ^{137}Cs by the rock.

4.2.5.3 Sorption onto small pieces of fracture material in the presence of colloids

In order to investigate the sorption behaviour of Cs and U on fracture material in the presence of colloids, small pieces of rock were used. As mentioned before, the fine-grained fracture filling material that requires dialysis bags for phase separation could not be used as U was strongly adsorbed by such bags.

Ten small pieces of rock were selected for each experiment. The samples of rock selected were of similar size and weight (1 - 2 g), in order to maintain similar solid to liquid ratios and surface areas. An example of a rock piece is shown in Fig. 4.34. Five of these were placed in a container filled with 40 ml of Grimsel groundwater and the other five were placed in a container with 40 ml of bentonite colloid suspension in Grimsel groundwater (Fig. 4.35). The aim of the experiment was to compare radionuclide partitioning in the two systems.

Fig. 4.34: Example of a piece of rock used for sorption experiments in the presence of bentonite colloids (cm scale).

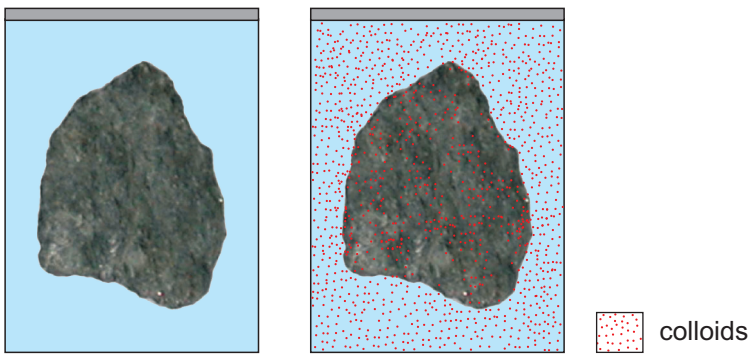

Fig. 4.35: Schematic representation of the experiment; the results are based on the comparison of sorption on the rock in the presence or absence of bentonite colloids.

After 1 week conditioning of the rock grains with the liquid phase, the water was spiked with ^{137}Cs ($2.95 \cdot 10^{-8}$ M) or ^{233}U ($3.5 \cdot 10^{-7}$ M) and the test tubes were then closed and gently shaken. This "shaking" was repeated twice a day for the duration of the experiment.

The continuous agitation of the system was avoided as small particles break off the rock pieces, as was clearly observed in preliminary experiments. The erosion of small particles from the rock samples can not be completely avoided, but it is minimised by this kind of agitation.

Sampling was performed following different contact times (from 1 day to 1 and 3 months for Cs and U respectively) and radionuclide activity was measured in all samples, both with and without colloids, without centrifuging.

The percentage of ^{137}Cs and ^{233}U adsorbed onto the rock, as a function of time, in presence or absence colloids, is shown in Fig. 4.36 and 4.37 respectively. The values are calculated as means and standard deviations of the five different samples.

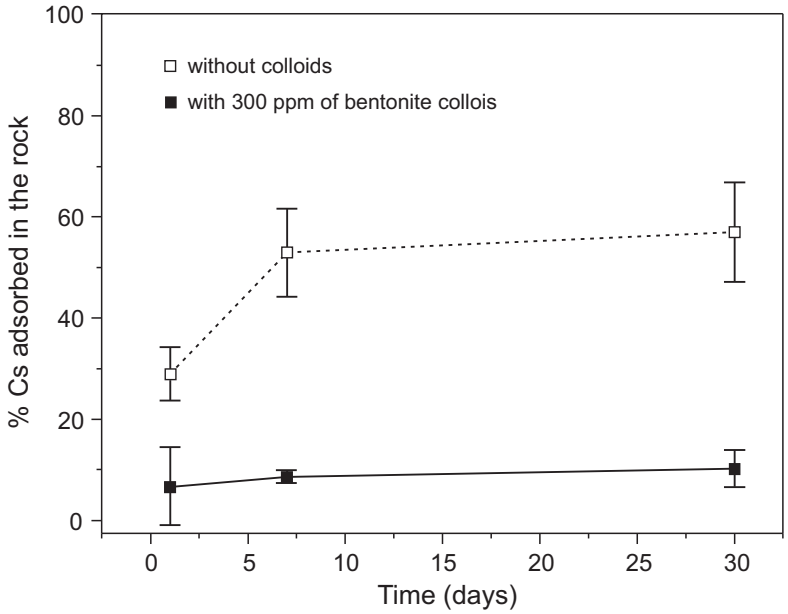

Fig. 4.36: Percentage of adsorbed ^{137}Cs on the rock calculated without colloids or in the presence of 0.3 g L^{-1} of bentonite colloids.

In the case of ^{137}Cs without colloids, sorption on the rock increases with time from 30 % to 60 %. Maintaining the same experimental conditions and adding 0.3 g L^{-1} bentonite colloids decreases the amount of ^{137}Cs adsorbed in the rock. Interestingly, the inventory of ^{137}Cs in the groundwater plus colloid suspension is practically constant.

A similar behaviour, even if less pronounced, is observed in the case of ^{233}U. The uranium sorbed in the rock without colloids varies with time from 13 to 22 %. In presence of 0.13 g L^{-1} of bentonite colloids, the adsorbed uranium is always slightly less, but this lies within the experimental error (Fig. 4.37).

The comparison of the system with and without colloids clearly indicates that, for both U and Cs, the presence of bentonite colloids appears to reduce the uptake of the element on the rock, this effect being more important in the case of ^{137}Cs. Colloids thus can act as a competitive

sorbant. These results indicate that, under Grimsel groundwater conditions, the presence of mobile bentonite colloids might enhance the migration of these two elements. However, due to known slow kinetics and sorption non-linearity of these elements, such simple datasets should not be over-interpreted.

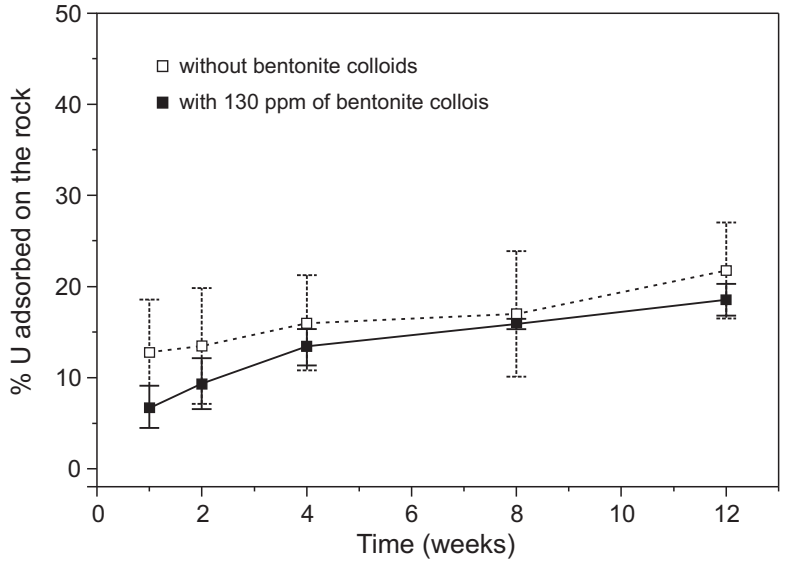

Fig. 4.37: Percentage of adsorbed ^{233}U in the rock calculated without colloids or in the presence of 0.13 g L^{-1} of bentonite colloids.

4.3 Batch sorption experiments with ^{237}Np, ^{244}Pu and ^{243}Am

4.3.1 Methodology

Batch sorption experiments were carried out under anaerobic conditions after previous equilibration of the sorbing phase with Grimsel groundwater. A dispersion of 20 mg L^{-1} bentonite colloids in Grimsel groundwater spiked with an actinide cocktail was used to study radionuclide sorption to colloids and the impact of colloids on sorption onto the rock, respectively. The colloid concentration was selected as it has been assumed appropriate for the *in situ* migration experiments. Bentonite colloids for these experiments were prepared by washing FEBEX bentonite repeatedly with MilliQ-water, followed by subsequent centrifugation. The last two washing steps were performed with Grimsel groundwater, in order to equilibrate the clay with this water. The colloidal fraction was finally separated from the coarser particles by centrifugation at 30,000 rpm. The resulting stock dispersion consists of about 3.8 g L^{-1} smectite colloids with a mean diameter of 70 nm and was stored under Ar-atmosphere.

Actinide desorption from bentonite colloids was studied by using a cation exchanger as competing ligand. In order to simplify the physical separation of the colloidal dispersion from the cation exchanger, a cation exchange filter was used, consisting of a Teflon backbone and chemically bound iminodiacetic acid functional groups (3M Empore, Chelating Extraction Disk). The filters are first equilibrated with Grimsel groundwater and then 2 filters are added to 50 ml of a groundwater solution containing 20 mg L^{-1} bentonite colloids with adsorbed actinides.

In the first set of batch experiments, crushed Grimsel granodiorite was taken and contacted with Grimsel groundwater containing the actinides at a solid to liquid ratio of 1:4 kg L^{-1} under Ar atmosphere. The approximate surface area determined by the BET method is around 0.2 m^2 g^{-1} for the crushed Grimsel granodiorite and 2 m^2 g^{-1} for the fracture filling material according to Bradbury (1989). The equilibrated Grimsel groundwater was separated after two weeks of conditioning and aliquots were spiked separately with ^{237}Np(V), ^{238}Pu(IV) and ^{241}Am(III) and solutions. The spike solutions consisted of:

- 10^{-4} M ^{237}Np(V) in 10^{-4} M HCl solution
- 10^{-4} M ^{238}Pu(IV) in 0.05 M HCl solution
- 10^{-4} M ^{241}Am(III) in 0.1 M HNO_3 solution.

Resulting initial concentrations and oxidation states for the individual actinides in the Grimsel groundwater after spiking were $3 \cdot 10^{-5}$ M ^{237}Np(V), $6 \cdot 10^{-9}$ M ^{238}Pu(IV) and $3 \cdot 10^{-10}$ M ^{241}Am(III). Those concentrations lie in the range used for the *in situ* experiments (see Tab. 2.4). Concentrations for all actinid ions are below solubility limits except for Pu(IV) according to speciation calculations (Duro et al. 2000). Dissolved species should be hydroxo and carbonato complexes. For Pu(IV) oversaturation with regard to $Pu(OH)_4$ is expected. The evolution of the actinide concentrations in solution without added solids was observed continuously by liquid scintillation counting (LSC), in order to study their stability in Grimsel groundwater. Another three aliquots of the spiked Grimsel groundwater samples were contacted with solid material (crushed fracture filling material and granodiorite). The decrease in the actinide concentration indicated the progress of the sorption reaction and this was monitored by LSC. Selected samples have been checked for colloids by ultrafiltration (average pore size: 1.8 nm).

In the second set of batch experiments, Grimsel granodiorite and fracture filling material have been crushed and the size fraction 250 - 800 µm (BET surface area for Grimsel granodiorite: 0.1 m^2 g^{-1}) was isolated by sieving, washed with MilliQ water and Grimsel groundwater, air dried and used in sorption experiments. The solid was contacted with Grimsel groundwater, previously spiked with an actinide cocktail containing the isotopes ^{237}Np, ^{244}Pu and ^{243}Am, which were also used in the *in situ* experiment. Analysis of actinides in the ultracentrifuged solution (90,000 rpm for 20 min) utilised an ICP-mass spectrometer equipped with an ultrasonic nebuliser. pH changes upon addition of the actinide cocktail did not exceed 0.2 units. Initial actinide concentrations were $1.3 \cdot 10^{-8}$ M ^{237}Np, $3.8 \cdot 10^{-11}$ M ^{244}Pu and $1.3 \cdot 10^{-9}$ M ^{243}Am. Differentiation of colloidal and dissolved actinide species (indicated as not centr. and centr. in the figures below, respectively) was made by ultracentrifugation at 90,000 rpm for 20 min under anaerobic conditions in closed vessels. Some tests on actinide sorption on different plastics were carried out to guide choice of materials for the field tests. They are described first.

4.3.2 Stability of the ^{237}Np, ^{244}Pu and ^{243}Am solution in Grimsel groundwater

In order to investigate possible colloid formation of these actinides in Grimsel groundwater in the absence of solids or bentonite colloids, a blank test was performed in HDPE (high density polyethylene) vials (see previous section).

Fig. 4.38 shows that Np(V) showed no changes in concentration and therefore seems to remain in the oxidised state. Ultra-centrifugation revealed no changes in the Np concentration and therefore the existence of colloidal species can be excluded.

In contrast, non-centrifuged ^{244}Pu and ^{243}Am samples both show a decrease in concentration over the test period. This decrease is interpreted as sorption of these nuclides onto container

walls. Sedimentation following precipitation can be excluded as samples are shaken prior to sampling. Ultra-centrifuged samples show a more dramatic decrease in concentration within the first 50 hours. This indicates that a fraction of these elements is either forming homogeneous radiocolloids (Am- or Pu-oxide / hydroxide / silicate colloids) or is bound to existing groundwater colloids (heterogeneous radiocolloids). After this period, the Am- and Pu-concentrations in the ultracentrifuged solution remain almost constant, within experimental uncertainties.

No measurable change in the Al concentration upon ultra-centrifugation was observed. This fact does not exclude the presence of groundwater colloids; these have clearly been shown to be present in the system based on previous measurements (see for example Degueldre et al. 1990, Möri 2004). However, due to the relatively high concentration background of dissolved Al in Grimsel groundwater, the colloid bound fraction could not be detected by the ultracentrifugation method by comparing total Al concentrations before and after within the analytical uncertainties. It should be noted here that the groundwater colloids were found to consist mainly of silica and may thus contain only minor fractions of Al (Degueldre 1996a).

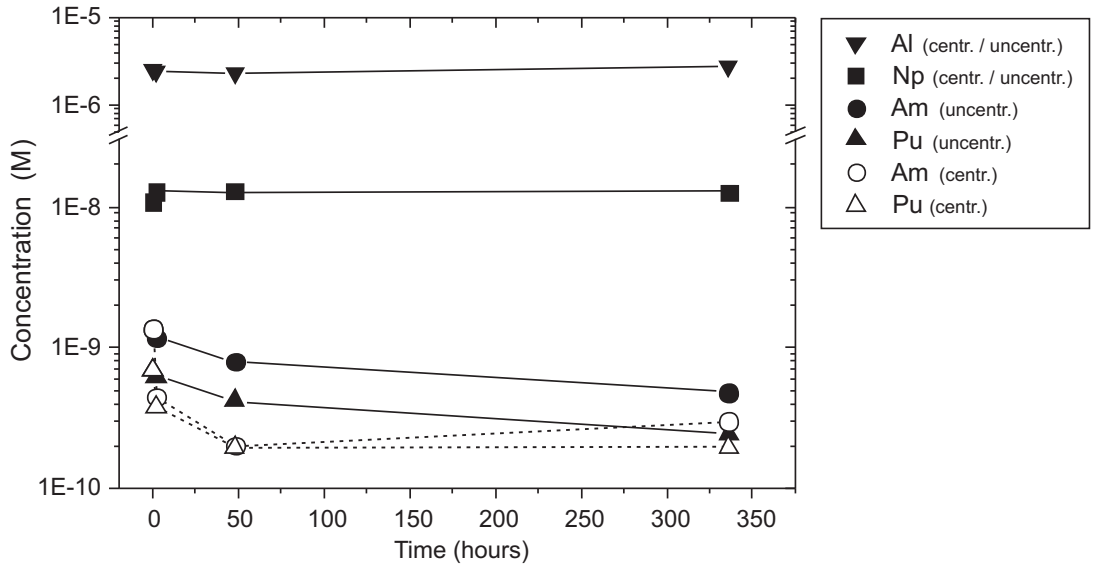

Fig. 4.38: Actinide concentrations in Grimsel groundwater (pH 9.4) as a function of time; HDPE vials, ultra-centrifuged (centr.) and non-centrifuged (uncentr.).

4.3.3 Sorption on bentonite colloids

Sorption of ^{237}Np, ^{244}Pu and ^{243}Am (experimental conditions of the "second set" noted in 4.3.1) on 20 mg L^{-1} bentonite colloids was studied as a function of time (see Fig. 4.39). After ultracentrifugation of the dispersion in the Grimsel groundwater, the concentration of Al decreased from a value of 1,500 µg L^{-1} that clearly indicates the presence of smectite colloids to the background concentration of the Grimsel groundwater. As Al can be taken as an indicator for bentonite colloids in this groundwater system, it can be concluded that bentonite colloids have been separated quantitatively: Al concentrations are the same in the groundwater and the colloid spiked groundwater after centrifugation: $2.5 \cdot 10^{-6}$ M. For Np, no decrease in concentration was observed in the ultracentrifuged solution, indicating that dissolved species prevail. This implies, again, that ^{237}Np remains in the (V) oxidation state. For Am and Pu, however, a decrease of the concentration by almost two orders of magnitude was found. Corresponding Rd values lie in the order of 10^5 to 10^6 L kg^{-1}.

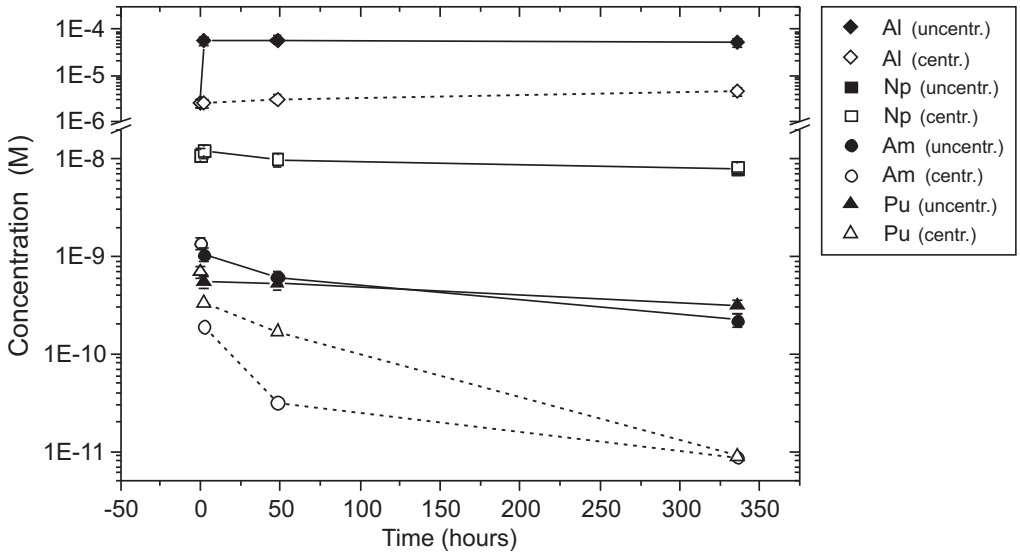

Fig. 4.39: Actinide sorption on FEBEX bentonite colloids (20 mg L^{-1}) as a function of time.

Tab. 4.7: Calculated Rd values (L kg^{-1}) for actinide sorption on bentonite colloids (S / L: 20 mg: 1 L); c_i: initial radionuclide concentration; c_{coll}: colloid concentration

	Distribution coefficient Rd (L kg^{-1})			
	Contact times			
	1 hour	1 day	1 week	3 weeks
	^{237}Np			
$c_i = 1 \cdot 10^{-6}$ M c_{coll}: 20 mg L^{-1}	$< 5 \cdot 10^3$	$< 5 \cdot 10^3$	$< 5 \cdot 10^3$	$< 5 \cdot 10^3$
	^{244}Pu			
$c_i = 4 \cdot 10^{-11}$ M c_{coll}: 20 mg L^{-1}	$1 \cdot 10^5 \pm 2 \cdot 10^4$	$1 \cdot 10^5 \pm 2 \cdot 10^4$	$1 \cdot 10^5 \pm 2 \cdot 10^4$	$8 \cdot 10^5 \pm 1.8 \cdot 10^4$
	^{243}Am			
$c_i = 9 \cdot 10^{-10}$ M c_{coll}: 20 mg L^{-1}	$3 \cdot 10^6 \pm 6 \cdot 10^5$	$3 \cdot 10^6 \pm 6 \cdot 10^5$	$2 \cdot 10^6 \pm 4 \cdot 10^5$	$1 \cdot 10^6 \pm 2 \cdot 10^5$

The actinides do not to show any sorption onto the container walls in the presence of bentonite colloids as concentrations for both elements remain invariant with time. ^{237}Np showed no concentration change, even after ultra-centrifugation (and presumed removal of bentonite colloids). Hence, no sorption was observed on either the container walls or the bentonite colloids and Np is assumed to remain in oxidation state V. Dissolved Pu, on the other hand, showed a significant decrease in concentration over the entire test duration. It appears that ^{244}Pu is strongly sorbed on bentonite colloids and that this effect is kinetically controlled. The kinetics of Am sorption on bentonite colloids appears to be somewhat faster than that for Pu. This might be attributed to the combined reduction / sorption reaction of a part of the Pu. It has been found (in separate investigations (see Fig. 4.45)) that the major part of the Pu spike used in these tests

was tetravalent while a small fraction (~ 5 %) existed in the hexavalent oxidation state. It is assumed that sorption of tetravalent Pu is quite rapid, while reduction of less strongly sorbing Pu(VI) is slow.

Based on the colloid survey in granitic systems (Degueldre 1994) an upper limit for the colloid concentration in the Grimsel groundwater of 200 ng ml^{-1} is given. If we assume that the Am Rd value for these colloids is the same as measured in the present study for bentonite colloids (~$1 \cdot 10^6$ L kg^{-1}), it turns out that ~ 17 % of the Am should be colloid bound. In presence of 20 mg L^{-1} bentonite colloids 98 % of the Am is attached to colloids according to this calculation.

The desorption behaviour of colloid-associated actinides derived by applying the ion-exchanger method is shown in Fig. 4.40. The actinide solution had been equilibrated with the bentonite colloids for 5 days and was then contacted with two filters. The chelating ion exchanger acts as a strong competing ligand, where the functional groups of the filter are present in excess compared to the sites on the bentonite colloids (20 mg L^{-1} bentonite colloids: ~ $2.3 \cdot 10^{-6}$ eq L^{-1} according to Kosakowski & Baeyens in Geckeis & Möri 2003, Appendix B; ion exchange filters: $1.8 \cdot 10^{-2}$ eq L^{-1}).

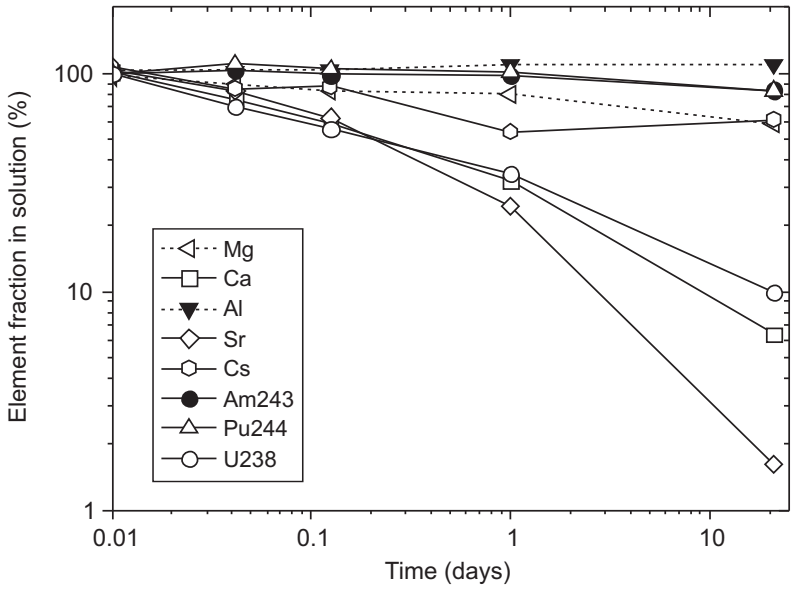

Fig. 4.40: Desorption behaviour of bentonite colloid-bound elements in the presence of a chelating filter membrane.

Equilibration time with 20 mg/L bentonite colloids: 5 d; Initial concentrations: c_i(Pu): $3.7 \cdot 10^{-9}$ mol/L; c_i(Am): $1.3 \cdot 10^{-9}$ mol/L.

The Al concentration remains virtually constant, showing that the bentonite colloids neither dissolve nor sorb on the ion exchange membrane. Most of Ca, Sr and ^{238}U which are naturally present in the bentonite colloids are desorbed from the colloids after 20 days and are fixed onto the membrane. It is likely that Ca and Sr are loosely bound to the colloid surface, on the permanently charged ion exchange groups of the smectite particles. Mg and Cs appear to be more strongly bound. Mg is reported to be partly bound in the crystalline smectite structure of the octahedral layers (see Section 3.2.2.1). Cs may be fixed in the smectite interlayers and only slowly released by the colloids (see also the comments above).

It is interesting to note that the actinides ^{243}Am and ^{244}Pu also very slowly dissociate from the colloids. After 20 days, about 75 - 80 % remains colloid-bound. Therefore, actinide desorption from the colloids is not expected to be significant under the experimental conditions of the *in situ* migration experiment.

4.3.4 Sorption on Grimsel granodiorite

The sorption behaviour of ^{243}Am, ^{244}Pu and ^{237}Np on Grimsel granodiorite is shown in Fig. 4.41 where Rd values were determined with both sets of batch experimental conditions (Section 4.3.1), with different initial radionuclide concentrations and different grain sizes for the Grimsel granodiorite (for details see Geckeis et al. 1999b). Rd values are plotted as a function of time for comparison.

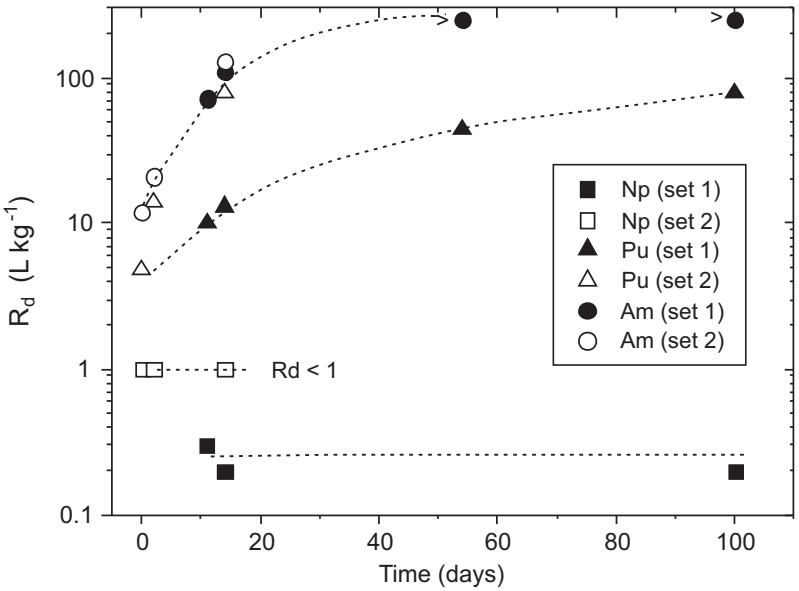

Fig. 4.41: Rd values for ^{237}Np, ^{244}Pu and ^{243}Am on Grimsel granodiorite: size fraction of 250 - 800 µm (set 2), compared with data obtained previously for Grimsel granodiorite without size fractionation (set 1).

Set 1: V/M: 4 L kg^{-1}; pH=9.5; surface area of solid: 0.2 m^2 g^{-1} Set 2: V/M: 7.5 L kg^{-1}; pH=9.3; surface area of solid: 0.1 m^2 g^{-1}; granodiorite grain size: 250-800 µm. Data points for Am Rd values at contact times > 50 days are lower limits due to analytical constraints.

Measured Rd values indicate slow sorption reaching equilibrium only after months. Pu-Rd values are somewhat lower than those for Am. Pu-Rd values determined in the second set experiments are higher by a factor of 6 to 7 as compared to data found for the somewhat different conditions in set 1experiments. This might be due to the lower initial concentration of the Pu in solution ($3.8 \cdot 10^{-11}$ M in set 2 as opposed to $6 \cdot 10^{-9}$ M in set 1) or by slightly different surface properties of the Grimsel granodiorite size fraction (crushed Grimsel granodiorite without size fractionation compared to grain sizes of 250 - 800 µm). A further explanation could be the influence of colloids which are dispersed from the crushed Grimsel granodiorite into the solution and which are not considered in the first set of experiments. In the second set, the solutions have been ultracentrifuged prior to analysis. From both sets of experiments, pronounced long-term sorption kinetics are evident, the origin of which is not yet understood. For ^{237}Np, almost no sorption was measured, resulting in Rd values of < 0.4 L kg^{-1}. Np

concentrations in the second set of experiments are determined by ICP-MS and are affected by a larger statistical uncertainty than in the LSC analysis used for the first set of experiments. Therefore, Np Rd values in the second set of experiments are simply given as Rd < 1 L kg^{-1}.

The influence of bentonite colloids (20 mg L^{-1}) on actinide sorption onto Grimsel granodiorite (second set: size fraction of the solid ranges from 250 to 800 µm) has also been studied. Within analytical error, the Al concentration remained constant during the experimental time, indicating the stability of bentonite colloids in the presence of Grimsel granodiorite surfaces.

Fig. 4.42 shows the temporal evolution of actinide concentrations in the presence of Grimsel granodiorite and bentonite colloids. For ^{237}Np, again no sorption was observed in either case. The slight, but consistent, decrease of Np concentration in absence of colloids has not been found in other experiments and therefore has to be verified. In case of ^{244}Pu and ^{243}Am, sorption to the granodiorite increased with time both in absence and presence of colloids. The calculated Rd values decreased by more than one order of magnitude in presence of bentonite colloids. Pu and Am concentrations show a comparable decrease with time in the absence of bentonite colloids, whereas the decrease in presence of bentonite colloids is less pronounced for Pu.

Tab. 4.8 gives an overview of calculated Rd values in the granodiorite-Grimsel groundwater system. The test durations and actinide concentrations are not completely the same for both sets. It should be noted once again: Rd values just provide the ratio for a given radionuclide between the solid and liquid phase where colloids are taken here as belonging to the liquid phase. As there are clear kinetic effects, possible precipitation / sorption non-linearity cannot be excluded and colloids are present in the natural Grimsel groundwater, those Rd values cannot be taken as Kd values considering only relatively rapid reversible sorption reactions.

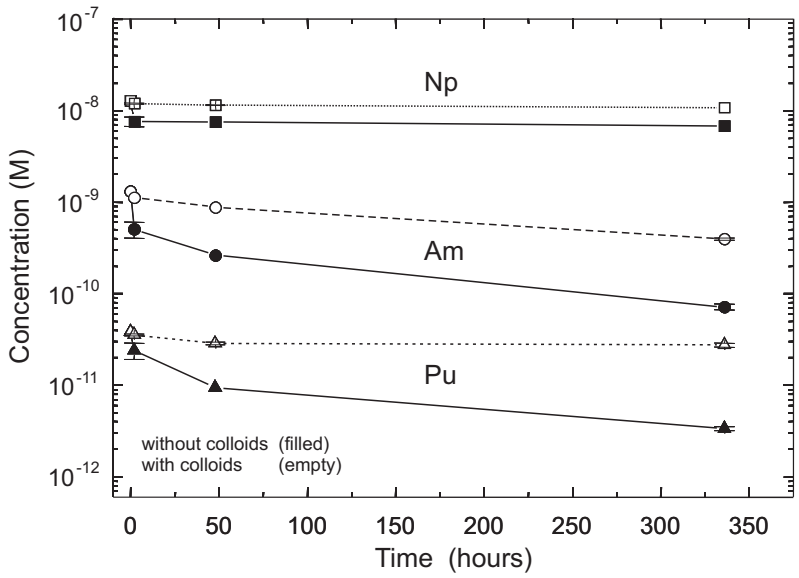

Fig. 4.42: Actinide sorption onto Grimsel granodiorite (second set, size fraction 250-800 µm) in the absence and presence of 20 mg L^{-1} bentonite colloids; filled symbols indicate actinide concentrations in absence of colloids (error bars correspond to the analytical uncertainty).

Tab. 4.8: Calculated Rd values ("base data set") for ^{237}Np, ^{244}Pu and ^{243}Am on granodiorite for Grimsel groundwater under anoxic conditions at different test durations. c_i: initial radionuclide concentration; c_{coll}: colloid concentration.

	Distribution coefficient Rd (L kg^{-1})					
	Contact times					
	2 hours	2 days	11 days	14 days	54 days	100 days
^{237}Np						
$c_i = 1.3 \cdot 10^{-8}$ M (2. set) $c_i = 3 \cdot 10^{-5}$ M* (1. set) [$c_i = 1.3 \cdot 10^{-8}$ M (coll)] c_{coll}: 20 mg L^{-1}	< 1 --- [< 1]	< 1 --- [< 1]	--- 0.3 ± 0.02* ---	< 1 0.2 ± 0.014* [< 1]	--- 0.04 ± 0.003* ---	--- 0.2 ± 0.014* ---
^{244}Pu						
$c_i = 3.8 \cdot 10^{-11}$ M (2. set) $c_i = 6 \cdot 10^{-9}$ M* (1. set) [$c_i = 3.8 \cdot 10^{-11}$ M (coll)] c_{coll}: 20 mg L^{-1}	4.8 ± 0.7 --- [0.6 ± 0.1]	14 ± 2 --- [2.5 ± 0.4]	--- 10 ± 1.4* ---	78 ± 11 13 ± 2* [3.0 ± 0.4]	--- 44 ± 6* ---	--- 78 ± 11* ---
^{243}Am						
$c_i = 1.3 \cdot 10^{-9}$ M (2. set) $c_i = 3 \cdot 10^{-10}$ M* (1. set) [$c_i = 1.3 \cdot 10^{-9}$M (coll)] c_{coll}: 20 mg L^{-1}	12 ± 2 --- [1.2 ± 0.2]	21 ± 3 --- [3.6 ± 0.5]	--- 72 ± 10* ---	130 ± 18 110 ± 15* [17 ± 2.4]	--- > 250* ---	--- > 250* ---

Sorption was investigated with crushed Grimsel granodiorite (surface area ~ 0.2 m^2 g^{-1}) and size fractionated material (250 - 800 µm, surface area: 0.1 m^2 g^{-1}).

* Sorption to crushed Grimsel granodiorite without size fractionation (exact experimental conditions for the first and second set, see explanation in the text).

Values in brackets stand for the respective sorption experiments on the size fractionated Grimsel granodiorite in presence of 20 mg L^{-1} bentonite colloids.

4.3.5 Sorption on fracture filling material

Batch experiments with fracture filling material were performed with a 250 - 800 µm size fraction and the following radionuclide concentrations: ^{237}Np ($c_i = 1.1 \cdot 10^{-8}$ M), ^{244}Pu ($c_i = 7 \cdot 10^{-10}$ M) and ^{243}Am ($c_i = 1.4 \cdot 10^{-9}$ M). The Al concentration was found to be lower in the ultracentrifuged samples indicating that colloids and particles derived from fracture filling material are present in the original solution (Al is an indicator for aluminosilicates in the fracture filling material). A slight increase of the dissolved (not colloidal) Al concentration might be due to the dissolution of aluminosilicate mineral phases or is possibly indicating that not all colloidal material is being removed by ultracentrifugation step.

Again, Np shows almost no sorption onto fracture filling material, with or without centrifugation (see Fig. 4.43).

Pu and Am, on the other hand, both show a considerable concentration decrease in contact with fracture filling material. After removing the colloidal fraction by ultra-centrifugation, the decrease is even more pronounced indicating the presence of colloidal species of these two radionuclides, presumable associated with the colloidal fraction of the fracture filling material. Equilibrium appears not to be reached within the 2 week test duration. Am shows a somewhat stronger affinity to colloidal fracture filling material than Pu.

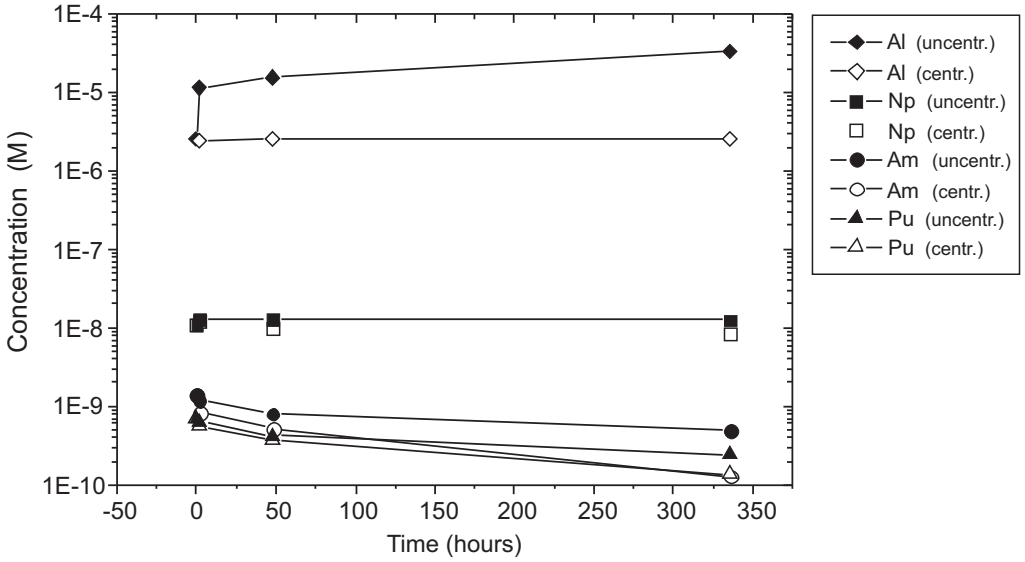

Fig. 4.43: Influence of sorption of actinides on fracture filling material on the resulting measured elemental concentrations in solution, with and without ultra-centrifugation.

In order to study the sorption behaviour of actinides onto fracture filling material at times of relevance to the *in situ* experiment (i.e. 1 hour or less), short duration sorption experiments with fracture filling material were performed, again with the 250 - 800 μm size fraction.

A rapid increase of the calculated Rd within the first 30 minutes was observed for the ultra-centrifuged samples (see Fig. 4.44). Non-centrifuged samples are insensitive to sorption onto the fracture filling material, showing a significant effect only after 30 minutes. This shows very clearly the influence of colloidal material on the sorption behaviour of these actinides. The general increasing trend of the Rd values observed in ultracentrifuged and non-centrifuged samples again shows that sorption is kinetically controlled.

Short term sorption studies have been repeated with a ^{244}Pu-stock solution electrochemically adjusted to the oxidation state Pu(IV). Absorption spectra of the old and the new Pu-stock solutions are shown in Fig. 4.45. It turned out that the old solution contained about 5 % ^{244}Pu in the oxidation state (VI). Calculated Rd values for Pu in the oxidation state (IV) were somewhat higher than found for the old solution (Fig. 4.45) and more similar to those of Am.

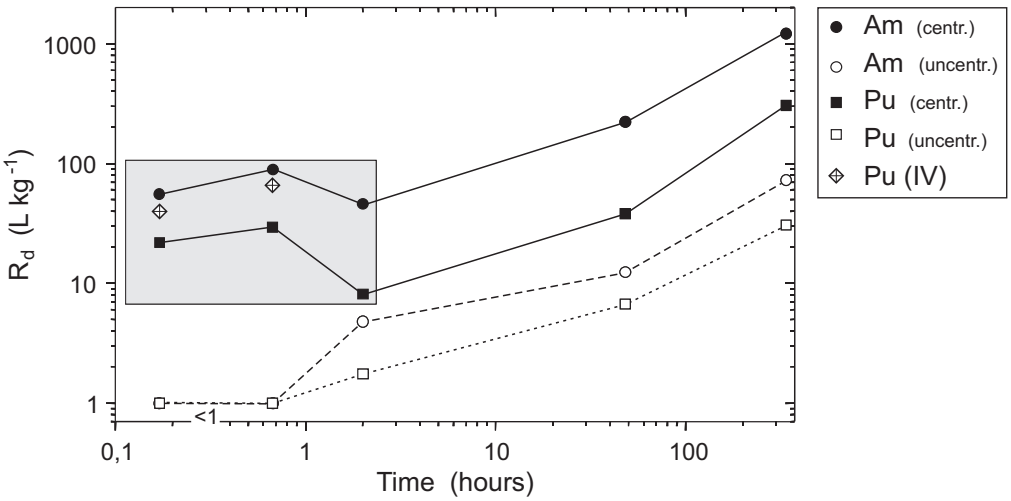

Fig. 4.44: Apparent sorption of ^{244}Pu and ^{243}Am onto fracture filling material as a function of time; fracture filling material: 250 - 850 µm.

Please note that sorption ratios (Rd) are defined as element concentration in the solid divided by element concentration in the liquid phase; in case of the uncentrifuged samples, the liquid phase contains also colloidal species; shaded area marks separately performed experiments with short contact times.

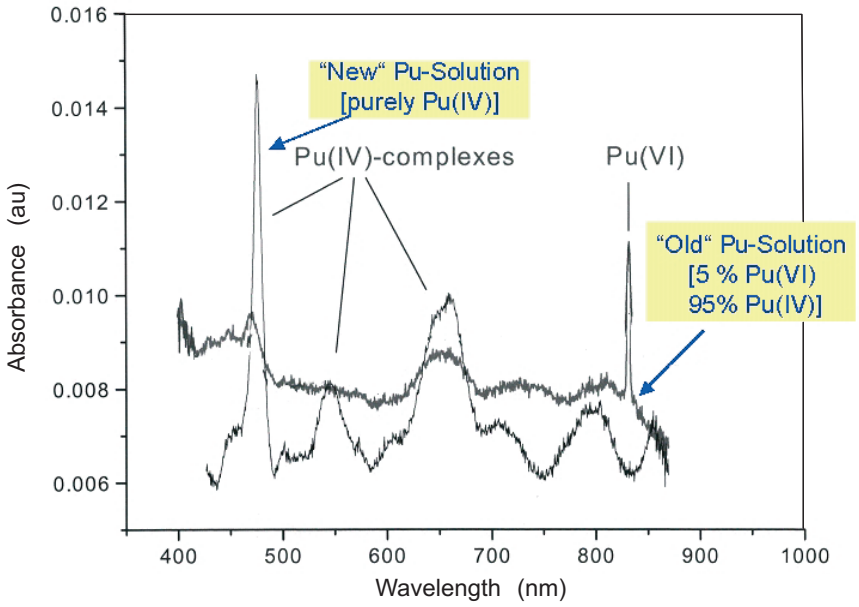

Fig. 4.45: Absorption spectrum of the "old" ^{244}Pu stock solution and the "new" electrochemically adjusted solution (1 M HNO_3).

Similarly to the case of granodiorite, the sorption of Np, Pu and Am onto fracture filling material was also studied in presence of 20 mg L^{-1} of bentonite colloids (see Fig. 4.46). For ^{237}Np almost no sorption was observed on either the bentonite colloids or the fracture filling material.

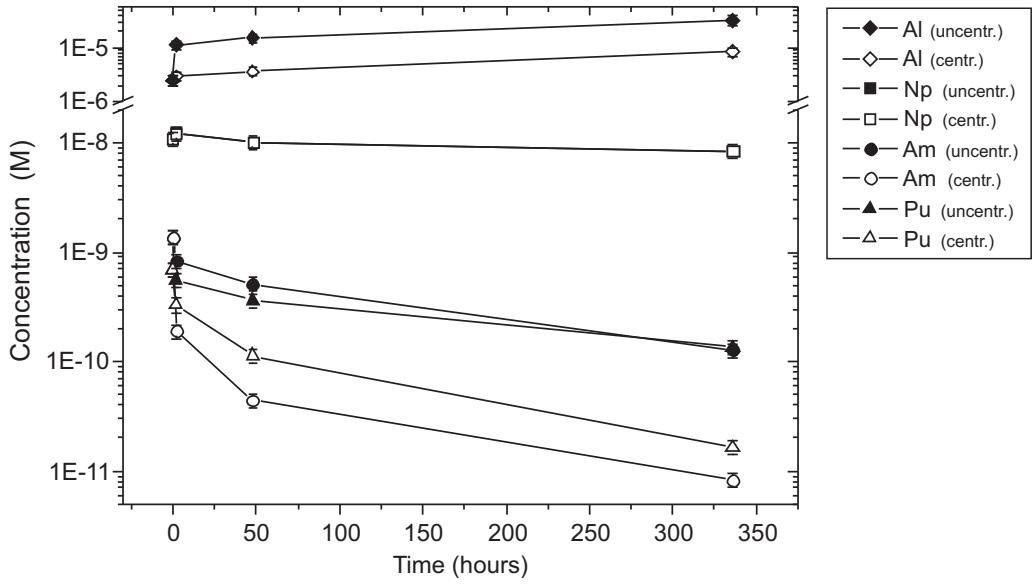

Fig. 4.46: Actinide sorption to fracture filling material in presence of 20 mg L^{-1} bentonite colloids.

Without ultra-centrifugation, the decrease of ^{244}Pu and ^{243}Am concentration is less pronounced than found in experiments without bentonite colloids (see Fig. 4.43). As the Pu and Am concentrations in the aqueous phase are completely dominated by colloid-bound species, the slight decrease of the actinide concentration with time could indicate at least partly and slowly reversible binding to colloids. Rd values of Np, Pu and Am on fracture filling material appear generally higher than those observed for Grimsel granodiorite after the same reaction time (compare Tab. 4.8 and 4.9).

Tab. 4.9: Rd values (L kg^{-1}) in a fracture filling material / Grimsel groundwater solution in presence and absence of bentonite colloids (20 mg L^{-1}). Size fraction 250 – 800 µm. c_i: initial radionuclide concentration; c_{coll}: colloid concentration.

	Distribution coefficient Rd (L kg^{-1})		
	Contact times		
	2 hours	24 hours	2 weeks
$^{237}Np^*$			
$c_i = 1.1 \cdot 10^{-8}$ M	<1	1.7 ± 0.3	3.6 ± 0.7
c_{coll} = 20 mg L^{-1}	[<1]	[1.8 ± 0.4]	[3.8 ± 0.8]
$^{244}Pu^*$			
$c_i = 7 \cdot 10^{-10}$ M	8 ± 2	38 ± 8	306 ± 60
c_{coll} = 20 mg L^{-1}	[2 ± 0.4]	[2.4 ± 0.5]	[9 ± 2]
$^{243}Am^*$			
$c_i = 1.4 \cdot 10^{-9}$ M	46 ± 9	223 ± 40	1223 ± 200
c_{coll} = 20 mg L^{-1}	[2 ± 0.4]	[9 ± 2]	[39 ± 8]

* values in brackets indicate Rd values in the presence of bentonite colloids

The sorption experiments with Am and Pu reveal two main features:

1. Pronounced sorption kinetics was observed over a period of weeks. The origin of the kinetics is not clear up to now, but might be due to surface diffusion of the actinide ions into the pores of the solid matrix (see also Axe & Trivedi 2002).
2. Sorption appears to be very sensitive to the presence of colloidal material. Addition of bentonite colloids clearly decreases the Rd values for both elements. In the absence of bentonite colloids, however, colloidal matter generated from the crushed fracture filling material or crushed granodiorite influences the sorption onto the solid phase.

Such rock derived colloids are detected indirectly by observing the Al-concentration in all solutions measured by ICP-MS. Plotting the calculated Am and Pu Rd values for the sorption on fracture filling material versus the measured Al concentration determined in ultra-centrifuged and non-centrifuged solutions demonstrates the colloid effect (Figs. 4.47 and 4.48).

The vertical grey line in both plots indicates the upper limit of Al concentrations measured in the Grimsel groundwater. This concentration is not further decreased upon ultracentrifugation within the analytical uncertainties. The data marked with ellipses represent those experiments performed with 20 mg L^{-1} bentonite colloids. All other data belong to experiments without addition of bentonite colloids or after removal of all kind of colloidal matter by ultra-centrifugation. It is quite reasonable to assume that increasing Al-concentrations indicate the presence of colloidal matter, which is responsible for the decreasing Rd values for actinide sorption to the fracture infill minerals. But all experiments show as well that sorption to fracture infill minerals increase with contact time irrespective of presence or absence of colloids.

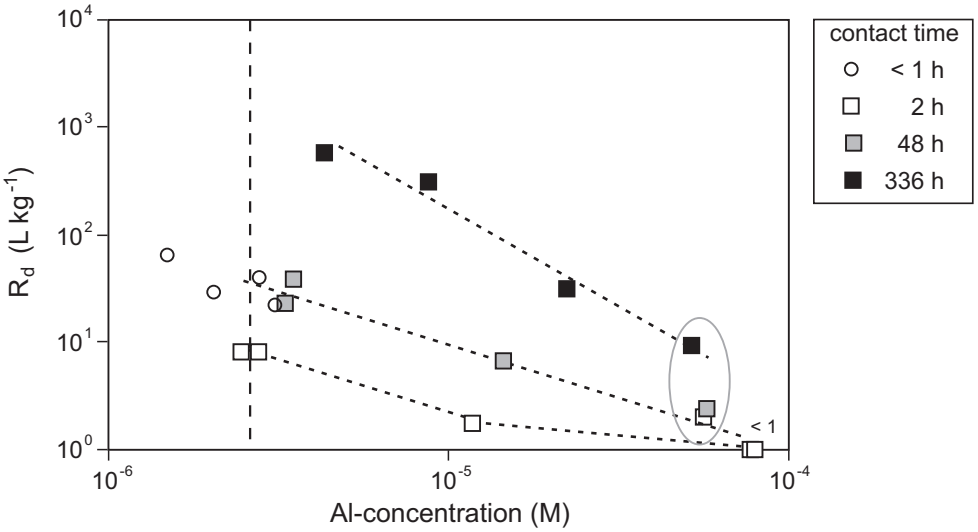

Fig. 4.47: Calculated Rd values for the sorption of ^{244}Pu to fracture filling as a function of time and Al-concentration measured in non-centrifuged and ultra-centrifuged sample solutions.

Dashed lines connect Rd values obtained after the same contact time as indicated in the graph; data for ultracentrifuged samples are represented by the lowest Al concentration in a sample series with the same contact time. The vertical dashed line marks the Al concentration of the groundwater; the ellipse marks those experimental data where 20 mg L^{-1} bentonite colloids have been added.

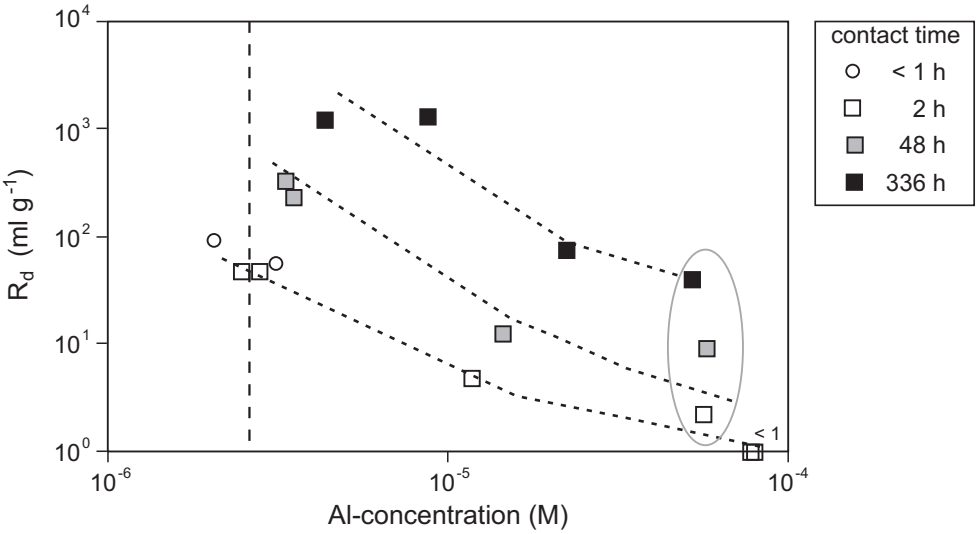

Fig. 4.48: Calculated Rd values for the sorption of ^{243}Am to fracture filling as a function of time and Al-concentration measured in non-centrifuged and ultra-centrifuged sample solutions.

Dashed lines connect Rd values obtained after the same contact time as indicated in the graph; data for ultracentrifuged samples are represented by the lowest Al concentration in a sample series with the same contact time; The vertical dashed line marks the Al concentration of the groundwater; the ellipse marks those experimental data where 20 mg L-1 bentonite colloids have been added.

4.4 Sorption on vial material and PEEK lines

The possible sorption of the actinides on vials, lines and tools (e.g. packers, pumps, flow meters etc.) had to be considered in the design of the experiment. In order to select appropriate materials showing the lowest degree of radionuclide sorption, a set of laboratory experiments were performed.

Aliquots of the spiked Grimsel groundwater were stored in either low density polyethylene (LDPE) or high density polyethylene (HDPE) vials in order to study the stability of the actinide cocktail as a function of time. Grimsel groundwater spiked with actinides and bentonite colloids were also observed for their stability in both these type of vials.

The decrease of the actinide concentration in solution in vials of different material can be seen in Fig. 4.49 and 4.50. In each case ^{237}Np shows little change in concentration (~ 5 - 10 %) implying that Np remained in oxidation state (V) and limited sorption onto container walls occurred.

However, in the cases of ^{244}Pu and ^{243}Am, considerable decrease of the solution concentration is observed. In these experiments the Pu concentration was erroneously selected very low ($c_0 = 3.8 \cdot 10^{-11}$ M) so that colloid formation / precipitation appears to be unlikely and it is assumed that it is sorption onto container walls which causes the actinide loss. Sorption to container walls is more pronounced within the experimental time period in case of LDPE vials (90 % loss) than for the HDPE vials (less than 60 % loss). It is proposed that compounds like phthalic acid currently used as softening agent could be responsible for this behaviour.

In the presence of 20 mg L^{-1} bentonite colloids no significant sorption of actinides to container walls is observed after 20 days (see Fig. 4.49). Sorption data for ^{137}Cs and ^{233}U are not shown here. Sorption on the surface of HDPE vials was found to be < 5 %.

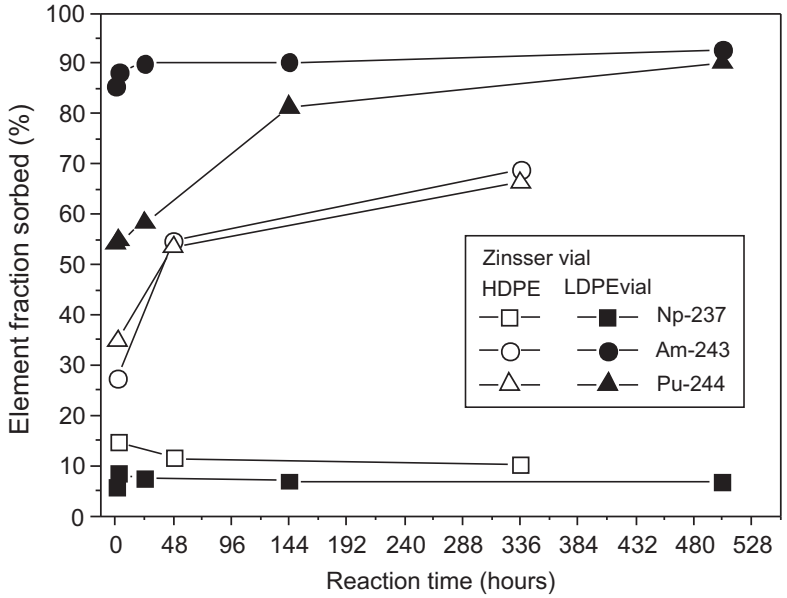

Fig. 4.49: Sorption behaviour of the actinides ^{237}Np, ^{244}Pu and ^{243}Am from Grimsel groundwater (pH = 9.2) on high density polyethylene (HDPE) and low density polyethylene (LDPE) vials.
(^{237}Np: $c_i = 1.3 \cdot 10^{-8}$ M; ^{243}Am: $c_i = 1.3 \cdot 10^{-9}$ M; ^{244}Pu; $c_i = 3.8 \cdot 10^{-11}$ M)

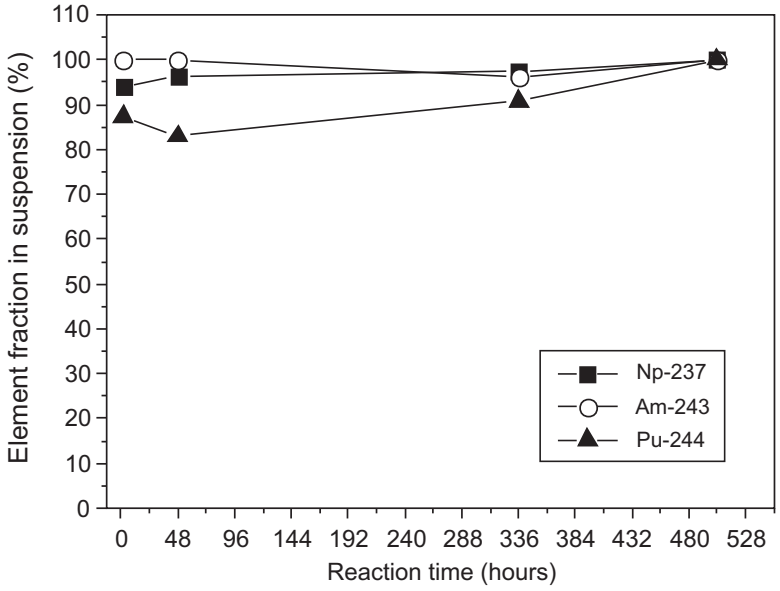

Fig. 4.50: Sorption behaviour of the actinides ^{237}Np, ^{244}Pu and ^{243}Am from Grimsel groundwater (Grimsel groundwater: pH = 9.2) low density polyethylene (LDPE) vials in the presence of 20 mg L^{-1} bentonite colloids (^{237}Np: $c_i = 1.3 \cdot 10^{-8}$ M; ^{243}Am: $c_i = 1.3 \cdot 10^{-9}$ M; ^{244}Pu; $c_i = 3.8 \cdot 10^{-11}$ M).

Experiments with PEEK tubing were performed to simulate radionuclide tracer behaviour during injection into the shear zone as planned for the *in situ* experiment (capillary length: 1.57 m; i.d.: 0.51 mm) revealed the following tracer losses: ^{99}Tc(IV): 54 %, ^{137}Cs: 1-2 % and ^{233}U: 5-8 %. Sorption of ^{99}Tc(IV) in the presence of bentonite colloids was not investigated, but

it is expected to be much smaller. The sorption of the actinides onto PEEK lines was investigated in field tracer tests and in the lab with the actinide homologues. In the absence of bentonite colloids, around 30 % of Tb(III) was sorbed onto the lines while, for Hf and Th, around 1 - 16 % was retained on the PEEK surface. In the presence of the bentonite colloids, the sorption to PEEK lines is reduced to 11 % for Tb(III) and < 2 % for the tetravalent Th and Hf. It is to be expected that the result would be very similar for Am(III) and Pu(IV).

Tracer experiments with the actinides Np(V) ($1 \cdot 10^{-8}$ M), Pu(IV) ($8 \cdot 10^{-9}$ M) and Am(III) ($8 \cdot 10^{-8}$ M) dissolved in Grimsel groundwater in absence of colloids were done by injecting 100 µl of this solution into a PEEK capillary (length: 1.57 m; i.d.: 0.51 mm). Residence time of the solution was about 60 s which is in the order of magnitude of the injection residence time of the injection solution in the PEEK line during the *in situ* experiments. Recoveries were 90 - 100 % for Np, 80-90 % for Pu and 70-80 % for Am. Those results are qualitatively consistent with the outcome of an experiment performed after a homologue tracer test (run #14 and, see Möri 2001). During that *in situ* test 1.1×10^{-8} M Hf(IV), $1.1 \cdot 10^{-8}$ M Tb(III), $9.2 \cdot 10^{-9}$ M Th(IV) in groundwater have been injected into the shear zone. After injection and flushing with groundwater, the injection PEEK line (injection flow rate: 10 ml min^{-1}; volume of flow line from point of tracer input to injection interval: 45 ml) has been flushed with HNO_3. Analysis of this solution showed that particularly the trivalent Tb(III) taken as a chemical homologue to Am(III) was sorbed to the PEEK line (20 - 30 %) while < 16 % of the Th(IV/Hf(IV) taken as homologues for tetravalent actinides were retained during injection.

All experiments revealed that it is unavoidable that certain amounts of tracer may sorb onto the equipment materials, i.e. storage vials and PEEK lines. Sorption becomes negligible in the presence of bentonite colloids.

4.5 Summary of sorption studies

Sorption of most radionuclides in the systems under investigation appears, in general, to be much more complicated than implied by the conventional Kd concept. Therefore the sorption data are represented as sorption ratios Rd where the radionuclide concentration in the liquid include colloidal and dissolved species.

The Rd values determined for Cs(I), Se(IV), Tc(IV/VII), Am(III), Pu(IV), Np(V) and U(VI) sorption to **bentonite colloids** (consisting mainly of smectite nanoparticles) are given in Tab. 4.12. They are highest for Am(III) and Pu(IV) and lie in the range of 10^5 - 10^6 L kg^{-1}. Lower values are found for Tc(IV), U(VI) and Cs(I) (10^2-10^4 L kg^{-1}). Under the high pH conditions it is not surprising that anionic species such as SeO_3^{2-} and TcO_4^- exhibit only weak interaction with colloids reflected by low Rd values. Low Rd values are also determined for Np(V) lying below the detection capabilities of the applied analytical techniques. The upper limit of 5×10^3 L kg^{-1} is anyhow in agreement with literature data. Bertetti et al. (1998) compiled data on Np(V) sorption onto a number of mineral phases including montmorillonite. Rd values for sorption to montmorillonite remained always below 5 10^2 L kg^{-1} even in absence of complexing ligands such as CO_3^{2-}. Pu sorption to colloids is relatively slow, possibly due to reduction of the residual Pu(VI) in the stock solution. Am did not show any measurable sorption kinetics. Cs and Tc(VII) again did not show any significant kinetic effects on the time-scale investigated. In the case of U(VI) sorption, slow kinetics were observed equilibrium might not have been reached in 18 weeks. Sorption was smaller and less time-dependent compared to that in presence of granodiorite. Se also showed almost the same kinetic effects as seen on granodiorite and fracture infill.

Sorption of most radionuclides onto **fracture filling material and granodiorite** increases with contact time. Even after experimental periods of 12 weeks, equilibrium appears not to be attained. Up to now, it is not clear what the underlying processes are (redox, precipitation and/or mineralisation reactions). This indicates again that a simple Kd approach cannot be applied to describe the sorption (or other uptake) processes in the system under investigation. More research is clearly necessary to clarify the uptake mechanisms involved in order to model the long term behaviour of such radionuclides. In general, Am sorption is somewhat greater than that of Pu and little sorption of Np is observed. U is more strongly sorbed to granodiorite than to the fracture filling material, whereas for Cs the opposite is true. The higher sorption of Cs, which mainly sorbs by ionic exchange, on fracture filling materials than granodiorite is most probably due to the higher content of layer silicates and in particular biotite. In case of Cs, the observed dependency of sorption on the fracture filling mineral grain size seems to disappear after 5 weeks and, in addition, the calculated Rd values were significantly higher, which may indicate kinetic effects, as have been observed in earlier studies (Aksoyoglu et al. 1990).

Figure 4.51 shows a summary of the Rd values obtained for sorption of all elements on the three main solids investigated.

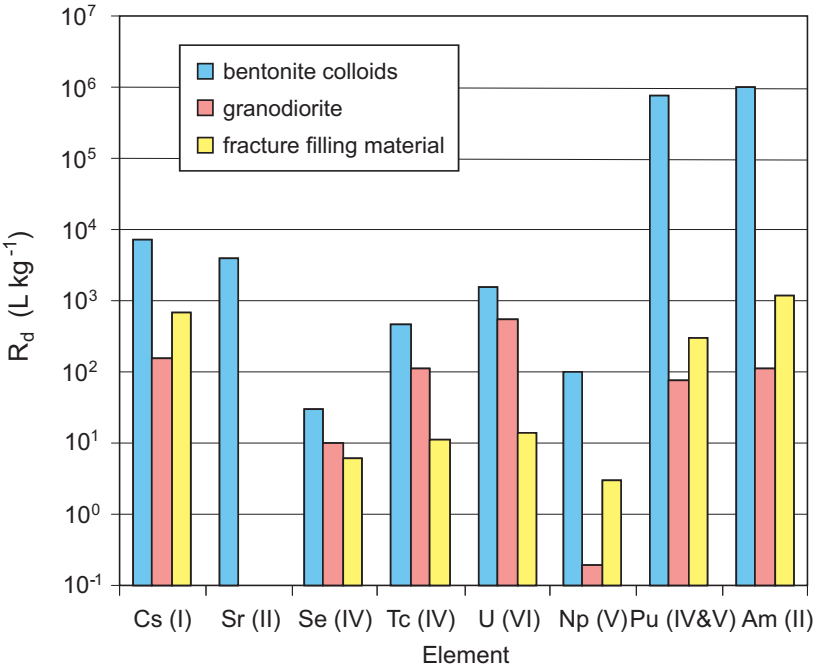

Fig. 4.51: Graphical summary of Rd values obtained in the present experiments.

It is assumed that, despite the low redox potential of the Grimsel groundwater in the batch experiments, Np remains in oxidation state (V) and, possibly, a part of the ^{244}Pu in oxidation state (VI) or (V). In the cases of Pu, U and Se, slow reduction might contribute to the sorption kinetics. For Tc(VII) a clear increase of sorption is found under anaerobic conditions, indicating that at least partial reduction to Tc(IV) is occuring. It is remarkable that Np(V) is almost non-sorbing and hence appears not to be reduced over the experimental time period. The same is true for Tc(VII) and U(VI) sorption to fracture filling material whereas for the sorption onto the granodiorite tentatively higher in Fe(II) containing mineral phases, reduction appears to be clear. Reduction of redox sensitive radionuclides very often is assumed to take place predominantly at Fe(II) containing mineral surfaces (e.g. Bondietti & Francis 1979). Depending

on the storage history of the material, it cannot be excluded that mineral surfaces are partly oxidised. Such processes might be responsible for the partly not or only incomplete reduction of Tc(VII), Se(VI), Np(V) and U(VI) in batch sorption studies. However, slow sorption kinetics are also found for the non-redox sensitive nuclides (e.g. Am(III)). This points to mechanisms other than redox reactions being responsible for the observed time dependencies. In the batch sorption experiments it is found that, even in the absence of bentonite colloids, Am and Pu may form significant quantities of colloidal species. Dissolution of such colloids or radionuclide desorption from colloids may also contribute to the observed kinetics. Further studies could focus on such colloids and their influence on the migration of these actinides.

Uptake of Pu and Am to **Grimsel granodiorite and fracture filling material** decreased by more than 1 order of magnitude **in the presence of 20 mg L^{-1} bentonite colloids**. No sorption of bentonite colloids onto Grimsel granodiorite or fracture filling material could be detected in these experiments. In the presence of granodiorite and fracture filling material, the sorption of Am and Pu with and without bentonite colloids showed a similar time-dependent trend which is an indication of reversible binding to the colloids. This finding is potentially very important for assessing the PA significance of colloids and should be verified in future experiments.

Both sorption and desorption processes and the underlying kinetics can be significant for the *in situ* migration experiment. For long residence times of the redox sensitive elements (Se, Tc, U, Np) in the undisturbed shear zone exceeding the experimental time periods used in our study, thermodynamic equilibria may be established and the reduced species may dominate in the system depending on the prevailing redox conditions. An important aspect which has previously not been investigated in detail is the desorption kinetics of radionuclides from both the solid phase (granodiorite / fracture filling material) and from the bentonite colloids. In case of very slow reaction rates, it is possible that the reactions can be considered "irreversible", at least for the time-scale of the *in situ* experiment.

Due to experimental constraints for the *in situ* tests, the contact time of the radionuclide cocktail with the surface of the fracture will be rather short – in the order of an hour. The cocktail itself will be prepared in the lab around 1 week in advance to injection. Having that in mind, it is clear that the kinetics of the sorption processes will be very important. In order to simulate the experiment, the relevant Rd values (short contact time for the sorption onto Grimsel granodiorite / fracture filling material and longer time for the radionuclide-colloid interaction) have to be used for modelling.

The following Tables summarise the calculated Rd values determined by the two laboratories (CIEMAT and FZK) in the framework of the CRR experiment.

Tab. 4.10: Selected Rd values (base data set for Grimsel granodiorite) for CRR relevant radionuclides in Grimsel groundwater under anoxic conditions at different test durations (solid : liquid ratio, 5g:20 ml).

Concentrations	**Distribution coefficient Rd (L kg^{-1})**									
	Contact times									
	1 h	2 h	1 d	2 d	11 d	14 d	28 d	54 d	84 d	100 d
^{75}Se(IV)										
$c_i = 1.71 \cdot 10^{-7}$ M	0.8	0.28	0.22	---	---	---	---	---	---	---
$c_i = 1.36 \cdot 10^{-7}$M	---	---	---	---	---	0.5	10	---	38	---
^{99}Tc(VII)										
$c_i = 2.79 \cdot 10^{-7}$ M	0.34	0.18	1.67	---	---	---	---	---	---	---
$c_i = 5.33 \cdot 10^{-7}$ M	---	---	---	---	---	150	141	---	122	---
^{99}Tc(IV)										
$c_i = 1.25 \cdot 10^{-8}$ M	91	---	107	---	---	110	114	---	---	---
^{137}Cs(I)										
$c_i = 5.76 \cdot 10^{-7}$ M	155	167	206	---	---	---	---	---	---	---
$c_i = 1.10 \cdot 10^{-7}$ M	---	---	---	---	---	63	45	---	60	---
^{233}U(VI)										
$c_i = 1.06 \cdot 10^{-7}$ M	9.9	12.2	20.3	---	---	---	---	---	---	---
$c_i = 4.04 \cdot 10^{-7}$ M	---	---	---	---	---	29	179	---	430	---
^{237}Np(V)										
$c_i = 1.3 \cdot 10^{-8}$ M (2. set)	---	< 1	---	< 1	---	< 1	---	---	---	---
$c_i = 3 \cdot 10^{-5}$ M* (1. set)	---	---	---	---	0.3*	0.2*	--	0.04*	--	0.2*
[$c_i = 1.3 \cdot 10^{-8}$ M (coll)]	---	[< 1]	---	[< 1]	---	[< 1]	---	---	---	---
^{244}Pu(IV)										
$c_i = 3.8 \cdot 10^{-11}$ M (2. set)	---	4.8	---	14	---	78	---	---	---	---
$c_i = 6 \cdot 10^{-9}$ M* (1. set)	---	---	--	---	10*	13*	--	44*	--	78*
[$c_i = 3.8 \cdot 10^{-11}$ M (coll)]	---	[0.6]	---	[2.5]	---	[3.0]	---	---	---	---
^{243}Am(III)										
$c_i = 1.3 \cdot 10^{-9}$ M (2. set)	---	12	---	21	---	130	---	---	---	---
$c_i = 3 \cdot 10^{-10}$ M* (1. set)	---		---	---	72*	110*	---	> 250*	--	> 250*
[$c_i = 1.3 \cdot 10^{-9}$ M (coll)]	---	[1.2]	---	[3.6]	---	[17.3]	---	---	---	---

^{237}Np, ^{244}Pu and ^{243}Am sorption was investigated with crushed Grimsel granodiorite (surface area ~2 $\cdot 10^{-1}$ m^2 g^{-1}) and size fractionated material (250-800 µm, surface area: 1 $\cdot 10^{-1}$ m^2 g^{-1}); ^{75}Se, ^{99}Tc, ^{137}Cs and ^{233}U sorption studies were performed with a grain size of < 64 µm.

* Sorption to crushed Grimsel granodiorite without size fractionation (exact experimental conditions for first and second set, see explanation in the text).

Values in brackets stand for the respective sorption experiments on the size fractionated Grimsel granodiorite in presence of 20 mg L^{-1} bentonite colloids.

Tab. 4.11: Rd values for all CRR relevant radionuclides on a fracture filling material / Grimsel groundwater solution; solid to liquid ratio for all experiments (5g:20mL).

	Distribution coefficient Rd (L kg^{-1})						
	Contact times						
	1 hour	2 hours	24 hours	1 week	2 weeks	4 weeks	6 weeks
Grain Size fraction (µm)	< 300	< 300	< 300	< 300	---	< 300	---
^{75}Se(IV)							
c_i = 2.12 x10^{-7} M	1.5	1.6	---	---	---	---	---
c_i = 2.9 ·10^{-7} M	---	---	---	3.3	---	---	5.1
^{99}Tc(VII)							
c_i = 3.45 ·10^{-7} M	0.3	0.4	---	---	---	---	---
c_i = 2.2 ·10^{-7} M	---	---	---	1.6	---	---	6.8
^{99}Tc(IV)							
c_i = 1.25 ·10^{-8} M	10	---	12	12	---	11	---
^{137}Cs							
c_i = 7.1 ·10^{-8} M	550	600	---	---	---	---	
c_i = 7.6 ·10^{-8} M	---	---	---	690	---	---	730
^{233}U							
c_i = 1.3 x10^{-7} M	5.0	5.6	3.6	4.2	5.6	6.3	
c_i = 6.8 x10^{-7} M	---	---	---	5.6	---	---	7.4

Grain size fraction (µm)	250 - 800	250 - 800	250 - 800	---	250 - 800	---	---
^{237}Np*							
c_i = 1.1 x10^{-8} M	---	<1 [< 1]	1.7 [1.8]	---	3.6 [3.8]	---	---
^{244}Pu*							
c_i = 7 x10^{-10} M	---	8 [2]	38 [2.4]	---	306 [9]	---	---
^{243}Am*							
c_i = 1.4 x10^{-9} M	---	46 [2]	223 [9]	---	1223 [39]	---	---

* values in brackets indicate Rd values in the presence of 20 mg L^{-1} bentonite colloids

Tab. 4.12: Rd values for bentonite colloid dispersions; solid to liquid ratios are indicated in terms of colloid concentrations c_{coll} (mg L^{-1}).

	Distribution coefficient Rd (L kg^{-1})						
	Contact Times						
	1 hour	1 day	1 week	2 weeks	3 weeks	4 weeks	12 weeks
$^{75}Se(IV)$							
$c_i = 1.36 \cdot 10^{-7}$M c_{coll}: 2 g L^{-1}	---	---	7	14	---	11	45
$^{99}Tc(VII)$							
$c_i = 5.33 \cdot 10^{-7}$M c_{coll}: 2 g L^{-1}	---	---	0	0	---	0	6.5
$^{99}Tc(IV)$							
$c_i = 4.5 \cdot 10^{-9}$M c_{coll}: 2 g L^{-1}	---	---	361	482	---	470	446
^{137}Cs							
$c_i = 1.10 \cdot 10^{-7}$M c_{coll}: 2 g L^{-1}	---	---	8'742	6'422	---	6'849	8'492
^{233}U							
$c_i = 4.04 \cdot 10^{-7}$M c_{coll}: 2 g L^{-1}	---	---	824	1'050	---	1'420	1'508
^{237}Np							
$c_i = 1.4 \cdot 10^{-8}$ M c_{coll}: 20 mg L^{-1}	$< 5 \cdot 10^3$	$< 5 \cdot 10^3$	$< 5 \cdot 10^3$	---	$5 \cdot 10^3$	---	---
^{244}Pu							
$c_i = 3.8 \cdot 10^{-11}$ M c_{coll}: 20 mg L^{-1}	$1 \cdot 10^5$	$1 \cdot 10^5$	$1 \cdot 10^5$	---	$8 \cdot 10^5$	---	---
^{243}Am							
$c_i = 9 \cdot 10^{-10}$ M c_{coll}: 20 mg L^{-1}	$3 \cdot 10^6$	$3 \cdot 10^6$	$2 \cdot 10^6$	---	$1 \cdot 10^6$	---	---

5 Conclusions

The aim of the laboratory experiments was to study the geochemical interaction of radionuclides in the system Grimsel groundwater - granodiorite / fracture filling material - bentonite. These laboratory experiments provided the necessary data for the final planning of the *in situ* migration experiment. Quantifying radionuclide sorption by simply measuring Rd values has to be considered carefully. Sorption of most radionuclides is very clearly shown to be much more complicated than implied by the conventional simple Kd concept. Sorption of most radionuclides exhibits strong kinetics and is partly influenced by colloid formation. Although distribution ratios have been calculated to conveniently represent the measured partitioning of radionuclides between 2 phases, this is not to be confused with sorption data considered by a more rigorous Kd concept where sorption constants represent fast, concentration-independent, reversible sorption that can be used directly in transport models. Quasi-mechanistic thermodynamic approaches to describe radionuclide sorption to mineral surfaces are evolving for some radionuclides and minerals (e.g. Degueldre et al. 1994, Bradbury et al. 2005). They allow taking variable geochemical conditions into account. The combination of experimental radionuclide speciation at surfaces by spectroscopic methods with the development of thermodynamic sorption models will allow gaining further understanding on sorption phenomena and more reliable thermodynamic modelling.

A thorough empirical study calls for the investigation of the dependency of sorption on radionuclide concentration, rock / water ratio, time, temperature, reaction direction, etc. A more mechanistic investigation could also consider effects of ionic strength, Eh and pH or even involve the application of spectroscopic techniques to determine the nature of dissolved and sorbed species. To pursue such an approach for this system is beyond the scope of this study. Sorption isotherms have been determined only for U, Sr and Cs, in order to illustrate the concentration dependency of the sorption of these elements. The experimental observations made in this work with regard to colloid formation and sorption kinetics of Pu and Am give an indication of the complexity of uptake processes in this multi-phase system.

Nevertheless, as a result of the experiments, a number of important and interesting properties of the investigated system emerged:

- The chemistry of the Grimsel groundwater favours the stabilization of aquatic colloids, specifically of colloidal smectite particles derived from bentonite barrier material. During sorption experiments using crushed Grimsel granodiorite and fracture filling, the increase of the Al-concentration, which decreased after ultracentrifugation, indicates also the release of colloidal particles into the water through dispersion processes.
- These colloids can considerably influence the transportation of the actinides U, Pu and Am and the fission product Cs. This becomes obvious when looking at the distribution of radionuclides between the aqueous and solid phases in presence and absence of colloids. For ^{75}Se(IV), ^{99}Tc(VII) and Np(V) the influence of colloids appears to be of less importance.
- The sorption reactions of Cs, U, Pu and Am are characterized by slow kinetics. In particular, sorption (or other uptake) reaction onto granodiorite and fracture filling do not appear to reach equilibrium on a timescale of weeks. The calculated Rd values increase by orders of magnitude over this time.
- The presence of smectite colloids decreases the extent of uptake of Cs, U and, in particular Pu and Am onto fracture filling or granodiorite. This can be explained in terms of competitive sorption, especially for Am and Pu which have very high Rd values for sorption to bentonite colloids (in the order of $1 \cdot 10^5 - 10^6$ L kg^{-1}).

- One of the most important questions for the assessment of the relevance of colloid mediated radionuclide migration involves the reversibility of the radionuclide / colloid binding. For Pu and Am, this question is certainly difficult to answer, but there are clear indications of, at least, partial reversibility over a timescale of days. This finding is potentially very important for assessing the PA significance of colloids and could be a priority issue to be addressed in future experiments.

6 References

Aksoyoglu S., Bajo C. & Mantovani M. (1990). Grimsel Test Site: Batch sorption Experiments with iodine, bromine, strontium, sodium and caesium on Grimsel mylonite. Nagra Technical Report NTB 91-06; Nagra, Wettingen, Switzerland (February 1991) also published as PSI Bericht Nr. 83; Paul Scherrer Institute, Villigen, Switzerland.

Alexander W. R. (1991). Redox state of the Grimsel Test Site (GTS) radionuclide Migration Experiment (MI) groundwater/rock system Unpubl. Nagra Internal Report. Nagra, Wettingen, Switzerland.

Alexander W. R., Frieg B., Ota K. & Bossart P. (1996). The RRP Project – Investigating radionuclide retardation in the host rock. Nagra Bulletin 27 (June, 1996), 43-55. Nagra, Wettingen, Switzerland.

Alexander W. R. & Kickmaier W. (2000). Radionuclide retardation in water conducting systems - lessons learned in the research programme in the Grimsel Test Site/ Radionuklidretardation in wasserführenden Systemen - Erfahrungen aus den Untersuchungsprogrammen im Felslabor Grimsel. Sanierung der Hinterlassenschaften des Uranerzbergbaus (Chancen und Grenzen der geochemischen und Transport-Modellierung bei der Verwahrung von Uranbergwerken und bei der Endlagerung radioaktiver Abfälle), 5th Workshop (18 - 18 May, 2000), Dresden, Germany.

Alexander W. R., MacKenzie A. B., Scott R. D. & McKinley I. G. (1990). Natural Analogue Studies in Crystalline Rock: The Influence of Water-bearing Fractures on Radionuclide Immobilisation in a Granitic Rock repository. Nagra Technical Report NTB 87-08; Nagra, Wettingen, Switzerland.

Alexander W. R., Ota K. & Frieg B. (eds.) (2003). The Nagra-JNC *in situ* study of safety relevant radionuclide retardation in fractured crystalline rock II: the RRP project methodology development, field and laboratory tests. Nagra Technical Report NTB 00-06. Nagra, Wettingen, Switzerland.

Axe L. & Trivedi P. (2002). Intraparticle surface diffusion of metal contaminants and their attenuation in microporous amorphous Al, Fe, and Mn oxides. J. Coll. Interf. Sci., 247, 259-265.

Baeyens B., Maes A. & Cremers A. (1985). *In situ* Physico-chemical Characterization of Boom Clay; Radioactive Waste Management and the Nuclear Fuel Cycle; 6, p. 391.

Bajo C., Hoehn E., Keil R. & Baeyens B. (1989). Chemical Characterisation of the Groundwater from Fault Zone AU 96m. In Grimsel Test Site-Laboratory Investigations in Support of the Migration Experiments; in M. Bradbury ed.; Nagra Technical Report NTB 88-23; Nagra, Wettingen, Switzerland, also published as PSI Report 28, April 1989. Paul Scherrer Institute, Würenlingen and Villigen, Switzerland.

Barcelona M. J. & Holm T.R. (1991). Oxidation–reduction capacities of aquifer solids. Environ. Sci. Tech. 25, 1565-1572.

Barringer E. A., Novich B. E. & Ring T. A. (1984). Determination of colloid stability using photon correlation spectroscopy, J. Coll. Interface Sci. 100, 584-586.

Baston G. M. N., Berry J. E. & Brownsword M. (2003). Effect of sorption kinetics. Section 3.4 in Alexander W. R., Ota K. & Frieg B. (2003) eds. The Nagra-JNC *in situ* study of safety relevant radionuclide retardation in fractured crystalline rock II: the RRP project methodology development, field and laboratory tests. Nagra Technical Report Series NTB 00-06, Nagra, Wettingen, Switzerland.

Bertetti F.P., Pabalan R.T. & Almendarez M.G. (1998). Studies of Neptunium(V) sorption on Quartz, Clinoptiloite, Montmorillonite, and g-Alumina, in E.A. Jenne (ed.) Adsorption of Metals to Geomedia, Academic press, San Diego, p. 131-148).

Bondietti E. A. & Francis C. W. (1979). Geologic migration potentials of technetium-99 and neptunium-237. Science 203, 1337-1340.

Bossart P. & Mazurek M. (1991). Grimsel Test Site: Structural Geology and Water Flow- Paths in the Migration Shear Zone. Nagra Technical Report NTB 91-12; Nagra, Wettingen, Switzerland.

Boult K. A., Cowper M. M., Heath T. G., Sato H., Shibutani T. & Yui M. (1998). Towards an understanding of the sorption of U(VI) and ^{75}Se(IV) on sodium bentonite. J. Contam. Hydrol., 35, 141-150.

Bradbury M. H. (ed.) (1989). Grimsel Test Site-Laboratory investigations in support of the Migration Experiments. Nagra Tech. Report NTB 88-23, Nagra, Wettingen, Switzerland, also published as PSI Report 28, April 1989. Paul Scherrer Institute, Villigen, Switzerland.

Bradbury M. H. & Baeyens B. (1992). Modelling the sorption of Cs – Application to the Grimsel Migration Experiment. PSI Annual Report 1992, Annex IV, 59-64, PSI, Villigen.

Bradbury M. H. & Baeyens B. (2000). A generalised sorption model for the concentration dependent uptake of caesium by argillaceous rocks. J. Contam. Hydrol., 42, 141–163.

Bradbury M. & Baeyens B. (2005). Modelling the sorption of Mn(II), Co(II), Ni(II), Zn(II), Cd(II), Eu(III), Am(III), Sn(IV), Th(IV), Np(V) and U(VI) on montmorillonite: Linear free energy relationships and estimates of surface binding constants for some selected heavy metals and actinides, Geochim Cosmochim. Acta 69 5391-5392.

Buck E. C. & Bates J. K. (1999). Microanalysis of colloids and suspended particles from nuclear waste glass alteration. Appl. Geochem. 14 (5), 635-653.

Buffle J. & Leppard G.G. (1995). Characterization of aquatic colloids and macromolecules. 1. Structure and behavior of colloidal material. Environ. Sci. Technol., 29, 2169-2175.

Chisholm-Brause C. J., Conradson S. D., Busher C. T., Eller P. & Morris D. E. (1994). Speciation of uranyl sorbed at multiple binding sites on montmorillonite. Geochim. Cosmochim. Acta, 58(17): 3625-3631.

Comans R. N., Holler M. & DePreter P. (1991). Sorption of ^{137}Cs on illite: non equilibrium behaviour and reversibility. Geochim. Cosmochim. Acta 55, 433-440.

Cuadros J. & Linares J. (1996). Experimental kinetic study of the smectite-to-illite transformation. Geochim. Cosmochim. Acta 60, 439-453.

Cui D. & Eriksen T. E. (1996). Reduction of pertechnetate in solution by heterogeneous electron transfer from Fe(II)-containing geological material. Environ. Sci. Technol. 30, 2263–2269.

Degueldre C. (1994). Colloid Properties in Groundwaters from Crystalline Formations. Nagra Technical Report NTB 92-05, Nagra, Wettingen, Switzerland.

Degueldre C., Grauer R., Laube A., Oess A. & Silby H. (1996b). Colloid properties in granitic groundwater systems, Part II: Stability and Transport Study. Appl. Geochem. 11, 697-710.

Degueldre C., Longworth G., Moulin V. & Vilks P. (1990). Grimsel Test Site-Grimsel Colloid Exercise: An International Intercomparison Exercise on the Sampling and Characterisation of Groundwater Colloids. Nagra Technical Report NTB 90-01; Nagra, Wettingen, Switzerland, also published as PSI Bericht Nr. 39; Paul Scherrer Institute, Villigen, Switzerland.

Degueldre C., Pfeiffer H.-R., Alexander W. R., Wernli B. & Bruetsch R. (1996a). Colloid properties in granitic groundwater systems. I: sampling and characterisation. Appl. Geochem. 11, 677-695.

Degueldre C., Ulrich H.J. & Silby H. (1994). Sorption of Am-241 onto montmorillonite, illite and hematite colloids, Radiochim. Acta 65, 173-179.

Dierckx A., Put M., De Cannière P., Wang L., Maes N., Aertsens M., Maes A., Vancluysen J., Verdickt W., Gielen R., Christians M., Warwick P., Hall A., Van der Lee J. (2000). TRANCOM-CLAY: Transport of radionuclides due to complexation with organic matter in clay formations. EUR19135EN, European Commission, Nuclear Science and Technology, Luxembourg.

Dodds J. (1982). La Chromatographie Hydrodynamique. Analysis, 10, 109-119.

Duro L., Bruno J., Rollin C., Guimerà J., Geckeis H., Schüßler W., Vejmelka P., Shibata M., Yoshida Y., Ota K. & Yui M. (2000)., Prediction of the solubility and speciation of RN in Febex and Grimsel waters. Colloid and Radionuclide Retardation project. Nagra Report, Nagra 99-218, Nagra, Wettingen, Switzerland.

Eikenberg J., Baeyens B. & Bradbury M. H. (1991). The Grimsel Migration Experiment: A Hydrogeochemical Equilibration Test. Nagra Technical Report NTB 90-39; Nagra, Wettingen, Switzerland, also printed as PSI Report 100, May 1991. Paul Scherrer Institute, Villigen, Switzerland.

Einarson M.B. & Berg J. (1993). Electrosteric stabilisation of colloidal latex dispersions. Colloid Interface Sci., 155, 165-172.

Fernández A. M., Baeyens B., Bradbury M. & Rivas P. (2004). Analysis of the porewater chemical composition of a Spanish compacted bentonite used in an engineered barrier. Physics and Chemistry of the Earth 29, 105-118.

Fierz Th., Geckeis H., Götz R., Geyer F. W. & Möri A. (ed.) (2001). GTS V/CRR: Tracer tests #1 - #16 (September 1999 – January 2001). Unpublished Nagra Internal Report. Nagra, Wettingen, Switzerland.

Finn P. A., Buck E. C., Gong M., Hoh J. C., Emery J. W., Hafenrichter L. D. & Bates J. K. (1994). Colloidal products and actinide species in leachate from spent nuclear fuel. Radiochim. Acta 66-67, 189-195.

Frick U., Alexander W. R., Baeyens B., Bossart P., Bradbury M. H., Bühler Ch., Eikenberg J., Fierz Th., Heer W., Hoehn E., McKinley I. G. & Smith P. A. (1992). Grimsel Test Site - The Radionuclide Migration Experiment-Overview of Investigations 1985 -1990. Nagra Technical Report NTB 91-04, Nagra, Wettingen, Switzerland.

García-Gutiérrez M. (2000). Base de datos de sorción, difusión y solubilidad para la evaluación del comportamiento. CIEMAT Informe técnico 931, CIEMAT, Madrid, Spain.

Gardiner M. P., Grindrod P. & Moulin V. (2001). The Role of Colloids in the Transport of Radionuclides from a Radioactive Waste Repository: Implication on Safety Assessment. Final Project Report EUR 19781, European Commission, Brussels, Belgium.

Geckeis H. (ed.) (1999a). Detailed and long term laboratory experiments. Colloid and Radionuclide Retardation project. Unpubl. Nagra Internal Report, Nagra, Wettingen, Switzerland.

Geckeis H., Grambow B., Loida A., Luckscheiter B., Smailos E. & Quinones J. (1998). Formation and stability of colloids under simulated near field conditions. Radiochim. Acta 82, 123-128.

Geckeis H., Grambow B., Loida A., Luckscheiter B., Smailos E. & Quinones J., (1999b). CRR Task 1c: Colloid generation under near-field conditons: -Evidences from experimental data obtained at INE, Conclusions drawn with respect to the expected radiocolloid stability in Grimsel groundwater and FEBEX porewater, Unpubl. Nagra Internal Report, Nagra, Wettingen, Switzerland.

Geckeis H., Klenze R. & Kim, J. I. (1999c). Solid-Water-Interface Reactions of Actinides and Homologues: Sorption onto Mineral Surfaces, Radiochim. Acta 87, 13 -21.

Geckeis H. & Möri A. (eds.) (2003). GTS V/CRR: Homologue, Br and Sr tracer tests. Unpubl. Nagra Internal Report, Nagra, Wettingen, Switzerland.

Guillaumont R.& Adloff J. P. (1992). Behavior of environmental plutonium at very low concentration, Radiochim. Acta 58-9, 53-60.

Hadermann J. (2001). Colloid-related Retention Processes. Conclusions of Working Group 3. In: Radionuclide Retention in Geologic Media, Workshop Proceedings, Oskarshamn, Sweden, 7-9 May 2001, OECD/NEA, Paris, France.

Hauser W., Geckeis H., Götz R., Geyer F.-W., Inderbitzin L., Fierz Th. & Möri A. (2003). GTS Phase V: CRR Experiment Laser-Induced Breakdown Detection of Natural Colloid Background at the Grimsel Test Site. Unpublished Nagra Internal Report, Nagra, Wettingen, Switzerland.

Hauser W., Geckeis H., Kim J. I. & Fierz Th. (2002). A mobile laser-induced breakdown detection system and its application for the *in situ* monitoring of colloid migration.-Coll. Surf. A: Physicochem. Eng. Aspects 203, 37-45.

Hauser W., Götz R., Geckeis H., & Kienzler B. (2005). *In situ* colloid detection in granite groundwater along the Äspö HRL access tunnel, in Laaksoharju M., Wold S., (eds.). The colloid investigations conducted at the Äspö Hard Rock Laboratory during 2000–2004, SKB Technical Report, TR-05-20, p. 57-76, SKB, Stockholm, Sweden.

Hockin S.L. & Gadd G. M. (2003). Linked Redox Precipitation of Sulfur and Selenium under Anaerobic Conditions by Sulfate-Reducing Bacterial Biofilms, Appl. Environ. Microbiol. 69, 7063-7072.

Hoehn E., Eikenberg J., Fierz Th., Drost W. & Reichlmayr E. (1998). The Grimsel Migration Experiment: field injection-withdrawal experiments in fractured rock with sorbing tracers. J. Contam. Hydrol., 34, 85-106.

Howard J. H (1977). Geochemistry of selenium: Formation of ferroselite and selenium behaviour in the vicinity of oxidizing sulphide and uranium deposits. Geochim. Cosmochim. Acta 41/11, 1665-1678.

Huertas F., Fuentes-Cantillana J. L., Jullien F., Rivas P., Linares J., Fariña P., Ghoreychi M., Jockwer N., Kickmaier W., Martínez M. A., Samper J., Alonso E. & Elorza F.J. (2000). Full-scale engineered barriers experiment for a deep geological repository for high-level radioactive waste in crystalline host rock (FEBEX project): Final report. EUR 19147 EN. European Commission, Brussels.

Huertas F., Fariña P., Farias J., García-Siñeriz J.L., Villar M.V., Fernández A.M., Martín P.L., Elorza F.J., Gens A., Sánchez M., Lloret A., Samper J. & Martinez M.A. (2006). FEBEX Updated Final Report (1994-2004). Enresa technical Publication 05-0/2006.

James S. C. & Chrysikopoulos C. V. (1999. Transport of Polydisperse Colloid Suspensions in a Single Fracture, Water Resources Research, 35 (3), 707-718.

JNC (2000). Properties of the Buffer. *In*: H12: Project to Establish the Scientific and Technical Basis for HLW Disposal in Japan, Supporting Report 2: Repository Design and Engineering Technology, Appendix B, JNC Technical Report, JNC TN1410 2000-003, JAEA, Tokai, Japan.

Kaplan D. I., Bertsch P. M., Adriano D. C. & Orlandini K. A. (1994). Actinide association with groundwater colloids in a coastal plain aquifer. Radiochim. Acta 66-67, 181-187.

Kersting A. B., Efurt D. W., Finnegan D. L., Rokop D. J., Smith D. K. & Thompson J. L. (1999). Migration of Plutonium in Groundwater at the Nevada Test Site, Nature, 397: 56 - 59.

Kim J. I. (1991). Actinide colloid generation in groundwater. Radiochim. Acta 52-53, 71-81.

Kim J. I., Delakowitz B., Zeh P., Klotz D. & Lazik D. (1994). A column experiment for the study of colloidal radionuclide migration in Gorleben aquifer systems. Radiochim. Acta 66-67, 165-171.

Kim Y., Cygan R. T. & Kirkpatrick R. J. (1996). ^{133}CsNMR and XPS investigation of ^{137}Cs adsorbed on clay minerals and related phases. Geochim. Cosmochim. Acta, 60 1041-1052.

Knopp R. & Klenze R. (1999). *In situ* detection of colloids in granitic Groundwaters by laser induced Breakdown Detection (LIBD). Institut für Nukleare Entsorgung, Forschungszentrum Karlsruhe, 76021 Karlsruhe, Germany.

Laaksoharju M. (1990). Colloidal particles in deep Swedish granitic groundwater. SKB report: AR-90-37, SKB, Stockholm Sweden.

Liang L. & Morgan J.J. (1990). Chemical aspects of iron-oxide coagulation in water-Laboratory studies and implications for natural systems. Aquat. Sci. 52, 32-55.

Linklater C. M., Albinsson Y., Alexander W. R., Casas I., McKinley I. G. & Sellin P. (1996). A natural analogue of high pH cement pore waters from the Maqarin area of northern Jordan: comparison of predicted and observed trace element chemistry of uranium and selenium. J. Contam. Hydrol. 21, pp 59-69.

Lovley D. R., Phillips J. P., Gorby Y. A. & Landa E. R. (1991): Microbial reduction of uranium. Nature, 350, 413-415.

Lu N., Cotter C. R., Kitten H. D., Bentley J. & Triay I. R. (1998). Reversibility of sorption of ^{239}Pu onto hematite and goethite colloids. Radiochim. Acta 83, 167-173.

Maiti T. C., Smith M. R. & Laul J.C. (1989). Colloid formation study of U, Th, Ra, Pb, Po, Sr, Rb, and ^{137}Cs in briny (high ionic strength) groundwaters: analog study for waste disposal. Nucl. Technol. 84, 82-87.

Mazurek M., Alexander W. R. & Meier P. M. (2001). Ch 4, Geological and hydrogeological characterisation of the MI shear zone. *in* Smith P. A., Alexander W. R., Heer W., Fierz Th., Meier P. M., Baeyens B., Bradbury M. H., Mazurek M. & McKinley I. G. (2001). The Nagra-JNC *in situ* study of safety relevant radionuclide retardation in fractured crystalline rock I: The radionuclide migration experiment-overview of investigations 1990-1996. Nagra Technical Report Series NTB 00-09, Nagra, Wettingen, Switzerland.

McCarthy J.F., Czerwinski K.R., Sanford W.E., Jardine P.M. & Marsh J.D. (1998). Mobilization of transuranic radionuclides from disposal trenches by natural organic matter. J. Contam. Hydrol. 30:49–77.

McKinley I. G. & Alexander W. R. (1993). Assessment of radionuclide retardation: uses and abuses of natural analogues, J. Contam. Hydro. 13, 249-259.

McKinley I. G. & Hadermann J. (1984). Radionuclide sorption database for Swiss safety assessments. Nagra Technical Report, NTB 84-40, Nagra, Wettingen, Switzerland.

McKinley J. P., Zachara J.M., Smith S. C. & Turner G. D. (1995). The influence of hydrolysis and multiple-site binding reactions on adsorption of U(VI) onto montmorillonite. Clay Clay Miner., 43, 568-598.

Meyer J., Mazurek M. & Alexander W. R. (1989). Petrographic and Mineralogical Characterisation of fault Zones AU 96 m and AU 126 m. In Grimsel Test Site: Laboratory Investigations in Support of the Migration Experiments; in Bradbury M. *ed*.; Nagra Technical Report NTB 88-23; Nagra, Wettingen, Switzerland, also published as PSI Report 28, April 1989. Paul Scherrer Institute, Würenlingen and Villigen, Switzerland.

Miller W. M., Alexander W. R., Chapman N. A., McKinley I. G. & Smellie J. A. (2000). Geological Disposal of Radioactive Wastes and Natural Analogues. Waste Management Series, vol. 2, Pergamon, Amsterdam, The Netherlands.

Missana T., Fernández V., Gutiérrez M. G., Alonso U. & Mingarro M. (2001). CRR project. Sorption Studies Final Report; Unpubl. CIEMAT internal report CIEMAT/DIAE/ 54431/2/2001, CIEMAT, Madrid, Spain.

Missana T., García-Gutiérrez M., Fernández V. & Gil P. (2002). Application of mechanistic models for the interpretation of radionuclide sorption in clays. Part (1) CIEMAT/ DIAE/54610/01/03.

Missana T. & García-Gutiérrez M. (2005). Experimental study and geochemical modelling of the cesium, calcium and strontium sorption on FEBEX smectite. Migration Conference 2003.

Missana T., Garcia-Gutierrez M. & Alonso U. (2004). Kinetics and irreversibility of cesium and uranium sorption onto bentonite colloids in a deep granitic environment, Appl. Clay Sci., 26, 137-150.

Möri A. (ed.) (2004). The CRR final project report series I: Description of the Field Phase - Methodologies and Raw Data. Nagra Technical Report NTB 03-01. Nagra, Wettingen, Switzerland.

Möri A. & Adler M. (2001). GTS, Excavation project (EP): The Nagra-JNC *in situ* study of safety relevant radionuclide retardation in fractured crystalline rock: Structural description and conceptual model of flow paths and radionuclide retardation sites. Unpubl. Nagra Internal Report, Nagra, Wettingen, Switzerland.

Möri A.; Biggin C.; Mäder U.; Eikenberg J.; Rüthi M. (2006a): Novel application of beta/ gamma autoradiography and collimated gamma-spectrometry to study in situ radionuclide migration paths in fractured rock.- Migration '05: Chemistry and migration behaviour of actinides and fission products in the geosphere: 10th international conference, Avignon, France, September 18-23, 2005.- Physics and Chemistry of the Earth 31 / 10-14, 511-516.

Möri A., Frieg B., Ota K. & Alexander W. R. (eds) (2006b). The Nagra-JNC *in situ* study of safety relevant radionuclide retardation in fractured crystalline rock III: the RRP project final report. Nagra Technical Report NTB 00-07 (*in prep*), Nagra, Wettingen, Switzerland.

Möri A., Mazurek M., Adler M., Schild M., Siegesmund S., Vollbrecht A., Ota K., Ando T., Alexander W. R., Smith P. A., Haag P. & Bühler Ch. (2003). The Nagra-JNC *in situ* study of safety relevant radionuclide retardation in fractured crystalline rock IV: The *in situ* study of matrix porosity in the vicinity of a water-conducting fracture. Nagra Technical Report NTB 00-08, Nagra, Wettingen, Switzerland.

Morris D. E., Chrisolm-Brause C. J., Barr M. E., Conradson S. D. & Eller P. G. (1994). Optical and spectroscopic studies of the sorption of uranyl species on a reference smectite. Geochim. Cosmochim. Acta, 58: 3626.

Moulin V., Billon A., Theyssier M. & Dellis T. (1991). Study of the interactions between organic matter and transuranic elements. Final Report (1986-1989), CEC Report EUR 13651 EN, Brussels.

Nagra (1994). Kristallin-I Safety Assessment Report. Nagra Technical Report NTB 93-22. Nagra, Wettingen, Switzerland.

Neall F. B. & Smith P. A. (ds.) (2003). H12: examination of safety assessment aims, procedures and results from a wider perspective. JNC Technical report JNC TY1400 2004-001, JAEA, Tokai, Japan.

Neck V., Müller R., Bouby M., Altmaier M., Rothe J., Denecke M. A. & Kim J. I. (2002). Solubility of amorphous Th(IV) hydroxide application of LIBD to determine the solubility product and EXAFS for aqueous speciation, Radiochim. Acta, 90 (9-11), 485 - 494.

Neretnieks I., Ernstsson I. & M.-L. (1997). A Note on Radionuclide Transport by Gas Bubbles. Materials Research Society Symposium Proceedings 467, 855 - 862.

Newman A. C. D. (ed.) (1987). Chemistry of Clay and Clay Minerals. Mineral Soc., Monograph N6.

Olofsson U., Allard B., Torstenfelt B. & Andersson K. (1982a). Properties and mobilities of actinide colloids in geologic systems. Scientific Basis for Nuclear Waste Management V: Proceedings of the Materials Research Society fifth international symposium, June 7-10, 1982, Berlin (Ed. W. Lutze). Mat. Res. Soc. Symp. Proc. 11. Elsevier Sci. Publ. Co., New York, 755-764.

Olofsson U., Allard B., Torstenfelt B. & Andersson K. (1982b): Formation and properties of americium colloids in aqueous systems.-Scientific Basis for Nuclear Waste Management IV: Proceedings of the Materials Research Society Annual Meeting, November 1981, Boston (ed. S.V. Topp). Mat, Res, Soc, Symp, Proc, 6. Elsevier Sci. Publ. Co., New York, 191-198.

Onodera Y., Iwasaki T., Ebina T., Hayashi H., Torii K., Chatterjee A. & Mimura H. (1998). Effect of layer charge on fixation of caesium ions in smectites. J. Contam. Hydrol., 35, 131-140.

Oscarson D. W., Watson R. L. & Miller H. G. (1987). The interaction of trace levels of caesium with montmorillonitic and illitic clays. Appl. Clay Sci., 2, 29-39.

Ota K., Möri A., Alexander W. R., Frieg B. & Schild M. (2003). Influence of the mode of matrix porosity determination on matrix diffusion calculations. J. Contam. Hydrol. 61, 131-145.

Parks G. A. (1965). The isoelectric points of solid oxides, solid hydroxides, and aqueous hydroxo complex systems. Chem. Rev. 65, 177-198.

Prieve D.C. & Hoysan P. M. (1978). Role of Colloidal Forces in Hydrodynamic Chromatography. J. Coll. Interf. Sci., 64/2, 201-213.

Pusch R. (1999). Clay colloid formation and release from MX-80 buffer. SKB Technical Report TR 99-31. SKB, Stockholm, Sweden.

RETROCK 2005. Treatment of radionuclide transport in geosphere within safety assessment. Final Report EUR 21230 EN.

Ryan J.N. & Elimelech M. (1996). Colloid mobilization and transport in groundwater, Coll. Surf. 107, 1-56.

Smith P. A., Alexander W. R., Heer W., Meier P. M., Baeyens B., Bradbury M. H., Mazurek M. & McKinley I. G. (2001a). The Nagra-JNC *in situ* study of safety relevant radionuclide retardation in fractured crystalline rock. In: The radionuclide migration experiment-overview of investigations 1990-1996. Nagra Technical Report NTB 00-09, Nagra, Wettingen, Switzerland.

Smith P. A., Alexander W. R., Kickmaier W., Ota K., Frieg B. & McKinley I. G. (2001b). Development and Testing of Radionuclide Transport Models for Fractured Rock: Examples from the Nagra/JNC Radionuclide Migration Programme in the Grimsel Test Site, Switzerland. J. Contam. Hydrol. 47, 335-348. *Also published in Japanese in JNC Technical Review 11, JNC TN1340 2001-006, JAEA, Tokai, Japan.*

Smith P. A., Guimerà J., Kosakowski G., Pudewills A. & Ibaraki M. (eds.) (2006). The CRR final project report series III: Results of the Supporting Modelling Programme. Nagra Technical Report NTB 03-03, Nagra, Wettingen, Switzerland.

Staunton S. & Roubaud M. (1997). Adsorption of caesium on montmorillonite and illite: effect of charge compensating cation, ionic strength, concentration of ^{137}Cs, K and fulvic acid. Clays and Clay Minerals, 45 (2), 251-260.

Sylvester E. R., Hudson E. A. & Allen P. G. (2000). The structure of U(VI) sorption complexes on silica, alumina and montmorillonite. Geochim. Cosmochim. Acta, 64 (14): 2431-2438.

Turner G. D., Zachara J. M, McKinley J.P. & Smith S. C. (1996). Surface-charge properties and UO22+ adsorption of a subsurface smectite. Geochim. Cosmochim. Acta, 60 (18) 3399-3414.

Turrero M.J., Gómez P., del Villar L.P., Moulin V., Magonthier M.C. & Menager M.T. (1995). Relation between colloid composition and the environment of their formation: application to the El Berrocal site (Spain). Appl. Geochem, 10, 119-131.

USDOE (2007). Basic Research Needs for Geosciences: Facilitating 21st Century Energy Systems.

Vandergraff T. T. & Ticknor K. V. (1994). A compilation and Evaluation of Sorption Coefficients Used in the Geosphere Model SYVAC for the 1990 Assessment of Whiteshell Research Area. AECL-10546, COG-92-59, AECL, Whiteshell, Canada.

van Olphen H. (1977). In: An Introduction to Clay Colloid Chemistry. Wiley Interscience.

Vieno T. & Nordman H. (1999). Safety assessment of spent fuel disposal in Hästholmen, Kivetty, Olkiluoto and Romuvaara. TILA-99. POSIVA 99-07, Posiva, Helsinki, Finland.

Vilks P., Frost L.H. & Bachinski D.B. (1997). Field-scale colloid migration experiments in a granitic fracture, J. Contam. Hydrol. 26, 203-214.

Vilks P., Miller H. & Doern D. (1991). Natural colloids and suspended particles in the Whiteshell Research Area, Manitoba, Canada, and their potential effects on radiocolloid formation. Appl. Geochem. 6, 565-574.

Wan J. & Wilson J. L. (1994). Visualization of the Role of the Gas-water Interface on the Fate and Transport of Colloids in Porous Media. Water Resources Research, 30, 11- 23.

Weiss C. A., Kirkpatrick R. J. & Altaner S. P. (1990). The structural environment of cations adsorbed onto clays: ^{133}Cs variable-temperature MAS NMR spectroscopic study of hectorite. Geochim. Cosmochim. Acta 54, 1655-1669.

Wersin P., Hochella M. F., Persson P., Redden G., Leckie J. O. & Harris D. W. (1994). Interaction between aqueous uranium (VI) and sulfide minerals: spectroscopic evidence for sorption and reduction. Geochim. Cosmochim. Acta 58, 2829 – 2843.

Wold S. & Eriksen T. E. (2003). Diffusion of lignosulfonate colloids in compacted bentonite, Appl. Clay Sci., 23, 43-50.

Zachara J. M. & McKinley J. P. (1993). Influence of hydrolysis on the sorption of metal cations by smectites: importance of edge coordination reactions. Aquat. Sci., 55, 250-261.

Zachara J. M., Smith S. C., Liu C., McKinley J. P., Serne R. J. & Gassman P. L. (2002). Sorption of $^{137}Cs^{+}$ to micaceous subsurface sediments from the Hanford site, USA. Geochim. Cosmochim. Acta 66, 193-211.

Appendix Short note on JNC's colloid erosion experiment

Experiment of colloid generation from compacted bentonite in Japan.

Kazuki Iijima, JAEA, Tokai, Japan

As a candidate buffer material for use in the geological disposal of high-level radioactive waste, densely compacted bentonite has a number of favourable properties, such as its low permeability and high capacity for radionuclide sorption. Furthermore, as the bentonite resaturates and swells following repository closure, fractures within the bentonite will be sealed, and the bentonite may also be extruded into fractures of the surrounding rock, diverting a part of the water flow away from the repository. This phenomenon is potentially advantageous to repository safety. However, if loss of bentonite into fractures due to extrusion and subsequent erosion of the extruding front by flowing groundwater is too pronounced, then the decrease in density of the bentonite within the repository may be sufficient to reduce its favourable properties. The eroding bentonite front may also provide a source of colloids. Colloids may then sorb radionuclides and, since colloids are not necessarily subject to the same retardation processes as solutes, they could provide a means by which radionuclides are transported relatively rapidly through the geosphere. Therefore, the extrusion and erosion of bentonite buffer from the disposal pit or tunnel should be quantitatively understand to evaluate long-term physical stability of the engineered barriers for the geological disposal of high-level radioactive waste. This study focuses on an experimental study on bentonite erosion. The objective of this experiment is to clarify the relationship between underground water velocity and generation rate of bentonite colloid.

EXPERIMENTAL EQUIPMENT

Fig. A-1 shows the experimental equipment for the erosion tests. The rock fracture is simulated by inserting a spacer between the upper and lower acrylic plates. The test water is supplied into this fracture. Water absorption and swelling behavior of the buffer specimens are observed from the top and the outflow distance (distances from the hole wall to the distal point of the extruded buffer material) are measured by photography. The simulated fracture width is set in the range of 0.3 to 1.5 mm. On top of the specimen, a sintered metal filter is installed and, under the specimen, a load cell (strain gauge type) is installed equipped with a piston (round rod made of stainless steel), and the swelling pressure of the simulated disposal pit is measured. A two-dimensional flow field is generated by supplying water into the simulated fracture through one of two holes made in the upper acrylic plate and draining through the other hole.

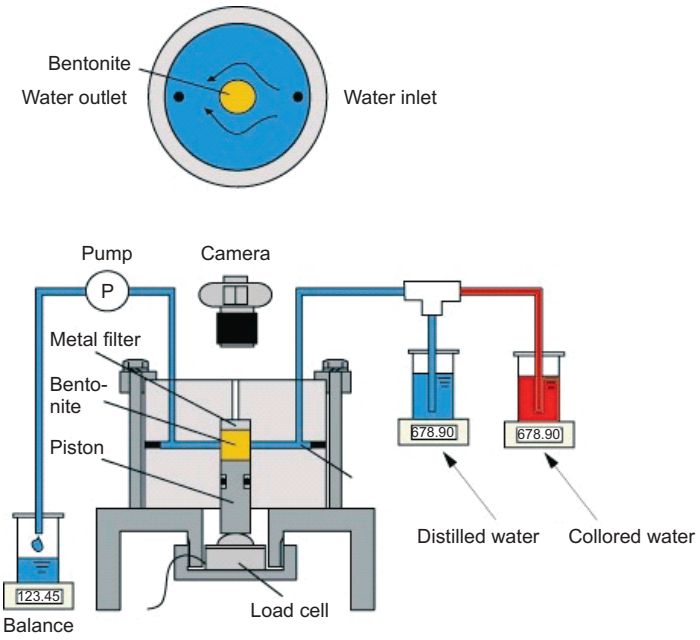

Fig. A-1: Experimental equipment.

TEST MATERIAL

Kunigel V1, made by Kunimine Industry Co., Ltd was used as the bentonite material. It consists mostly of montmorillonite (59.3 %) and quartz (30 %). The other important minerals are feldspar (6 %) and calcite (4 %). The dry density is at 1.8 Mg m^{-3} under the distilled water conditions.

EXPERIMENTAL PROCEDURE AND CONDITIONS

A single annular slot is located within a plexiglass cell and the compacted bentonite specimen is placed in a hole in the center of the plexiglass cell. Water is supplied to the slot by a pump, which fills the slot with water and begins to saturate the bentonite specimen. In this experiment, the particle size and concentration of bentonite colloid in drainage water are measured continuously. Test conditions are shown in Tab. A-1.

Tab. A-1: Experimental conditions.

Bentonite	Kunigel V1 bentonite
Specimen size [mm]	ϕ 10 × H 10
Dry density [Mg/m^3]	1.80
Initial water content of specimen [%]	10.0
Aperture [mm]	0.3, 0.5, 1.0, 1.5
Temperature [°C]	20
Type of water	Distilled water
Water velocity [m/sec]	$1.04 \cdot 10^{-5}$ ~ $1.71 \cdot 10^{-4}$

TEST RESULTS

Fig. A-2 shows the relationship between water velocity and concentration of bentonite colloid. The concentration of bentonite colloid in distilled water was observed to decrease with increasing water velocity.

Fig. A-3 shows particle size distribution of bentonite colloid. Fig. A-4 shows relationship between particle size of bentonite colloid and water velocity. The particle size of bentonite colloid was observed to be large with increasing water velocity from these experimental results.

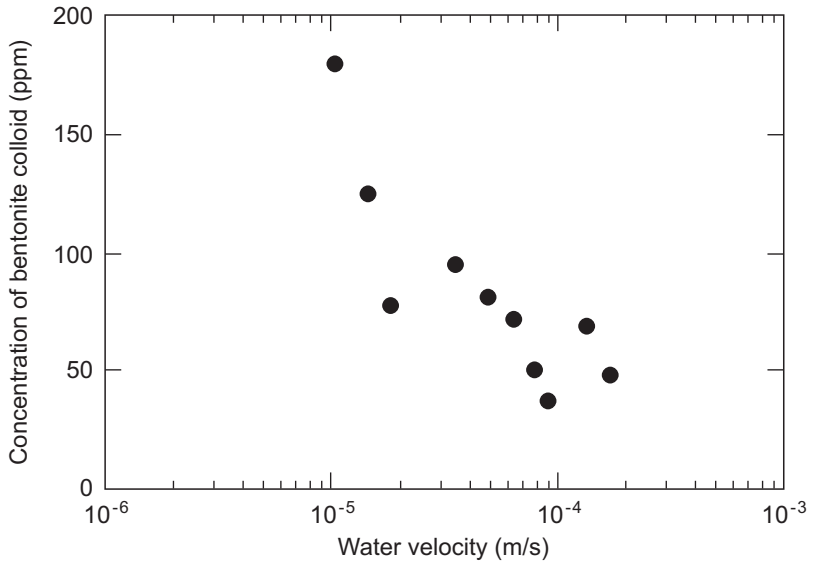

Fig. A-2: Relationship between water velocity and concentration of bentonite colloid.

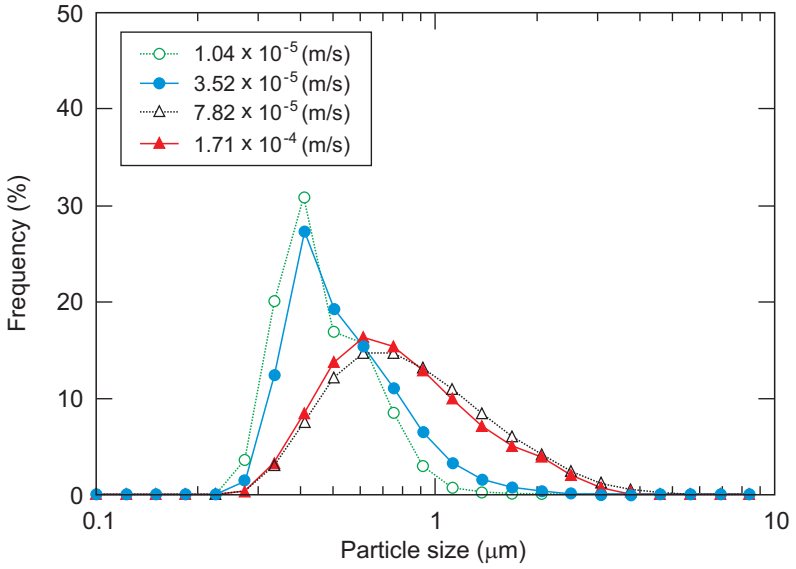

Fig. A-3: Particle size distribution of bentonite colloids.

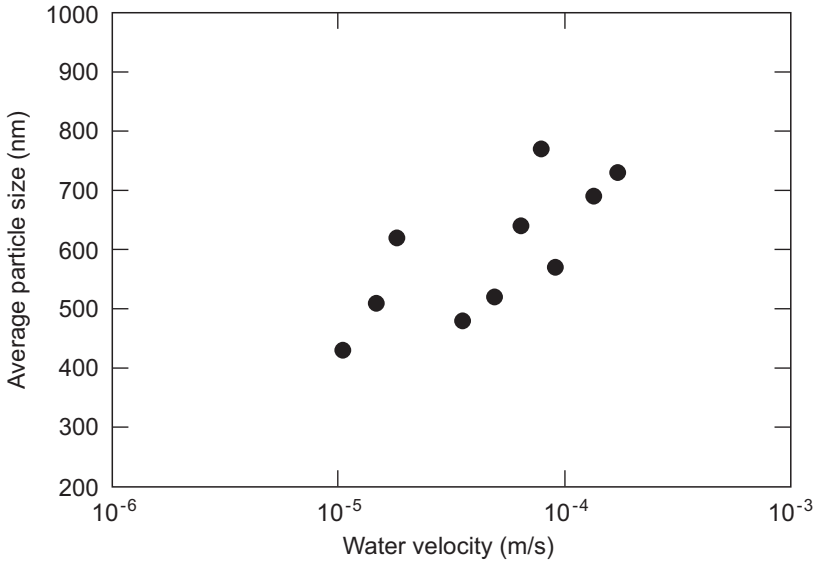

Fig. A-4: Relationship between particle size of bentonite colloids and water velocity.

CONCLUSIONS

The major conclusions obtained in this study are as follows;

1. The concentration of bentonite colloids in distilled water was observed to decrease with increasing water velocity.
2. The particle size of bentonite colloid was observed to be large with increasing water velocity.

The results suggest that the concentration of bentonite colloid in distilled water can only be evaluated by analysing the relationship between bentonite colloid concentration and water velocity.